THEORY AND PHENOMENOLOGY OF HIGGS BOSONS IN LEFT-RIGHT SUPERSYMMETRIC MODELS

By

AYON PATRA

Bachelor of Science in Physics
Calcutta University
Kolkata, West Bengal, India
2005

Master of Science in Physics
Indian Institute of Technology, Kanpur
Kanpur, Uttar Pradesh, India
2007

Submitted to the Faculty of the
Graduate College of
Oklahoma State University
in partial fulfillment of
the requirements for
the Degree of
DOCTOR OF PHILOSOPHY
May, 2014

THEORY AND PHENOMENOLOGY OF HIGGS BOSONS IN LEFT-RIGHT SUPERSYMMETRIC MODELS

Dissertation Approved:

Kaladi S. Babu

Dissertation advisor

Satyanarayan Nandi

Girish S. Agarwal

Eduardo G. Yukihara

Subhash Kak

TABLE OF CONTENTS

LIST OF TABLES

LIST OF FIGURES

CHAPTER 1

INTRODUCTION

In this chapter I briefly review the highly successful Standard Model of particle physics. We also identify its problems, both theoretical and experimental. This leads us to discuss possible extensions based on both supersymmetry and left-right symmetry. The motivations for considering these extensions are discussed in the subsequent sections. Universal extra dimensional models, which can lead to alternate solutions to the problems in Standard Model is also discussed briefly.

1.1 The Standard Model

The Standard Model of particle physics is a hugely successful model which combines the electromagnetic and weak forces under a more unified framework. It describes the various interactions existing in nature not including gravity. The Standard Model is based on the gauge group $SU(3)_C \times SU(2)_L \times U(1)_Y$ [1] under which the fermions transform as

$$Q_i(1,2,1/3) = \begin{pmatrix} u_{iL} \\ d_{iL} \end{pmatrix};\ L_i(1,2,-1) = \begin{pmatrix} \nu_{iL} \\ e_{iL} \end{pmatrix};$$

$$u_i^c(3^*,1,-4/3);\ d_i^c(3^*,1,2/3);\ e_i^c(1,1,2), \tag{1.1}$$

where $i = 1-3$ denotes the generation and the numbers in brackets are the $SU(3)_C$, $SU(2)_L$ and $U(1)_Y$ quantum numbers respectively. The Q and L are the quark and lepton doublets, while u^c, d^c and e^c (with $\psi^c = (\psi^c)_L = C\overline{\psi}_R^T$) are the charge conjugates of the right-handed up-type quark, down-type quark and charged lepton.

We see that the left-handed fields are doublets under $SU(2)_L$ while the right-handed fields are singlets. The hypercharge Y is defined in such a way that the electric charge $\mathcal{Q}$ satisfies the relation $\mathcal{Q} = T_{3L} + \frac{Y}{2}$ where T_{3L} is the third component of isospin of the $SU(2)_L$ group.

A scalar Higgs boson doublet, which transforms as

$$H(1,2,1) = \begin{pmatrix} H^+ \\ H^0 \end{pmatrix} \tag{1.2}$$

under the Standard Model gauge group, is required to generate mass for all the particles via the Higgs mechanism.

The success of the Standard Model lies in the fact that essentially all of its predictions have been experimentally verified since it was first proposed. The existence of massive charged W-bosons, massive neutral Z-boson, the charm and top quarks were all predicted by the Standard Model before they were experimentally observed. It can predict the anomalous magnetic moment of the electron to an accuracy of part per billion in agreement with experiments. It can also quantitatively explain the CP violation and mass splitting seen in the neutral K-mesons. With the recent discovery of Higgs boson at the Large Hadron Collider, it seems that Standard Model has all the essential ingredients to explain the observed phenomenon in High Energy colliders.

In spite of all the successes of the Standard Model, some experimental observations compel us to think that it is not complete and may be a remnant of some higher symmetry. The strong CP problem, which deals with the experimentally observed fact that the weak interaction sector admits CP-violation while nothing similar has been observed in the strong interactions although one can write down such interactions consistent with symmetries, cannot be naturally explained in the framework of the Standard Model. The experimentally observed neutrino oscillations suggest that the neutrinos have finite albeit small masses while the Standard Model neutrinos are massless. The existence of dark matter has been well established from the rotation

curves of galaxies and gravitational lensing observations. The Standard Model has no such invisible particle which can be considered as a dark matter candidate. The baryonic asymmetry in the universe cannot be explained as the asymmetry produced by Standard Model is too small compared to the observed value.

The main focus of this dissertation is dedicated to the study of models involving the left-right supersymmetric extensions of the Standard Model. We now briefly discuss some of the aforementioned problems of the Standard Model which can be easily explained in framework of left-right supersymmetric models.

1.1.1 Strong CP problem

The weak interactions have been experimentally seen to violate CP-symmetry, for example in the neutral kaon and B meson decays. One would expect such a phenomenon to appear in the strong interactions as well. The QCD Lagrangian admits a term

$$\mathcal{L}_{QCD} = \frac{\theta g^2}{32\pi^2} G^a_{\mu\nu} \widetilde{G}_{a\mu\nu} \tag{1.3}$$

where $\widetilde{G}_{a\mu\nu}$ is the dual field strength for the gluon. This term violates P and T and hence from the conservation of CPT symmetry, it is CP violating as well.

The physically observable parameter is a combination of θ in Eq. (1.3) and the phases of the quark masses and is given as

$$\overline{\theta} = \theta + \text{Arg}\left[\text{Det}(M_q)\right], \tag{1.4}$$

where M_q is the quark mass matrix.

The experimental limits on the neutron electric dipole moment provides stringent constraint on the value of $\overline{\theta}$ to be less than 10^{-10} [2] [3]. A fundamental dimensionless parameter appearing in the Standard Model Lagrangian should naturally be of order one but its observed smallness from the experimental measurement is what is known as the strong CP problem.

1.1.2 Neutrino oscillation and neutrino mass

Experiments with solar, atmospheric and reactor neutrinos have provided compelling evidence of neutrino oscillations [4–7]. During their flight, neutrinos of different flavor ν_e, ν_μ, ν_τ can oscillate into one another due to non-zero neutrino masses and neutrino mixing. In the formalism of local quantum field theory this means that the flavor eigenstates of neutrinos are linear combinations of three (or more) neutrinos ν_j, with masses $m_j \neq 0$:

$$\nu_{lL}(x) = \sum_j U_{lj}\nu_{jL}(x),\ l = e, \nu, \tau \tag{1.5}$$

where ν_{jL} is the left-handed component of the field ν_j possessing a mass m_j and U is the neutrino mixing matrix, also known as the Pontecorvo-Maki-Nakagawa-Sakata (PMNS) matrix.

For a simplified version with only two flavor of neutrinos, the PMNS matrix is parametrized by a single Euler angle θ and the oscillation probability of $\nu_\alpha \to \nu_\beta$ with $\alpha \neq \beta$ is given by

$$P(\nu_\alpha \to \nu_\beta) = 4\sin^2\theta\cos^2\theta\sin^2\left(\frac{\Delta m^2_{21}L}{4E}\right) \tag{1.6}$$

where the relativistic energy-momentum relation $E = \sqrt{m^2 + |\vec{p}|^2}$ with $m << |\vec{p}|$ has been used. The parameter L is called the oscillation length and $\Delta m^2_{21} = m^2_2 - m^2_1$. A non-zero oscillation probability not only requires the neutrinos to be massive but also non-degenerate.

From current experimental results, the mass-squared difference for the three neutrino mass eigenstates are [8]:

$$\Delta m^2_{21} = \ 7.59^{+0.20}_{-0.18} \times 10^{-5}\ eV^2$$

$$\Delta m^2_{31} = \begin{cases} (2.45 \pm 0.09) \times 10^{-3}\ eV^2 & \text{for normal hierarchy;} \\ -(2.34^{+0.10}_{-0.09}) \times 10^{-3}\ eV^2 & \text{for inverted hierarchy;} \end{cases}$$

Neutrino experiments this far have not been sensitive to the sign of Δm^2_{31} and hence there are two possible cases. Of the two cases, normal hierarchy refers to the case where $m_1 < m_2 < m_3$ and inverted hierarchy is one for which $m_3 < m_1 < m_2$.

These experimentally observed mass-squared differences mean that the neutrinos must have small non-degenerate masses. In the Standard Model this is not possible because of the absence of any right-handed neutrino. An extension of the Standard Model with a singlet right-handed neutrino will allow us to write mass terms and hence can solve this problem. If we consider the neutrino ν as a four-component spinor and $\nu_{L,R}$ as it left and right chiral projections, a Dirac mass term $\mathcal{L}_D$ coming from the Yukawa coupling terms in the Lagrangian can be written as

$$\mathcal{L}_D = m_D \overline{\nu}_L \nu_R + h.c. \tag{1.7}$$

where m_D is a complex matrix obtained after electroweak symmetry breaking. The singlet right-handed neutrino can have a Majorana mass term $\mathcal{L}_M$ given as

$$\mathcal{L}_M = m_R \nu_R^T C^{-1} \nu_R \tag{1.8}$$

where m_R is the Majorana mass matrix. The Dirac mass term in the Lagrangian is invariant under a global $U(1)$ symmetry under which $\nu \to e^{i\theta}\nu$. This global symmetry can be identified as the lepton number. The Majorana mass term, on the other hand, has no such symmetry and breaks the lepton number by two units. In presence of $\mathcal{L}_M$, the $\Delta L = 2$ type lepton-number-violating processes such as neutrinoless double β decay will take place. Observation of such processes can be a strong indication of Majorana character of neutrinos though presently this remains an open question.

Using these terms in the Lagrangian, the neutrino mass matrix looks like:

$$M = \begin{pmatrix} 0 & m_D \\ m_D^T & m_R \end{pmatrix}. \tag{1.9}$$

The light neutrino mass matrix is then given as

$$M_\nu = m_D m_R^{-1} m_D^T \tag{1.10}$$

Here $m_D = Y_\nu v$ with Y_ν being the Dirac Yukawa coupling matrix and $v \equiv \langle H^0 \rangle = 174$ GeV is the electroweak vacuum expectation value. This mechanism of generation of light neutrino mass is known as the **seesaw** mechanism.

For a single neutrino generation the light neutrino mass will be $(Y_\nu v)^2/m_D$. To get the light neutrino mass to be of the order of 0.1 eV as suggested by oscillation data, we either need the Yukawa couplings to be very small ($Y_\nu \sim 10^{-12}$) or the heavy neutrino to be very heavy ($m_R \sim 10^{14}$ GeV) or a combination of these two possibilities (e.g. $Y_\nu \sim 10^{-6}$ and $m_D \sim \mathcal{O}(TeV)$).

1.1.3 Dark Matter

The existence of Dark matter [9] and that its abundance in our universe is much higher than ordinary baryonic matter is one of the most astounding revelations of the twentieth century. Our universe consists of around 26.8% dark matter, 4.9% baryonic matter and the rest is contributed to what we call Dark energy. One of the earliest evidences of dark matter came from the astronomical observations that various luminous objects move faster than one would expect if they were only affected by the gravitational force of other visible objects. This led to the conclusion that there must be some other form of invisible matter which exerts gravitational force on the visible objects in the universe.

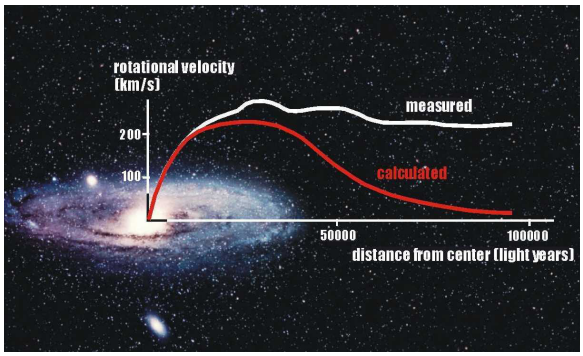

Figure 1.1: *Rotation curve for M33 galaxy(Credit Queens University)*

At the galactic scale, the evidence of dark matter can be seen from the rotation curves of galaxies. The *galactic rotation curve* is a graph of circular velocities of stars and gas as a function of their distance from the galactic center. The rotation curve for the M33 galaxy in shown in Fig 1.1. The rotation curve exhibits a flat behavior at large distance from the galactic center while for an inverse-square law like gravity we expect the rotation speed of the distant stars to fall off as the mass density decreases away from the galactic center. There must exist some other form of matter which is almost uniformly spread over the galaxy and hence explains the flat nature of the rotation curve.

The *bullet cluster* seen in 2006 consists of two colliding cluster of galaxies. It is shown in Fig 1.2. During the collision, most of the stars easily pass each other while the gas cloud from the merging galaxies slowed down and were concentrated mostly at the center. Using gravitational lensing technique, astronomers measured the mass of the stars that were now separated from the gas. This measurement showed that the stars were much more massive compared to their calculated mass. The explanation can be that there is some other form of matter which interacts very weakly and could easily pass the collision and thus was contributing to the total observed mass.

Figure 1.2: *The Bullet Cluster showing two colliding galaxies.(Credit nasa.gov)*

These and other experiments have proved beyond doubt that there exists some form of matter which exerts gravitational force but is otherwise invisible. If such a particle exists in nature, any particle physics model should have a viable dark matter candidate. Unfortunately Standard Model has no such particle and hence we need to look for some other models which will have a weakly interacting particle with the required abundance to be a dark matter candidate. Any new model though has to eventually give us the Standard Model at low energies.

1.2 Supersymmetry

Supersymmetry is a generalization of the space-time symmetries of quantum field theory that transforms fermions into bosons and vice verse. It extends the Poincaré algebra through introduction of four anticommuting spinor generators into the SuperPoincaré algebra. Supersymmetry also provides a framework for the unification of particle physics with gravity [10] under supergravity.

In supersymmetric models, each boson(fermion) of Standard Model has a supersymmetric partner which is a fermion(boson). These superpartners have the same internal quantum numbers except their spin which differs by half. Together, a particle with its supersymmetric partner forms what is called a supermultiplet. A *superpotential* is constructed consisting of gauge invariant, holomorphic terms which are linear, quadratic or cubic functions of the superfields as higher order terms will lend the theory non-renormalizable. The coefficients of the quadratic functions of the Higgs boson fields in the superpotential are known as the μ parameters and have the dimension of mass. The cubic terms in the superpotential gives rise to three particle vertices and are called the Yukawa coupling terms. This superpotential gives rise to the so called F-terms in the supersymmetric Lagrangian.

In Standard Model, one can calculate the radiative corrections to the Higgs bo-

son mass from all the particles that couple with the Higgs boson. This calculation, unfortunately, gives a result which is quadratically divergent with the cut-off scale. This yields a natural Higgs boson mass which is of the order of Ultraviolet cut-off of the theory, generically around the Planck scale ($\sim 10^{19}$ GeV). We need a large fine-tuning to get the Higgs boson mass to be the experimentally observed value of 125 GeV. This is known as the *hierarchy problem*. Supersymmetry has an ingenious mechanism to bypass this problem. This resides in the fact that bosonic couplings provide radiative corrections which are opposite in sign with respect to fermion loops. Since supersymmetry has both bosonic and fermionic particles in the same supermultiplet, there is an exact cancellation of these quadratically divergent contributions thus solving the *hierarchy problem*. In any realistic model supersymmetry must be broken in such a way so as not to introduce any quadratic divergence.

Supersymmetric models allow for the existence of renormalizable baryon and lepton number violating terms is the superpotential. These terms are dangerous since the lepton and baryon number violating processes are strongly constrained by experiments, especially from proton stability. These unwanted terms can be prohibited by requiring the superpotential to be invariant under a $\mathbb{Z}_2$ symmetry known as R-parity which is defined as

$$R = (-1)^{3(B-L)+2S}, \tag{1.11}$$

where S is the spin of the particle and B and L are the baryon and lepton number respectively. All the Standard Model particles have R-parity of $+1$ while their superpartners have R-parity -1. Hence if R-parity is conserved, the lightest supersymmetric particle (LSP) cannot decay and can be identified as a dark matter candidate. The dark matter annihilation cross-section of order 0.1pb, which is natural in supersymmetric models, leads to the correct relic abundance.

In an exact supersymmetric theory, the particles and their superpartners would be degenerate in mass. Since no such supersymmetric particle has been observed in

experiments, supersymmetry must be a broken symmetry. Supersymmetry breaking can be achieved by writing a soft supersymmetry breaking [11] potential which consists of terms which are either linear, quadratic or cubic functions of the fields. These terms break supersymmetry softly by not introducing any ultraviolet divergences in the scalar masses, thus maintaining the cancellation of quadratic divergence as discussed earlier. The cubic terms in the soft supersymmetry breaking Lagrangian are called the trilinear A-term and their coefficients are denoted by A_i. The μ-terms in the superpotential along with the trilinear A-terms can lead to additional sources of CP violation and give rise to the SUSY CP problem [12]. Experimental limits from the electron and the neutron electric dipole moments imply that the SUSY phases must be $\lesssim 10^{-2}$, which is known as the SUSY CP problem.

Field	$SU(3)_c$	$SU(2)_L$	$U(1)_Y$
$\hat{L} = \begin{pmatrix} \hat{\nu}_{eL} \\ \hat{e}_L \end{pmatrix}$	1	2	-1
$\hat{E}^c$	1	1	2
$\hat{Q} = \begin{pmatrix} \hat{u}_L \\ \hat{d}_L \end{pmatrix}$	3	2	$\frac{1}{3}$
$\hat{U}^c$	3^*	1	$-\frac{4}{3}$
$\hat{D}^c$	3^*	1	$\frac{2}{3}$
$\hat{H}_u = \begin{pmatrix} \hat{h}_u^+ \\ \hat{h}_u^0 \end{pmatrix}$	1	2	1
$\hat{H}_d = \begin{pmatrix} \hat{h}_d^0 \\ \hat{h}_d^- \end{pmatrix}$	1	2	-1

Table 1.1: *Matter and Higgs superfield content of the MSSM*

The minimal supersymmetric extension of the Standard Model (MSSM) consists of extending the Standard Model particle spectrum by adding their superpartners. The matter and the Higgs superfields of the MSSM is given in Table 1.1. An extra Higgs boson doublet field is needed to generate masses for both the "up"-type and "down"-type quarks (and charged leptons) in a way consistent with supersymmetry. The superpotential is given by

$$W_{MSSM} = Y_u \hat{Q} \hat{H}_u \hat{U}^c + Y_d \hat{Q} \hat{H}_d \hat{D}^c + Y_l \hat{L} \hat{H}_d \hat{E}^c + \mu \hat{H}_u \hat{H}_d \tag{1.12}$$

where Y_u, Y_d and Y_l are the up, down and lepton Yukawa coupling matrices. The F-term and the soft supersymmetry breaking terms of the Lagrangian can be derived from the superpotential while a D-term can be written for the scalar superfields. The Lagrangian would thus consist of the Kinetic terms for all the superfields along with the F-term, D-term and the soft supersymmetry breaking terms. This generates all the masses and couplings of the particles except the neutrino mass which requires either the introduction of a right-handed neutrino or R-parity violating couplings.

1.3 Left-Right Symmetry

The chiral structure of the Standard Model and its inability to explain the origin of parity violation in weak interactions compels us to think of a theory which has a left and right chiral symmetric structure. This left-right symmetry would extend the gauge group of the Standard Model into $SU(3)_c \times SU(2)_L \times SU(2)_R \times U(1)_{B-L}$ [13]. This would imply that the fundamental weak-interaction Lagrangian is invariant under parity symmetry at scales much above the electroweak scale and the parity asymmetry observed in nature arises from the vacuum being noninvariant under parity symmetry. The origin of parity violation can be explained as the $SU(2)_R$ symmetry is broken at some high scale leading to the observed parity asymmetry at lower energies. New effects associated with the parity non-invariance of the Lagrangian are expected

to manifest themselves as the existence of a second neutral Z' boson, W_R bosons, right-handed charged currents, right-handed neutrino, etc. The mass scales at which these new effects appear is the energy scale at which the right-handed symmetry is broken.

The existence of a non-zero albeit small neutrino mass can also be easily understood in the framework of the left-right symmetric models. The existence of a heavy right-handed neutrino is warranted by parity invariance and its spontaneous breaking at a high scale. This heavy right-handed neutrino can produce a small left-handed neutrino mass via the seesaw mechanism as has been explained earlier.

The chiral fermion sector in this model becomes

$$\begin{aligned} Q_L &= \begin{pmatrix} u \\ d \end{pmatrix}_L \sim \left(3, 2, 1, \frac{1}{3}\right), \; Q_R = \begin{pmatrix} u \\ d \end{pmatrix}_R \sim \left(3, 1, 2, \frac{1}{3}\right), \\ L_L &= \begin{pmatrix} \nu \\ e \end{pmatrix}_L \sim (1, 2, 1, -1), \; L_R = \begin{pmatrix} \nu \\ e \end{pmatrix}_R \sim (1, 1, 2, -1), \end{aligned} \tag{1.13}$$

where the numbers in the brackets denote the quantum numbers under $SU(3)_C \times SU(2)_L \times SU(2)_R \times U(1)_{B-L}$ gauge groups. The electric charge of a particle in left-right symmetric models is defined as

$$\mathcal{Q} = I_{3L} + I_{3R} + \frac{B - L}{2} \tag{1.14}$$

where I_{3L} and I_{3R} are the third component of the isospin of the $SU(2)_L$ and $SU(2)_R$ respectively, B and L are the baryon and lepton numbers. This definition of the charge is physically much more attractive compared to the Standard Model definition where the hypercharge $U(1)$ lacks any physical meaning and is arbitrarily adjusted according to the actual charge of a particle.

Many Grand Unified Theories as well as fundamental Planck scale theories such as string theory can more easily lead to left-right symmetric gauge structure and thus

it is a distinct possibility that the Standard Model will eventually become part of a left-right symmetric structure.

1.4 Minimal Left-Right Supersymmetric Model with automatic R-parity

The minimal Left-Right Supersymmetric model [14] is a supersymmetric extension of the left-right symmetric model of 1.3. The gauge group is extended to $SU(3)_C \times SU(2)_R \times SU(2)_L \times U(1)_{B-L}$. This extended gauge symmetry allows for parity to be defined as an exact symmetry which can only be spontaneously broken. As a consequence of the parity invariance, the Yukawa couplings and the corresponding SUSY breaking A terms are hermitian, and the μ term are real. This leads to a vanishing electric dipole moment of fermions which solves the strong CP problem and the SUSY CP problem. R-parity is part of the gauge symmetry as it is contained in $B - L$. The model also has all the ingredients to explain the neutrino mass and an unbroken R-Parity provides a stable dark matter candidate.

Unlike Standard Model, the quarks and leptons in this model consists of left-handed and right-handed doublets. The right-handed lepton doublet has a right-handed neutrino which is necessary for the generation of left-handed neutrino mass. The Higgs sector, in one version, consists of two $SU(2)_R$ and two $SU(2)_L$ Higgs triplet fields. The $SU(2)_R$ triplet fields are needed for breaking the $SU(2)_R \times U(1)_{B-L}$ symmetry. It also has two bidoublet fields which are doublets under both $SU(2)_R$ and $SU(2)_L$. These generate the quark and lepton masses and the CKM mixings. There is also an optional singlet Higgs field which makes sure that the right-handed symmetry breaking occurs in the supersymmetric limit.

The $SU(2)_R \times U(1)_{B-L}$ symmetry is broken down to $U(1)_Y$ by the $SU(2)_R$ Higgs triplets. This generates a Majorana term for the ν^c field. If this symmetry breaking takes place at a high scale, it will generate a large mass for the right-handed neutrino. The heavy right-handed neutrino Majorana mass term can, through the seesaw

mechanism, explain the small left-handed neutrino mass without the need to consider unnaturally small Yukawa couplings. Thus, this model can explain the existence of small neutrino mass.

The conservation of R-parity, which is a part of the gauge symmetry, prevented the lightest supersymmetric particle from decaying and hence was considered to be the dark matter particle. In this model, R-parity is automatically conserved and the lightest neutralino can be considered as the dark matter.

We have seen how the Minimal Left-Right Supersymmetric model solves many of the problems of the Standard Model and can naturally explain the existence of neutrino mass and dark matter. As one might expect, this LRSUSY model is not without its own set of problems. The tree-level Higgs potential in the model can be shown to be lower for a charge breaking vacuum compared to the charge conserving one. Also at the tree level, it can be seen that the computation of the doubly-charged Higgs boson mass-square matrix yields a negative eigenvalue. This problem can be solved by calculating the one loop correction to the potential and the doubly-charged Higgs boson mass as will be discussed in details in chapter 2.

1.5 Universal Extra Dimension

Extra dimensional theories have seen a renewed interest since the advent of String theory. String theory, the most promising theory to quantize gravity and unify it with the other gauge forces, seems to require both extra dimensions, beyond the known four, and supersymmetry as crucial ingredients for its consistency. The idea of extra dimension, though, was first introduced by Kaluza and Klein [15] who were trying to unify Electromagnetism and Gravity by assuming that the photon field originates from the fifth component of a five dimensional metric tensor. In the Kaluza Klein (KK) framework, the particles are free to move in the entire space formed by all the dimensions and hence the length of the extra dimension must be small in order to be

consistent with experimental observations. In the case of a product space formed of the four-dimensional Minkowski space and a circle $M_4 \times S^1$, the wave function of a scalar field can be expanded in Fourier series along S^1 to be

$$\phi(x, y) = \frac{1}{\sqrt{2\pi R}} \sum_{n \epsilon \mathbb{Z}} e^{in\frac{y}{R}} \phi_n(x) \tag{1.15}$$

where x stands for the regular 4D coordinate, y is the coordinate of the extra dimension of radius R and n is the eigenvalue of the one-dimensional angular momentum operator. The Klein-Gordon equation of the scalar field thus becomes

$$p^\mu p_\mu = -p_0^2 + \vec{p}^2 = -\frac{n^2}{R^2} \tag{1.16}$$

where p_μ is the momentum four-vector. Thus we can see that in the four-dimensional space, this is equivalent to a tower of particles of masses given by n/R. For energy scales below $1/R$, only massless modes with $n = 0$ can be excited and hence the low energy physics is effectively four-dimensional.

Extra dimensional models with a low cutoff scale can provide a solution to the hierarchy problem [16] [17]. The radiative corrections to the Higgs boson mass in extra dimensional models are also quadratically divergent similar to the Standard Model. The advantage of a low scale extra dimensional model is that the ultraviolet cutoff scale is $\mathcal{O}$(TeV) and hence the correction to the Higgs mass is of the electrowek scale thus solving the hierarchy problem.

Recent interest in extra dimensional theories have given rise to two broad subcategory of models. The first corresponds to those where the Standard Model fields are confined to our regular (3+1) dimensions while only gravity can propagate in the extra dimension. The other class of models are the ones in which some or all of the Standard Model fields can access the extended space-time manifold. Universal Extra dimension corresponds to the second class of models and is characterized by flat extra dimension with small compactification radius of $\mathcal{O}(\text{TeV}^{-1})$. For the case of minimal universal extra dimension (mUED), there is only one extra dimension

which is compactified on a S^1/Z_2 orbifold. This orbifolding is crucial in generating chiral zero modes for fermions, which would otherwise be vector-like. The UED Lagrangian, in general, has KK number conservation which is broken by the boundary conditions in mUED leading to the conservation of KK parity defined as $(-1)^n$. This discrete symmetry ensures that the lightest KK particle is stable and can be a dark matter candidate. The conserved KK parity also means that any contribution from the KK modes to the electroweak processes is at the loop level and is thus sufficiently suppressed to not effect the experimental observations even for a relatively small KK-spacing. The experimental observation of the Higgs boson and its observed properties have put severe constraints on mUED as will be discussed later.

1.6 Organisation of this Dissertation

This dissertation is organized as follows. In chapter 2, I look at several variations of left-right supersymmetric models differentiated by their symmetry breaking mechanism. I calculate the masses of the Higgs bosons and Higgsinos and show that in some cases one can easily obtain the experimentally observed Higgs boson mass even for a relatively light stop squark which is not possible in the Minimal Supersymmetric Standard Model. This is a new result that we have obtained which helps to explain the current experimental Higgs boson mass even for a relatively light supersymmetric particle spectrum.

In Chapter 3, I study the collider phenomenology of the production and decay of the doubly-charged Higgs boson and Higgsinos at the Large Hadron Collider. A new channel for the observation of these doubly-charged particles is suggested. I analyze the final signal of four leptons and missing energy. I look at the invariant mass, missing energy and angular separation plots for the final state particles and see that the signal produced by our model would be very easy to distinguish from other competing models.

In chapter 4, I study the properties of the neutral Higgs boson in the framework of mUED and compare them to the experimental observations. I specifically look at the constraints on the mUED model from measured Higgs boson signal strength in its various decay channels. This helps to put a lower bound on the size parameter of the mUED model.

CHAPTER 2

LIGHT HIGGS BOSON MASS IN SUPERSYMMETRIC LEFT-RIGHT MODELS

2.1 Introduction

Models based on the left–right symmetric gauge group $G_{3221} \equiv SU(3)_c \times SU(2)_L \times SU(2)_R \times U(1)_{B-L}$ [13] are attractive extensions of the Standard Model (SM) with several interesting features. At the fundamental level Parity is a good symmetry in these models. The observed Parity violation in weak interactions is explained by the spontaneous breaking of $SU(2)_R \times U(1)_{B-L}$ down to $U(1)_Y$ at a scale v_R well above the masses of the W and Z bosons. The gauge structure requires the existence of the right–handed neutrino, and thus leads naturally to small neutrino masses via the seesaw mechanism. In fact, with the right–handed neutrino included, G_{3221} is the maximal gauge symmetry that can be realized at a scale of order TeV, relevant to the ongoing LHC experiments.* Because of Parity invariance these models can potentially solve the strong CP problem [3] without introducing a global Peccei–Quinn symmetry and the resulting axion.

Supersymmetric versions of left–right gauge models, denoted here as SUSYLR models, preserve the merits of G_{3221} noted above, and in addition, solve the gauge

*There is a natural embedding of G_{3221} into the Pati–Salam symmetry $G_{422} \equiv SU(4)_c \times SU(2)_L \times SU(2)_R$ [18], however, the scale of G_{422} symmetry breaking must be of order 10^5 GeV, from $K_L \to \mu e$ decay constraints. Embedding G_{3221} (or G_{422}) into the unified symmetry group of $SO(10)$ is very natural, but that symmetry breaking scale must be of order 10^{15} GeV, from constraints on nucleon decay and gauge coupling unification.

hierarchy problem. It has been noted that the puzzle of small phases in the SUSY breaking sector (required by electric dipole moment constraints) has a natural explanation in the SUSY left–right models, by virtue of Parity symmetry [12]. Several versions of the SUSYLR models have been proposed and studied in the literature, with differing Higgs boson sectors used for symmetry breaking [14, 19–23]. Here we undertake a systematic study of the Higgs potential in various realizations of these models, focusing on the lightest neutral Higgs boson mass m_h. In many cases we find that the tree–level constraint $m_h \leq m_Z$ of the MSSM is modified to less stringent constraint. [19]. This difference in the upper limit arises from the non-decoupling D–terms of $SU(2)_R \times U(1)_{B-L}$, which occurs when the symmetry breaking scale v_R and the SUSY breaking scale are of the same order. Thus, these models would predict additional $W_R^{\pm}$ and Z_R gauge bosons within reach of LHC experiments, in addition to SUSY particles. In the MSSM heavy stops ($m_{\tilde{t}} > 2$ TeV) with large mixing are needed in order to accommodate the Higgs boson of mass 126 GeV discovered recently at LHC. Such a large mass of the stop puts the gauge hierarchy problem in a different perspective, since some amount of tuning would be required. With the increased mass of m_h, SUSYLR models would allow for the stops to be much lighter and less mixed, and thus would alleviate the tuning problem.

Our analysis focuses on two basic classes of models which have been developed in the literature. In one class Higgs triplets are introduced for $SU(2)_R$ symmetry breaking along with $SU(2)_L \times SU(2)_R$ bi-doublets which break the electroweak symmetry [14, 21–23]. Fermion mass generation is via direct Yukawa couplings in this class of models, including the Majorana mass of the right-handed neutrino. In a second class, Higgs doublets are used to break $SU(2)_R$ symmetry, with doublets and/or bi-doublets breaking the electroweak symmetry. Additional fermions are necessary in this class for fermion mass generation, at least in the neutrino sector. A specific example studied incorporates the inverse seesaw mechanism for neutrino masses with

the inclusion of gauge singlet fermions. Another example, termed alternate left–right model [19, 20], has an E_6 inspired particle spectrum. A third example uses a universal seesaw mechanism for quarks and leptons by introducing vector–like gauge singlet fermions [24].

Non–decoupling D–term effects on the lightest Higgs boson mass in extensions of the MSSM have been studied by various authors. In Ref. [19] symmetry breaking in SUSYLR models with an E_6 inspired particle spectrum was studied and a relation $m_h \leq \sqrt{2}\, m_W$ was derived. In Ref. [23] symmetry breaking of SUSYLR models with Higgs triplets was studied and an enhancement of m_h compared to the MSSM result was observed. Ref. [25] has studied extended gauge sectors, including an extra $SU(2)$ added to the SM gauge symmetry. In this case there is an unknown gauge coupling, which was chosen so that it remains perturbative all the way to a GUT scale, and significant increase in m_h was observed. In Ref. [26] non–decoupling effects of an additional $U(1)$ gauge symmetry was studied, which also showed a modest increase in m_h. Our aim in this chapter is systematically study the Higgs boson sectors of various realizations of SUSYLR models, which results in some overlap with earlier studies. In one case we reproduce and generalize the results of Ref. [19]. In another case studied, we provide an analytic formula for the upper limit on m_h that interpolates between the decoupling and non–decoupling limits of left–right symmetry, where our results agree roughly with the numerical results of Ref. [23].

When gauge singlets that couple to the MSSM Higgs fields are present in the theory, additional F–term contributions to m_h arises. In several cases this contribution is non–decoupling, a well-known case being the NMSSM [27]. Modes increase in m_h can arise from this contribution, although we find the non–decoupling D–term to be more significant.

The remainder of this chapter is organized as follows. In Sec. 2.2 we briefly explain the symmetry breaking mechanism, lepton mass and light neutrino mass

generation mechanism for each of the models. In Sec. 2.3 we analyze the Higgs potential of SUSYLR models with triplet scalars breaking the $SU(2)_R \times U(1)_{B-L}$ symmetry. Various scenarios are discussed here. For electroweak symmetry breaking we allow for one or two bi-doublets. We also allow for a gauge singlet that facilitates LR symmetry breaking in the SUSY limit. We focus on the lightest neutral Higgs boson mass and derive the tree–level constraint for m_h. In Sec. 2.4, Sec. 2.5 and Sec. 2.6 Higgs potentials involving doublet fields are studied with several variations: inverse seesaw, E_6 inspired spectrum, and universal seesaw for quarks and leptons. In Sec.2.7 we calculate the radiative correction to the doubly-charged Higgs boson mass and show that the one-loop corrections can make it positive. Finally, we summarize the results.

2.2 The Left–Right Supersymmetric Model

In left-right symmetric models, the gauge group is extended to $SU(3)_c \times SU(2)_L \times SU(2)_R \times U(1)_{B-L}$. The models we consider are supersymmetric versions of the left-right symmetric model. We consider different symmetry breaking sectors leading to several variations of the left-right supersymmetric models. The right-handed symmetry breaking can be achieved either by triplet or doublet Higgs boson fields while the electroweak symmetry is broken using bidoublets or doublet Higgs boson fields. Each model has a common chiral fermion sector consisting of three families of quark and lepton superfields given as

$$\begin{aligned} Q &= \begin{pmatrix} u \\ d \end{pmatrix} \sim \left(3, 2, 1, \frac{1}{3}\right), \; Q^c = \begin{pmatrix} d^c \\ -u^c \end{pmatrix} \sim \left(3^*, 1, 2, -\frac{1}{3}\right), \\ L &= \begin{pmatrix} \nu \\ e \end{pmatrix} \sim (1, 2, 1, -1), \; L^c = \begin{pmatrix} e^c \\ -\nu^c \end{pmatrix} \sim (1, 1, 2, 1), \end{aligned} \tag{2.1}$$

where the numbers in the brackets denote the quantum numbers under $SU(3)_C \times SU(2)_L \times SU(2)_R \times U(1)_{B-L}$ gauge groups.

All the models discussed below must meet three main criterion. First, a right-handed symmetry breaking mechanism consistent with the experimental limits for the heavy gauge boson masses has to be present. Second, we must be able to generate the fermion masses and thirdly, there must be a mechanism to generate a small neutrino mass. We now briefly describe the models that have been studied in this work while a detailed calculation of the Higgs sector will be discussed later.

2.2.1 Models involving triplet and bidoublet Higgs fields

This is the most straightforward way to satisfy our requirements for a consistent model. A right-handed triplet Higgs field Δ^c can couple directly to the right-handed neutrino giving it a Majorana mass as well as break the right-handed symmetry as its neutral component acquires a vacuum expectation value. The bidoublet field Φ can have Yukawa couplings with the fermions generating the quark and leptons masses. Being a supersymmetric theory the right-handed Δ^c field must be accompanied by another right-handed triplet $\overline{\Delta}^c$ field to achieve the right-handed symmetry breaking without inducing any R-parity violating couplings. In a left-right symmetric model, the right-handed triplets must also be accompanied by left handed triplets Δ and $\overline{\Delta}$ for parity conservation. Additionally, one or more bidoublet fields denoted by Φ_a which are needed for generation of quark and lepton masses and CKM matrices. We consider cases with and without an extra singlet field. In the absence of the singlet field, it is not possible to break the right-handed symmetry in the supersymmetric limit. This is perfectly consistent as long as we consider the right-handed symmetry breaking and the supersymmetry breaking to be at the same scale. The singlet is only needed to decouple the two symmetry breaking scales allowing the right-handed symmetry to be broken at a much higher scale. Thus, the Higgs boson fields in this

model are given as

$$\begin{aligned}
\Delta(1,3,1,2) &= \begin{pmatrix} \frac{\delta^+}{\sqrt{2}} & \delta^{++} \\ \delta^0 & -\frac{\delta^+}{\sqrt{2}} \end{pmatrix}, \ \overline{\Delta}(1,3,1,-2) = \begin{pmatrix} \frac{\overline{\delta}^-}{\sqrt{2}} & \overline{\delta}^0 \\ \overline{\delta}^{--} & -\frac{\overline{\delta}^-}{\sqrt{2}} \end{pmatrix}, \\
\Delta^c(1,1,3,-2) &= \begin{pmatrix} \frac{\delta^{c^-}}{\sqrt{2}} & \delta^{c^0} \\ \delta^{c^{--}} & -\frac{\delta^{c^-}}{\sqrt{2}} \end{pmatrix}, \ \overline{\Delta}^c(1,1,3,2) = \begin{pmatrix} \frac{\overline{\delta}^{c^+}}{\sqrt{2}} & \overline{\delta}^{c^{++}} \\ \overline{\delta}^{c^0} & -\frac{\overline{\delta}^{c^+}}{\sqrt{2}} \end{pmatrix}, \\
\Phi_i(1,2,2,0) &= \begin{pmatrix} \phi_1^+ & \phi_2^0 \\ \phi_1^0 & \phi_2^- \end{pmatrix}_i (i=1,2), \ S(1,1,1,0). \qquad (2.2)
\end{aligned}$$

The fields getting non-zero vev are given by

$$\left\langle \delta^{c^0} \right\rangle = v_R, \ \left\langle \overline{\delta}^{c^0} \right\rangle = \overline{v}_R, \ \left\langle \phi_{1_i}^0 \right\rangle = v_{u_i}, \ \left\langle \phi_{2_i}^0 \right\rangle = v_{d_i}, \qquad (2.3)$$

while all other fields do not get any vacuum expectation value. We take the limit where $v_R, \overline{v}_R >> v_u, v_d$.

The Yukawa terms in the superpotential for these models are

$$\mathcal{L}_Y = \sum_{j=1}^{2} Y_q^j Q^T \tau_2 \Phi_j \tau_2 Q^c + Y_l^j L^T \tau_2 \Phi_j \tau_2 L^c + i f L^T \tau_2 \Delta L + i f^c L^{cT} \tau_2 \Delta^c L^c, \qquad (2.4)$$

where Y_q^j and Y_l^j are the quark and lepton Yukawa coupling matrices and f is the Majorana neutrino Yukawa coupling matrix. This superpotential is invariant under parity transformation under which $\Phi \to \Phi^\dagger, \Delta \to \Delta^{c^*}, \overline{\Delta} \to \overline{\Delta}^{c^*}, S \to S^*, Q \to Q^{c^*}, L \to L^{c^*}, \theta \to \overline{\theta}$ etc. Parity invariance requires the Yukawa coupling matrices Y_q^j and Y_l^j to be hermitian and $f^c = f$. The Majorana mass term for the right-handed neutrino is heavy and this facilitates the generation of a small left-handed neutrino mass via the seesaw mechanism.

There are three heavy gauge bosons in these cases – two heavy right-handed W-bosons and one heavy right-handed Z-boson. In the limit where the right-handed vevs are much bigger than the electroweak vev, we can neglect the mixing between the left-handed and the right-handed gauge bosons and obtain the mass of the heavy

W-bosons as

$$M^2_{W^{\pm}_R} \simeq \frac{1}{2} g^2_R (2v^2_R + 2\overline{v}^2_R + v^2_{u_i} + v^2_{d_i}), \tag{2.5}$$

and mass of the heavy Z-boson is

$$M^2_{Z_R} \simeq \frac{g^2_R}{2\cos^2\theta_W \cos 2\theta_W} \left[4(v^2_R + \overline{v}^2_R)\cos^4\theta_W + (v^2_{u_i} + v^2_{d_i})\cos^2 2\theta_W\right], \tag{2.6}$$

where i runs over the number of bidoublets in the model, g_R is the $SU(2)_R$ gauge coupling and θ_W is the Weinberg angle.

These expressions for the gauge boson masses must be consistent with the experimental limit and will be relevant in setting a lower limit for the right-handed symmetry breaking scale.

2.2.2 Inverse seesaw model

The right-handed symmetry breaking in the previous case was achieved using $SU(2)_R$ triplet Higgs bosons but we can also use $SU(2)_R$ doublet Higgs field for the symmetry breaking. This simplifies the Higgs boson sector considerably. A couple of bidoublet are also present in the Higgs spectrum which can generate the quark and lepton masses and CKM mixing. The problem with doublet Higgs boson fields is that they do not directly couple to the right-handed neutrino and cannot produce a Majorana mass term for them. Hence we need to introduce an extra heavy singlet neutrino N for each generation of leptons in addition to the chiral matter fields that are given in Eq. (2.1). This heavy neutral singlet would get a Majorana mass and can produce a light neutrino mass. The Higgs sector thus consists of two right-handed doublet fields needed for anomaly cancellation and another two left-handed doublets for parity symmetry. The Higgs sector is given by the following Higgs fields

$$H_L(1,2,1,-1) \;=\; \begin{pmatrix} H^0_L \\ H^-_L \end{pmatrix}, \overline{H}_L(1,2,1,1) = \begin{pmatrix} \overline{H}^+_L \\ \overline{H}^0_L \end{pmatrix}, H_R(1,1,2,1) = \begin{pmatrix} H^+_R \\ H^0_R \end{pmatrix},$$

$$\overline{H}_R(1,1,2,-1) \;=\; \begin{pmatrix} \overline{H}_R^0 \\ \overline{H}_R^- \end{pmatrix}, \Phi_a(1,2,2,0) = \begin{pmatrix} \phi_1^+ & \phi_2^0 \\ \phi_1^0 & \phi_2^- \end{pmatrix}_a (a=1,2), \tag{2.7}$$

and the vev of the neutral fields are given as

$$\left\langle H_L^0 \right\rangle = v_L,\ \left\langle \overline{H}_L^0 \right\rangle = \overline{v}_L,\ \left\langle H_R^0 \right\rangle = v_R,\ \left\langle \overline{H}_R^0 \right\rangle = \overline{v}_R,\ \left\langle \phi_{1_i}^0 \right\rangle = v_{u_i},\ \left\langle \phi_{2_i}^0 \right\rangle = v_{d_i}, \tag{2.8}$$

The superpotential terms required for the quark and lepton mass generation in this case is given as

$$W_Y = \sum_{j=1}^{2} Y_q^j Q^T \tau_2 \Phi_j \tau_2 Q^c + Y_l^j L^T \tau_2 \Phi_j \tau_2 L^c + i f L^T \tau_2 \overline{H}_L N + i f^c L^{cT} \tau_2 \overline{H}_R N + \frac{1}{2} \mu_N N N \tag{2.9}$$

where Y_q^j and Y_l^j are the quark and lepton Yukawa coupling matrix, f and f^c are the left-handed and right-handed neutrino Yukawa couplings matrices with the singlet neutrino and μ_N is the Majorana mass term for N. Again from parity invariance, the Yukawa coupling matrices must be hermitian, $f^c = f$ and μ_N is real. Here only the heavy neutrino has a Majorana mass term while the ν and ν^c fields get Dirac masses by couplings among themselves and with the heavy neutrino. For each neutrino generation, we get a 3×3 neutrino mass matrix given as

$$\begin{pmatrix} 0 & Y_l v_1 & f\overline{v}_L \\ Y_l v_1 & 0 & f^c \overline{v}_R \\ f\overline{v}_L & f^c \overline{v}_R & \mu_N \end{pmatrix}. \tag{2.10}$$

In the limit where $\overline{v}_L$ and μ_N become zero, one of the eigenvalues of this matrix vanishes. So, for small values of these parameters one can understand the existence of a small neutrino mass. This is known as the inverse seesaw mechanism for generation of neutrino mass.

The heavy gauge boson masses in this case are given as:

$$M^2_{W_R^\pm} \simeq \frac{1}{2} g_R^2 (v_R^2 + \overline{v}_R^2 + v_1^2 + v_2^2), \tag{2.11}$$

and

$$M^2_{Z_R} \simeq \frac{g_R^2}{2\cos^2\theta_W \cos 2\theta_W}\left[(v_R^2+\overline{v}_R^2)\cos^4\theta_W + (v_1^2+v_2^2)\cos^2 2\theta_W\right] \tag{2.12}$$

where g_R is the $SU(2)_R$ gauge coupling, θ_W is the Weinberg angle and v_L, v_R, v_2 are the vev of the ${H_L}^0, {H_R}^0, \phi_2^0$ fields respectively. Comparing these masses with the experimental limit for the heavy gauge bosons we will be able to set a lower limit for vev of the right-handed Higgs boson fields.

2.2.3 Universal seesaw model

One can choose an even simpler Higgs boson sector in order to achieve the symmetry breaking. We can have a right-handed doublet field H_R to break the $SU(2)_R$ symmetry and a left-handed doublet H_L for $SU(2)_L$ symmetry breaking. For a supersymmetric model one would also need $\overline{H}_R$ and $\overline{H}_L$ fields for anomaly cancellation. This Higgs boson sector, without a bidoublet, will not be able to generate the quark and lepton masses and we need to introduce additional heavy quark and lepton fields for this purpose. The chiral matter sector in this case would consist of the quarks and leptons given in Eq. (2.1) along with a set of heavy singlet quarks and leptons for each generation. There are a pair of heavy singlet quarks $P(3,1,1,-\frac{4}{3})$, $N(3,1,1,\frac{2}{3})$ and a singlet lepton $E(1,1,1,2)$ along with their conjugate fields $P^c(3,1,1,\frac{4}{3}), N^c(3,1,1,-\frac{2}{3})$ and $E^c(1,1,1,-2)$ respectively. We can also include a neutral singlet lepton given as $S(1,1,1,0)$ which can generate the light neutrino mass. This is not essential as the neutrino mass can also be generated at the two-loop level by contribution from W_L and W_R exchange.. The Higgs sector in this case is given by:

$$\begin{aligned} H_L(1,2,1,-1) &= \begin{pmatrix} {H_L}^0 \\ {H_L}^- \end{pmatrix}, \overline{H}_L(1,2,1,1) = \begin{pmatrix} {\overline{H}_L}^+ \\ {\overline{H}_L}^0 \end{pmatrix}, \\ H_R(1,1,2,1) &= \begin{pmatrix} {H_R}^+ \\ {H_R}^0 \end{pmatrix}, \overline{H}_R(1,1,2,-1) = \begin{pmatrix} {\overline{H}_R}^0 \\ {\overline{H}_R}^- \end{pmatrix}. \end{aligned} \tag{2.13}$$

The absence of bidoublet fields prevent any direct coupling between the left-handed and the right-handed fermions. The only possible Yukawa interaction terms would involve the heavy singlet fermions and the light fermions as given below:

$$\begin{aligned} W_Y &= y_u Q\overline{H}_L P - y_d Q H_L N - y_l L H_L E + y_\nu L\overline{H}_L S \\ &+ y_u^c Q^c\overline{H}_R P^c - y_d^c Q^c H_R N^c - y_l^c L^c H_R E^c + y_\nu^c L^c\overline{H}_R S \\ &+ m_u P P^c + m_d N N^c + m_l E E^c + m_\nu S S \end{aligned} \tag{2.14}$$

where y_i and y_i^c represent the 3×3 Yukawa coupling matrices and m_i are the heavy singlet fermions Majorana mass matrices. From parity invariance, the Yukawa matrices must be hermitian while $y_i^c = y_i$ and all m_i must be real. This gives a 2×2 mass matrix for the fermions and helps them get their masses in a way similar to the seesaw mechanism.

The heavy gauge boson masses can be obtained from Eq. (2.11) and Eq. (2.12) by substituting v_1 and v_2 to be zero.

We investigate two variations of this model with and without a singlet Higgs boson since the mass of the lightest CP-even Higgs boson comes out to be very different in the two cases as will be shown later.

2.2.4 E_6 motivated left-right supersymmetric model

This model is motivated by the low energy manifestation of superstring theory where the matter supermultiplets belong to the **27** representation of E_6 group. The particle content of this representation under the subgroup given by $SU(3) \times SU(2) \times SU(2) \times U(1)$ is given as:

$$\begin{aligned} &(u,d)_L : (3,2,1,\frac{1}{3}),\ d_L^c : (\overline{3},1,1,\frac{2}{3}),\ (h^c,u^c)_L : (\overline{3},1,2,-\frac{1}{3}),\ (e^c,n)_L : (1,1,2,1), \\ &\begin{pmatrix} \nu_e & E^c \\ e & N_E^c \end{pmatrix} : (1,2,2,0),\ h_L : (3,1,1-\frac{2}{3}),\ (\nu_E,E)_L : (1,2,1,-1),\ N_L^c : (1,1,1,0), \end{aligned} \tag{2.15}$$

where the numbers in brackets represent their quantum numbers under $SU(3)_c$, $SU(2)_L$, $SU(2)_R$ and $U(1)_{B-L}$ groups respectively. We can define an R-parity quantum number in this case under which the u, d, ν_e, e fields are even while the h, E, ν_E, N_E^c, n fields are odd. The superpartners of these fields have opposite R-parity. The Higgs fields can be identified as:

$$\begin{aligned} H_L(1,2,1,-1) &= \begin{pmatrix} {H_L}^0 \\ {H_L}^- \end{pmatrix} = \begin{pmatrix} \tilde{\nu}_E \\ \tilde{E} \end{pmatrix}, \; H_R(1,1,2,1) = \begin{pmatrix} {H_R}^+ \\ {H_R}^0 \end{pmatrix} = \begin{pmatrix} \tilde{e}^c \\ \tilde{n} \end{pmatrix}, \\ \Phi(1,2,2,0) &= \begin{pmatrix} \phi_1^+ & \phi_2^0 \\ \phi_1^0 & \phi_2^- \end{pmatrix} = \begin{pmatrix} \tilde{E}^c & \tilde{N}_E^c \\ \tilde{\nu}_e & \tilde{e} \end{pmatrix}. \end{aligned} \tag{2.16}$$

The fermions and the gauge bosons have odd and even R-parity respectively, except for the second W boson which must be odd as it links particles of opposite R-parity. A small neutrino mass can be generated by the mixing of the n, ν_E and the N_E^c fields.

The heavy gauge boson masses can be obtained from Eq. (2.11) and Eq. (2.12) by substituting $\overline{v}_R$ to be zero.

2.3 The Left–Right Supersymmetric Model involving Triplet fields

In this section, we concentrate on the Higgs sector of the model, build the superpotential and calculate the mass spectrum for the Higgs bosons and Higgsinos. We look at the neutral CP-even Higgs boson mass and see how it gets modified with respect to the Minimal Supersymmetric Standard Model.

2.3.1 Case with two pair of triplets, a bidoublet and a singlet

We first look at the case with the triplet Higgs fields $\Delta, \overline{\Delta}, \Delta^c, \overline{\Delta}^c$, one bidoublet Higgs field Φ and a singlet Higgs boson S. For a fully realistic model, we need two bidoublet fields to generate the quark mixing but for simplicity we will only use a

single bidoublet for our calculations. This does not significantly affect the Higgs boson masses as will be shown in a later section. The exact structure of the individual fields in these multiplets are given in Eq. (2.2). The most general superpotential terms involving only the Higgs boson fields in this case is given as:

$$\begin{aligned} W &= S\left[\mathrm{Tr}(\lambda\Delta\overline{\Delta}) + \mathrm{Tr}(\lambda^c\Delta^c\overline{\Delta}^c) + \frac{\lambda'}{2}\mathrm{Tr}(\Phi^T\tau_2\Phi\tau_2) - M^2\right] \\ &+ \mathrm{Tr}\left[\mu_1\Delta\overline{\Delta} + \mu_2\Delta^c\overline{\Delta}^c + \frac{\mu}{2}\left(\Phi^T\tau_2\Phi\tau_2\right)\right] + \frac{\mu_S}{2}S^2, \end{aligned} \tag{2.17}$$

where $\lambda^c = \lambda^*$, $\mu_1 = \mu_2^*$ and λ', M^2, μ and μ_S are real from parity invariance.

The Higgs potential consists of the F-term, D-term and soft supersymmetry-breaking terms, and is written as:

$$V_{Higgs} = V_F + V_D + V_{Soft}. \tag{2.18}$$

In this case, the relevant terms in the Higgs potential are given by:

$$\begin{aligned} V_F &= \mathrm{Tr}\left|(\lambda\Delta\overline{\Delta}) + (\lambda^*\Delta^c\overline{\Delta}^c) + \frac{\lambda'}{2}(\Phi^T\tau_2\Phi\tau_2) - M^2 + \mu_S S\right|^2 + \mathrm{Tr}\left|\mu\Phi + \lambda' S\Phi\right|^2 \\ &+ \mathrm{Tr}\left[\left|\mu_1\Delta + \lambda S\Delta\right|^2 + \left|\mu_1\overline{\Delta} + \lambda S\overline{\Delta}\right|^2 + \left|\mu_2\Delta^c + \lambda^* S\Delta^c\right|^2\right. \\ &+ \left.\left|\mu_2\overline{\Delta}^c + \lambda^* S\overline{\Delta}^c\right|^2\right], \end{aligned} \tag{2.19}$$

$$\begin{aligned} V_D &= \frac{g_L^2}{8}\sum_{a=1}^{3}\left|\mathrm{Tr}(2\Delta^\dagger\tau_a\Delta + 2\overline{\Delta}^\dagger\tau_a\overline{\Delta} + \Phi^\dagger\tau_a\Phi)\right|^2 \\ &+ \frac{g_R^2}{8}\sum_{a=1}^{3}\left|\mathrm{Tr}(2\Delta^{c\dagger}\tau_a\Delta^c + 2\overline{\Delta^c}^\dagger\tau_a\overline{\Delta}^c + \Phi^\dagger\tau_a\Phi)\right|^2 \\ &+ \frac{g_V^2}{2}\left|\mathrm{Tr}(\Delta^\dagger\Delta - \overline{\Delta}^\dagger\overline{\Delta} - \Delta^{c\dagger}\Delta^c + \overline{\Delta^c}^\dagger\overline{\Delta}^c)\right|^2, \end{aligned} \tag{2.20}$$

$$\begin{aligned} V_{Soft} &= m_1^2\mathrm{Tr}(\Delta^{c\dagger}\Delta^c) + m_2^2\mathrm{Tr}(\overline{\Delta}^{c\dagger}\overline{\Delta}^c) + m_3^2\mathrm{Tr}(\Delta^\dagger\Delta) + m_4^2\mathrm{Tr}(\overline{\Delta}^\dagger\overline{\Delta}) \\ &+ m_S^2|S|^2 + m_5^2\mathrm{Tr}(\Phi^\dagger\Phi) + \left[\lambda A_\lambda S\mathrm{Tr}(\Delta\overline{\Delta} + \Delta^c\overline{\Delta}^c) + h.c.\right] \\ &+ \left[\lambda' A_{\lambda'} S\mathrm{Tr}(\Phi^T\tau_2\Phi\tau_2) + h.c.\right] + (\lambda C_\lambda M^2 S + h.c.) + \left(\mu_S B_S S^2 + h.c.\right) \\ &+ \left[\mu_1 B_1\mathrm{Tr}\left(\Delta\overline{\Delta}\right) + \mu_2 B_2\mathrm{Tr}\left(\Delta^c\overline{\Delta}^c\right) + \mu B\mathrm{Tr}\left(\Phi^T\tau_2\Phi\tau_2\right) + h.c.\right]. \end{aligned} \tag{2.21}$$

We use this potential to calculate the Higgs boson mass-squared matrices for the charged, neutral CP-even and neutral CP-odd Higgs bosons. The vacuum structure

that we choose is given by:

$$\langle \Delta^c \rangle = \begin{pmatrix} 0 & v_R \\ 0 & 0 \end{pmatrix}, \ \langle \overline{\Delta}^c \rangle = \begin{pmatrix} 0 & 0 \\ \overline{v}_R e^{i\phi_R} & 0 \end{pmatrix}, \ \langle \Phi \rangle = \begin{pmatrix} 0 & v_2 \\ v_1 e^{i\phi_1} & 0 \end{pmatrix}, \langle S \rangle = v_S e^{i\phi_S}. \tag{2.22}$$

while the Δ and $\overline{\Delta}$ fields do not get any vacuum expectation values(or VEV). For simplicity we assume $\phi_R = 0$, $\phi_1 = 0$ and $\phi_S = 0$. This choice of phases negates the mixing between the scalar and the pseudo-scalar Higgs bosons but does not significantly affect the mass of the lightest CP-even Higgs boson. The values of v_R and $\overline{v}_R$ are of the order of the right-handed symmetry breaking while v_1 and v_2 are of electroweak scale and hence $v_R, \overline{v}_R >> v_1, v_2$. We first look at the CP-even Higgs boson which is the main focus of this chapter. To easily identify the field corresponding to the lightest eigenvalue, we take a linear combination of the Higgs fields so that only two of the newly defined fields get a non-zero vacuum expectation value – one at the high right-handed symmetry breaking scale and the other at the electroweak symmetry breaking scale. The field redefinition that we use is given as:

$$\rho_1 = \frac{v_1\phi_1^0 + v_2\phi_2^0}{\sqrt{v_1^2+v_2^2}}, \ \rho_2 = \frac{v_2\phi_1^0 - v_1\phi_2^0}{\sqrt{v_1^2+v_2^2}}, \ \rho_3 = \frac{v_R\delta^{c0} + \overline{v}_R\overline{\delta}^{c0}}{\sqrt{v_R^2+\overline{v}_R^2}}, \ \rho_4 = \frac{\overline{v}_R\delta^{c0} - v_R\overline{\delta}^{c0}}{\sqrt{v_R^2+\overline{v}_R^2}}. \tag{2.23}$$

In this rotated basis we calculate the mass matrix subject to the following minimization conditions:

$$\begin{aligned}
0 =& v_1[4m_5^2 + g_L^2(-v_2^2+v_1^2) + g_R^2(-v_2^2+v_1^2-2v_R^2+2\overline{v}_R^2)] - 8\lambda' A_{\lambda'} v_2 v_S - 8\mu B v_2 \\
&+ 4\lambda' v_2(M^2 - \lambda v_R\overline{v}_R + \lambda' v_1 v_2 - \mu_S v_S) + 4v_1(\mu + \lambda' v_S)^2, \\
0 =& v_2[4m_5^2 + g_L^2(v_2^2-v_1^2) + g_R^2(v_2^2-v_1^2+2v_R^2-2\overline{v}_R^2)] - 8\lambda' A_{\lambda'} v_1 v_S - 8\mu B v_1 \\
&+ 4\lambda' v_1(M^2 - \lambda v_R\overline{v}_R + \lambda' v_1 v_2 - \mu_S v_S) + 4v_2(\mu + \lambda' v_S)^2, \\
0 =& 2m_1^2 v_R + g_R^2 v_R(-v_1^2+v_2^2+2v_R^2-2\overline{v}_R^2) + 2[g_V^2 v_R(v_R^2-\overline{v}_R^2) + \lambda A_\lambda \overline{v}_R v_S + \mu_2 B_2 \overline{v}_R \\
&+ v_R(\lambda v_S + \mu_2)^2 + \lambda\overline{v}_R(-M^2 + \lambda v_R\overline{v}_R - \lambda' v_1 v_2 + \mu_S v_S),
\end{aligned}$$

$$
\begin{aligned}
0 =& 2m_2^2\overline{v}_R + g_R^2\overline{v}_R(v_1^2 - v_2^2 - 2v_R^2 + 2\overline{v}_R^2) + 2[g_V^2\overline{v}_R(-v_R^2 + \overline{v}_R^2) + \lambda A_\lambda v_R v_S + \mu_2 B_2 v_R \\
&+ \overline{v}_R\left(\lambda v_S + \mu_2\right)^2 + \lambda v_R(-M^2 + \lambda v_R\overline{v}_R - \lambda' v_1 v_2 + \mu_S v_S), \\
0 =& 2m_S^2 v_S + 2C_\lambda M^2\lambda - 4\lambda' A_{\lambda'} v_1 v_2 + 2\lambda A_\lambda v_R\overline{v}_R + 2[\lambda'^2(v_1^2 + v_2^2) + \lambda^2(v_R^2 + \overline{v}_R^2)]v_S + 4\mu_S B_S v_S \\
&2\mu\lambda'(v_1^2 + v_2^2) + 2\lambda\mu_2(v_R^2 + \overline{v}_R^2) + 2\mu_S\left(-M^2 + \lambda v_R\overline{v}_R - \lambda' v_1 v_2 + \mu_S v_S\right). \quad (2.24)
\end{aligned}
$$

We first look at the scalar Higgs boson mass. The neutral components of the left-handed Δ and $\overline{\Delta}$ fields decouple and form a 2×2 mass-squared matrix with heavy eigenvalues while we get a 5×5 mass-squared matrix in the basis $(\mathrm{Re}\rho_1, \mathrm{Re}\rho_2, \mathrm{Re}\rho_3, \mathrm{Re}\rho_4, \mathrm{Re}S)$ where one of the eigenvalues would remain light. The relevant terms in this 5×5 mass-squared matrix are given as:

$$
\begin{aligned}
M_{11} &= \frac{g_L^2(v_1^2 - v_2^2)^2 + g_R^2(v_1^2 - v_2^2)^2 + 8v_1^2 v_2^2\lambda'^2}{2(v_1^2 + v_2^2)}, \\
M_{12} &= \frac{v_1 v_2(v_1^2 - v_2^2)(g_L^2 + g_R^2 - 2\lambda'^2)}{(v_1^2 + v_2^2)}, \\
M_{13} &= \frac{-g_R^2(v_1^2 - v_2^2)(v_R^2 - \overline{v}_R^2) - 4\lambda\lambda' v_1 v_2 v_R\overline{v}_R}{\sqrt{(v_1^2 + v_2^2)(v_R^2 + \overline{v}_R^2)}}, \\
M_{14} &= -\frac{2[g_R^2(v_1^2 - v_2^2)v_R\overline{v}_R - \lambda\lambda' v_1 v_2(v_R^2 - \overline{v}_R^2)]}{\sqrt{(v_1^2 + v_2^2)(v_R^2 + \overline{v}_R^2)}}, \\
M_{15} &= \frac{2\lambda'[-2A_{\lambda'} v_1 v_2 + (v_1^2 + v_2^2)(v_S\lambda' + \mu) - \mu_S v_1 v_2]}{\sqrt{v_1^2 + v_2^2}}, \\
M_{22} &= \Big[(2g_L^2 + 2g_R^2)v_1^2 v_2^2 + 2m_5^2(v_1^2 + v_2^2) + \lambda'^2(v_1^2 - v_2^2)^2 + 2\lambda'^2 v_S^2(v_1^2 + v_2^2) \\
&+ 4\lambda'\mu v_S(v_1^2 + v_2^2) + 2\mu^2(v_1^2 + v_2^2)\Big]/(v_1^2 + v_2^2), \\
M_{23} &= \frac{2\left[g_R^2 v_1 v_2(-v_R^2 + \overline{v}_R^2) + \lambda\lambda'(v_1^2 - v_2^2)v_R\overline{v}_R\right]}{\sqrt{v_1^2 + v_2^2}\sqrt{v_R^2 + \overline{v}_R^2}}, \\
M_{24} &= \frac{-4g_R^2 v_1 v_2 v_R\overline{v}_R - \lambda\lambda'(v_1^2 - v_2^2)(v_R^2 - \overline{v}_R^2)}{\sqrt{v_1^2 + v_2^2}\sqrt{v_R^2 + \overline{v}_R^2}}, \\
M_{25} &= \frac{\lambda'(v_1^2 - v_2^2)(2A_{\lambda'} + \mu_S)}{\sqrt{v_1^2 + v_2^2}}, \\
M_{33} &= \frac{2\left[(g_R^2 + g_V^2)\left(v_R^2 - \overline{v}_R^2\right)^2 + 2\lambda^2 v_R^2\overline{v}_R^2\right]}{v_R^2 + \overline{v}_R^2}, \\
M_{34} &= \frac{2v_R\overline{v}_R(v_R^2 - \overline{v}_R^2)^2\left(2g_R^2 + 2g_V^2 + \lambda^2\right)}{v_R^2 + \overline{v}_R^2},
\end{aligned}
$$

$$
\begin{aligned}
M_{35} &= \frac{2\lambda\left[A_\lambda v_R \overline{v}_R + v_R^2(\lambda v_S + \mu_2) + \overline{v}_R^2(\lambda v_S + \mu_2) + v_R \overline{v}_R \mu_S\right]}{\sqrt{v_R^2 + \overline{v}_R^2}}, \\
M_{44} &= \left[8(g_R^2 + g_V^2) v_R^2 \overline{v}_R^2 + (m_1^2 + m_2^2)(v_R^2 + \overline{v}_R^2) + \lambda^2 (v_R^2 - \overline{v}_R^2)^2\right. \\
&+ \left. 2(\lambda v_S + \mu_2)^2 (v_R^2 + \overline{v}_R^2)\right] / (v_R^2 + \overline{v}_R^2), \\
M_{45} &= -\frac{(v_R^2 - \overline{v}_R^2)\lambda(A_\lambda + \mu_S)}{\sqrt{v_R^2 + \overline{v}_R^2}}, \\
M_{55} &= m_S^2 + \lambda'^2 (v_1^2 + v_2^2) + \lambda^2 (v_R^2 + \overline{v}_R^2) + \mu_S^2 + 2\mu_S B_S.
\end{aligned} \tag{2.25}
$$

From our choice of basis, we can guess that the M_{11} element of the mass-matrix along with the corrections from the off-diagonal elements would approximately be the lightest eigenvalue for this matrix. We calculate the corrections to lightest eigenvalue coming from the off-diagonal M_{12}, M_{13}, M_{14} and M_{15} elements. It can be seen that the M_{12} element is proportional to the square of the light vev while the diagonal M_{22} element comes out to be proportional to the square of the heavy vev. Hence the M_{12} term gives a negligible correction to the lightest eigenvalue. Further we choose parameters λ', $A_{\lambda'}$ and A_λ such that they make M_{13}, M_{15} and M_{35} zero respectively. Using this choice of parameters we calculate the correction and it can be shown that in the limit where the soft supersymmetry breaking term m_1 is much bigger than the right-handed symmetry breaking scale, the contribution vanishes and the M_{11} is the lightest mass eigenvalue for this case [†]. This gives us:

$$
M_{h_{tree}}^2 = 2M_W^2 \cos^2 2\beta + \lambda^2 v^2 \sin^2 2\beta, \tag{2.26}
$$

where $\tan\beta = \frac{v_1}{v_2}$ and $v^2 = v_1^2 + v_2^2$.

Including the radiative corrections from the top and stop sector, the Higgs boson mass is:

$$
M_h^2 = (2M_W^2 \cos^2 2\beta + \lambda^2 \sin^2 2\beta)\Delta_1 + \Delta_2 \tag{2.27}
$$

[†]If we choose μ_S to be much greater than all the other mass scales in the model, we get back the familiar result where the tree level CP-even neutral Higgs boson mass is bound by M_Z.

where

$$\begin{aligned}\Delta_1 &= \left(1 - \frac{3}{8\pi^2}\frac{m_t^2}{v^2}t\right), \\ \Delta_2 &= \frac{3}{4\pi^2}\frac{m_t^4}{v^2}\left[\frac{1}{2}\tilde{X}_t + t + \frac{1}{16\pi^2}\left(\frac{3}{2}\frac{m_t^2}{v^2} - 32\pi\alpha_3\right)\left(\tilde{X}_t t + t^2\right)\right], \end{aligned} \tag{2.28}$$

and m_t is the top running mass, $v = \sqrt{v_1^2 + v_2^2} \approx 174$ GeV, α_3 is the running QCD coupling, $\tilde{X}_t$ is stop squark mixing parameter, and $t = \log\frac{M_S^2}{M_t^2}$ with M_t being the top pole mass and M_S being the geometric mean of the two stop squark masses.

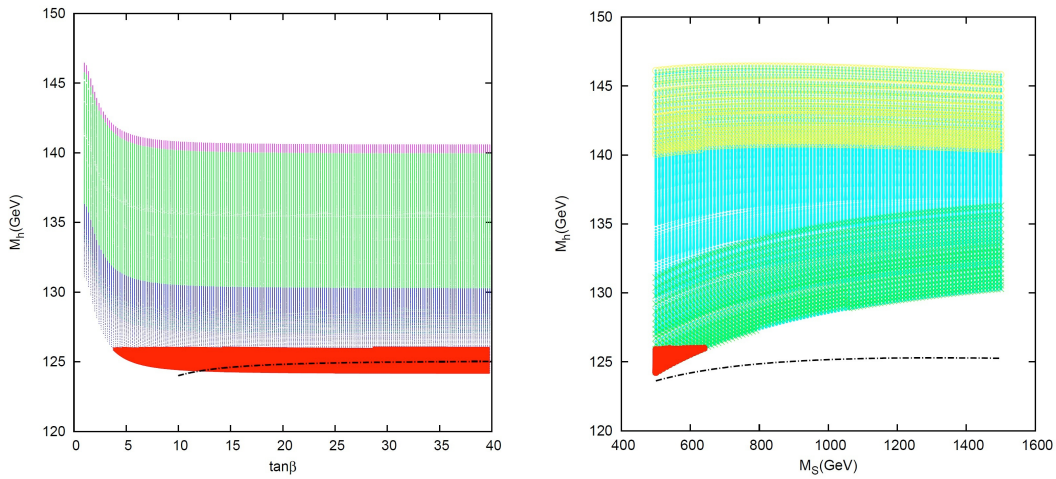

Figure 2.1: *(a) Variation of Higgs boson mass with* $\tan\beta$*, (b) Higgs boson mass as a function of* M_S

The Higgs boson mass in this case is plotted in Fig. 2.1(a) as a function of $\tan\beta$. The red region in the figure represents the band where the mass is between 124 GeV and 126 GeV. Anything below this has not been included as that will be ruled out by experiments. Any point above this can always be lowered by choosing a different set of parameters, as one must remember that we have chosen our parameter space so as to maximize the lightest Higgs boson mass. The light blue region represents the area where the stop squark mixing is minimum i.e. $X_t = 0$ while the pink upper region is for maximal mixing where $X_t = 6$. The green region is for all values of Higgs mass greater than 126 GeV and it is overlapped by the blue and the pink region.

Fig. 2.1(b) represents the Higgs mass and as a function M_S in Fig. 2.1(b). Again the red band is where the Higgs boson mass is between 124 GeV and 126 GeV, green region is for $X_t = 0$, yellow region represents $X_t = 6$ and blue region is for all values of Higgs mass greater than 126 GeV which is overlapped by the green and the yellow regions. The black dotted line in each case represents the MSSM Higgs mass. We can see that a Higgs mass of 124 GeV can be very easily achieved in this case for a very small mass of stop squark and even for minimal mixing between them.

The 2×2 mass-squared matrix corresponding to the neutral left-handed triplet scalar Higgs fields in the original basis is given as

$$\begin{bmatrix} m_3^2 + \frac{g_L^2}{2}(v_1^2 - v_2^2) + g_V^2(-v_R^2 + \overline{v}_R^2) + (\lambda v_S + \mu_1)^2 & \lambda(M^2 - \lambda v_R \overline{v}_R + \lambda' v_1 v_2 - \mu_S v_S) - \lambda A_\lambda v_S - \mu_1 B_1 \\ \lambda(M^2 - \lambda v_R \overline{v}_R + \lambda' v_1 v_2 - \mu_S v_S) - \lambda A_\lambda v_S - \mu_1 B_1 & m_4^2 - \frac{g_L^2}{2}(v_1^2 - v_2^2) + g_V^2(v_R^2 - \overline{v}_R^2) + (\lambda v_S + \mu_1)^2 \end{bmatrix} \tag{2.29}$$

We now look at the pseudo-scalar Higgs boson masses in this model. The structure of this sector is very similar to the scalar Higgs boson in the sense that the left-handed triplet fields decouple to form a 2×2 matrix which is exactly the same as given in Eq. (2.29) while the imaginary component of the other neutral Higgs bosons form a 5×5 matrix. We choose a basis given as

$$g_1 = \frac{v_1 \phi_1^0 - v_2 \phi_2^0}{\sqrt{v_1^2 + v_2^2}},\ g_2 = \frac{v_R \delta^{c^0} - \overline{v}_R \overline{\delta}^{c^0}}{\sqrt{v_R^2 + \overline{v}_R^2}},\ h_1 = \frac{v_2 \phi_1^0 + v_1 \phi_2^0}{\sqrt{v_1^2 + v_2^2}},\ h_2 = \frac{\overline{v}_R \delta^{c^0} + v_R \overline{\delta}^{c^0}}{\sqrt{v_R^2 + \overline{v}_R^2}}. \tag{2.30}$$

The $\mathrm{Im}g_1$ and $\mathrm{Im}g_2$ fields can be identified as the Goldstone bosons which are absorbed by the Z_R-boson and the Z-boson to make them massive. Integrating out these Goldstone states, the resulting 3×3 matrix in the basis $(\mathrm{Im}h_2, \mathrm{Im}h_1, \mathrm{Im}S)$ is given as

$$\begin{aligned} M_{11} &= m_1^2 + m_2^2 + \lambda^2(v_R^2 + \overline{v}_R^2 + 2v_S^2) + 2\mu_2(2\lambda v_s + \mu_2), \\ M_{12} &= \lambda\lambda' \sqrt{(v_1^2 + v_2^2)(v_R^2 + \overline{v}_R^2)}, \\ M_{13} &= \lambda(\mu_S - A_\lambda)\sqrt{v_R^2 + \overline{v}_R^2}, \end{aligned}$$

$$
\begin{aligned}
M_{22} &= 2m_5^2 + \lambda'^2(v_1^2 + v_2^2 + 2v_S^2) + 2\mu(2\lambda' v_S + \mu), \\
M_{23} &= \lambda'(2A_{\lambda'} - \mu_S)\sqrt{v_1^2 + v_2^2}, \\
M_{33} &= m_S^2 + \lambda^2(v_R^2 + \overline{v}_R^2) + \lambda'^2(v_1^2 + v_2^2) - \mu_S(2B_S - \mu_S).
\end{aligned} \tag{2.31}
$$

The charged Higgs boson sector has six singly-charged Higgs boson fields in this model. Their mass-squared matrix can be split into two block diagonal matrices. There is a 2×2 matrix corresponding to the δ^+ and $\overline{\delta}^-$ fields which in its original basis is given as

$$
\begin{pmatrix}
g_V^2(\overline{v}_R^2 - v_R^2) + m_3^2 + \mu_1^2 & B_1\mu_1 \\
B_1\mu_1 & g_V^2(v_R^2 - \overline{v}_R^2) + m_4^2 + \mu_1^2
\end{pmatrix}. \tag{2.32}
$$

The other 4×4 block has two Goldstone bosons which are absorbed by W_R and W gauge bosons to get mass. The Goldstone eigenstates can be identified as

$$
g_1^+ = \frac{v_1\phi_1^+ - v_2\phi_2^{-^*}}{\sqrt{v_1^2 + v_2^2}},\ g_2^+ = \frac{\sqrt{2}(v_1^2 + v_2^2)(\overline{v}_R\overline{\delta}^{c^+} + v_R\delta^{c^{-^*}}) + (v_2^2 - v_1^2)(v_2\phi_1^+ + v_1\phi_2^{-^*})}{\sqrt{2(v_1^2 + v_2^2)^2(v_R^2 + \overline{v}_R^2) + (v_2^2 - v_1^2)^2(v_1^2 + v_2^2)}}. \tag{2.33}
$$

In the basis given by

$$
h_1^+ = \frac{v_R\overline{\delta}^{c^+} - \overline{v}_R\delta^{c^{-^*}}}{\sqrt{v_R^2 + \overline{v}_R^2}},\ h_2^+ = \frac{-\sqrt{2}(v_1^2 + v_2^2)(v_2\phi_1^+ + v_1\phi_2^{-^*}) + (v_2^2 - v_1^2)(\overline{v}_R\overline{\delta}^{c^+} + v_R\delta^{c^{-^*}})}{\sqrt{2(v_1^2 + v_2^2)^3 + (v_2^2 - v_1^2)^2(v_R^2 + \overline{v}_R^2)}}, \tag{2.34}
$$

the 2×2 singly-charged Higgs boson mass-squared matrix elements are given as

$$
\begin{aligned}
M_{11} &= -\frac{g_R^2(v_R^2 - \overline{v}_R^2)\left[v_1^4 + 2v_1^2(-v_2^2 + v_R^2 + \overline{v}_R^2) + v_2^4 + 2v_2^2(v_R^2 + \overline{v}_R^2)\right]}{(v_1^2 - v_2^2)(v_R^2 + \overline{v}_R^2)}, \\
M_{12} &= \frac{2g_R^2 v_R\overline{v}_R\sqrt{v_1^4 + 2v_1^2(-v_2^2 + v_R^2 + \overline{v}_R^2) + v_2^2[v_2^2 + 2(v_R^2 + \overline{v}_R^2)]}}{v_R^2 + \overline{v}_R^2}, \\
M_{22} &= \left[g_R^2\left\{v_R^4(-v_1^2 + v_2^2 - 2v_R^2 - 2\overline{v}_R^2) + \overline{v}_R^4(-v_1^2 + v_2^2 + 2v_R^2 + 2\overline{v}_R^2) - 6(v_1^2 - v_2^2)v_R^2\overline{v}_R^2\right\}\right. \\
&+ \left. 4g_V^2(v_R^2\overline{v}_R^4 - v_R^6 - v_R^4\overline{v}_R^2 + \overline{v}_R^6) - 2(m_1^2 - m_2^2)(v_R^2 + \overline{v}_R^2)^2\right]/(v_R^4 - \overline{v}_R^4).
\end{aligned} \tag{2.35}
$$

In this case, there is no constraint on the m_3, m_4, μ_1 and B_1. So there is lot of freedom in choosing a parameter space for calculating the masses in the 2×2 sector

corresponding to the Δ and $\overline{\Delta}$ fields. Instead we look at the other sectors and eliminate m_2, m_5, B, B_2 and C_λ from the minimization conditions given in Eq. (2.24). We had also fixed the values of λ', A_λ and $A_{\lambda'}$ when we were calculating the scalar Higgs boson mass. Using all these constraints and choosing $g_R = g_L = 0.653$, $g_V = 0.48$, $\lambda = 0.7$, $v_1 = 30$ GeV, $v_2 = 171$ GeV, $v_R = 2.5$ TeV, $\overline{v}_R = 2$ TeV, $m_1 = 4$ TeV, $\mu_2 = 2$ TeV, $\mu = 1$ TeV, $\mu_S = 2$ TeV, $m_S = 2$ TeV, $v_S = 800$ GeV and $B_S = 1$ TeV, we get the numerical values of the charged Higgs boson mass (denoted by $M_{h_i^+}$) for this choice of parameters are $M_{h_3^+} = 8$ TeV and $M_{h_4^+} = 1.43$ TeV while the masses of the pseudo-scalar Higgs bosons (denoted by H_{A_i}) are $M_{A_3} = 7.86$ TeV, $M_{A_4} = 929$ GeV and $M_{A_5} = 1.19$ TeV.

Chargino and Neutralino masses

The particle spectrum of this model is much richer compared to the Minimal Supersymmetric Standard Model and hence the study of the chargino and neutralino masses is crucial for determining the lightest supersymmetric particle. The higgsino and the gauginos mix to form the chargino and the neutralino. The chargino mass term in this case is written as

$$\mathcal{L}_{ch} = -\frac{1}{2}\begin{pmatrix}\widetilde{\delta}^{c^-} & \widetilde{\overline{\delta}}^{-} & \widetilde{\phi}_2^- & \lambda_R^- & \lambda_L^-\end{pmatrix}\begin{pmatrix}\mu_2+\lambda^* v_S & 0 & 0 & -\sqrt{2}g_R v_R & 0\\ 0 & \mu_1+\lambda v_S & 0 & 0 & 0\\ 0 & 0 & \mu+\lambda' v_S & g_R v_2 & g_L v_2\\ \sqrt{2}g_R\overline{v}_R & 0 & g_R v_1 & M_R & 0\\ 0 & 0 & g_L v_1 & 0 & M_L\end{pmatrix}\begin{pmatrix}\widetilde{\overline{\delta}}^{c^+}\\ \widetilde{\delta}^{+}\\ \widetilde{\phi}_1^+\\ \lambda_R^+\\ \lambda_L^+\end{pmatrix}, \tag{2.36}$$

and the neutralino mass matrix in the basis $\begin{pmatrix}\widetilde{\delta}^{c^0} & \widetilde{\overline{\delta}}^{c^0} & \widetilde{\delta}^0 & \widetilde{\overline{\delta}}^0 & \widetilde{\phi}_1^0 & \widetilde{\phi}_2^0 & \lambda_0 & \lambda_{R_3} & \lambda_{L_3} & \widetilde{S}\end{pmatrix}$

is given as

$$\begin{pmatrix}
0 & \mu_2+\lambda^* v_S & 0 & 0 & 0 & 0 & -\sqrt{2}g_V v_R & \sqrt{2}g_R v_R & 0 & \lambda^*\overline{v}_R \\
\mu_2+\lambda^* v_S & 0 & 0 & 0 & 0 & 0 & \sqrt{2}g_V \overline{v}_R & -\sqrt{2}g_R \overline{v}_R & 0 & \lambda^* v_R \\
0 & 0 & 0 & \mu_1+\lambda v_S & 0 & 0 & 0 & 0 & 0 & 0 \\
0 & 0 & \mu_1+\lambda v_S & 0 & 0 & 0 & 0 & 0 & 0 & 0 \\
0 & 0 & 0 & 0 & 0 & -\mu-\lambda' v_S & 0 & -\frac{g_R v_1}{\sqrt{2}} & -\frac{g_L v_1}{\sqrt{2}} & -\lambda' v_2 \\
0 & 0 & 0 & 0 & -\mu-\lambda' v_S & 0 & 0 & \frac{g_R v_2}{\sqrt{2}} & \frac{g_L v_2}{\sqrt{2}} & -\lambda' v_1 \\
-\sqrt{2}g_V v_R & \sqrt{2}g_V \overline{v}_R & 0 & 0 & 0 & 0 & M_1 & 0 & 0 & 0 \\
\sqrt{2}g_R v_R & -\sqrt{2}g_R \overline{v}_R & 0 & 0 & -\frac{g_R v_1}{\sqrt{2}} & \frac{g_R v_2}{\sqrt{2}} & 0 & M_R & 0 & 0 \\
0 & 0 & 0 & 0 & -\frac{g_L v_1}{\sqrt{2}} & \frac{g_L v_2}{\sqrt{2}} & 0 & 0 & M_L & 0 \\
\lambda^* \overline{v}_R & \lambda^* v_R & 0 & 0 & -\lambda' v_2 & -\lambda' v_1 & 0 & 0 & 0 & \mu_S
\end{pmatrix}. \tag{2.37}$$

2.3.2 Case with two pair of triplets, a bidoublet and a heavy singlet

We now look at the case where the single Higgs S is heavy and can be integrate it out from the model to give the following superpotential:

$$W = \mu_1 \mathrm{Tr}(\Delta\overline{\Delta}) + \mu_2 \mathrm{Tr}(\Delta^c\overline{\Delta}^c) + \epsilon \mathrm{Tr}\left[\Delta^c\overline{\Delta}^c\right]^2 + \frac{1}{2}\mu \mathrm{Tr}(\Phi^T\tau_2\Phi\tau_2). \tag{2.38}$$

Here ϵ is proportional to $1/M_S$ with M_S being the scale at which the singlet is integrated out. Since ϵ is very small, we only kept the $\epsilon \mathrm{Tr}(\Delta^c\overline{\Delta}^c)^2$ term in the superpotential as other terms will have no significant effect to the lightest CP-even Higgs boson mass.

The D-term of the Higgs potential is exactly same as in Eq. (2.20) but there will be different contributions to the F-term and the soft supersymmetry breaking terms. They are given by:

$$\begin{aligned}
V_F &= |\mu_1|^2 \mathrm{Tr}(\Delta^\dagger\Delta + \overline{\Delta}^\dagger\overline{\Delta}) + \mathrm{Tr}\left[\left|\mu_2^2\Delta^c + 2\epsilon\Delta^c\overline{\Delta}^c\Delta^c\right|^2 + \left|\mu_2^2\overline{\Delta}^c + 2\epsilon\overline{\Delta}^c\Delta^c\overline{\Delta}^c\right|^2\right] \\
&+ |\mu|^2 \mathrm{Tr}(\Phi^\dagger\Phi), \qquad (2.39) \\
V_{Soft} &= m_1^2 \mathrm{Tr}(\Phi^\dagger\Phi) + \left[B\mu \mathrm{Tr}(\Phi^T\tau_2\Phi\tau_2) + h.c.\right] + m_3^2 \mathrm{Tr}(\Delta^\dagger\Delta) + m_4^2 \mathrm{Tr}(\overline{\Delta}^\dagger\overline{\Delta}) \\
&+ m_5^2 \mathrm{Tr}(\Delta^{c\dagger}\Delta^c) + m_6^2 \mathrm{Tr}(\overline{\Delta}^{c\dagger}\overline{\Delta}^c) + \mathrm{Tr}(B_1\mu_1\Delta\overline{\Delta} + h.c.)
\end{aligned}$$

$$+ \quad \mathrm{Tr}(B_2\mu_2\Delta^c\overline{\Delta}^c + h.c.) + \left[\epsilon D_\epsilon \mathrm{Tr}(\Delta^c\overline{\Delta}^c)^2 + h.c.\right]. \tag{2.40}$$

We use the same basis field redefinition as in Eq. (2.23). The minimization conditions are given as:

$$\begin{aligned}
0 &= -4B\mu v_2 + v_1\left(4{m_1}^2 + {g_L}^2({v_1}^2 - {v_2}^2) + {g_R}^2\left({v_1}^2 - {v_2}^2 + 2{v_R}^2 - 2\overline{v}_R^2\right) + 4\mu^2\right), \\
0 &= -4B\mu v_1 + v_2\left(4{m_1}^2 + {g_L}^2\left(-{v_1}^2 + {v_2}^2\right) + {g_R}^2\left(-{v_1}^2 + {v_2}^2 - 2{v_R}^2 + 2\overline{v}_R^2\right) + 4\mu^2\right), \\
0 &= 2B_2\mu_2\overline{v}_R + \left[2{m_5}^2 + 2{\mu_2}^2 + {g_R}^2\left({v_1}^2 - {v_2}^2\right)\right]v_R + 2\left({g_R}^2 + {g_V}^2\right)v_R\left(-{\overline{v}_R}^2 + v_R^2\right) \\
&+ 4\epsilon\overline{v}_R\left[D_\epsilon v_R\overline{v}_R + \mu_2(3v_R^2 + \overline{v}_R^2) + 2\epsilon v_R\overline{v}_R(2v_R^2 + \overline{v}_R^2)\right], \\
0 &= 2B_2\mu_2 v_R + \left[2{m_6}^2 + 2{\mu_2}^2 + {g_R}^2\left(-{v_1}^2 + {v_2}^2\right)\right]\overline{v}_R + 2\left({g_R}^2 + {g_V}^2\right)\overline{v}_R\left(-{v_R}^2 + \overline{v}_R^2\right) \\
&+ 4\epsilon v_R\left[D_\epsilon v_R\overline{v}_R + \mu_2(v_R^2 + 3\overline{v}_R^2) + 2\epsilon v_R\overline{v}_R(v_R^2 + 2\overline{v}_R^2)\right].
\end{aligned} \tag{2.41}$$

Calculating the neutral CP-even Higgs boson mass-squared matrix subject to these minimization conditions, the matrix elements can be obtained from Eq. (2.25) by putting all the triplet and bidoublet couplings to the singlet Higgs to be zero with some extra terms in the M_{33}, M_{34}, M_{44} elements. The relevant terms in the mass-squared matrix are:

$$\begin{aligned}
M_{11} &= \frac{(g_L^2 + g_R^2)(v_1^2 - v_2^2)^2}{2(v_1^2 + v_2^2)}, \\
M_{13} &= \frac{g_R^2(v_R^2 - \overline{v}_R^2)(v_1^2 - v_2^2)}{\sqrt{(v_1^2 + v_2^2)(v_R^2 + \overline{v}_R^2)}}, \\
M_{14} &= \frac{2g_R^2 v_R\overline{v}_R(v_1^2 - v_2^2)}{\sqrt{(v_1^2 + v_2^2)(v_R^2 + \overline{v}_R^2)}}, \\
M_{33} &= \frac{2(g_R^2 + g_V^2)v_R^3 - B_2\mu_2\overline{v}_R - 2\epsilon\overline{v}_R\left[\mu_2(\overline{v}_R^2 - 3v_R^2) - 8\epsilon v_R^3\overline{v}_R\right]}{v_R},
\end{aligned} \tag{2.42}$$

$$\begin{aligned}
M_{34} &= B_2\mu_2 - 2(g_R^2 + g_V^2)v_R\overline{v}_R + \epsilon\left[3\mu_2(v_R^2 + \overline{v}_R^2) + 2v_R\overline{v}_R(D_\epsilon + 4\epsilon(v_R^2 + \overline{v}_R^2)\right], \\
M_{44} &= \frac{2(g_R^2 + g_V^2)\overline{v}_R^3 - B_2\mu_2 v_R + 2\epsilon v_R\left[\mu_2(3\overline{v}_R^2 - v_R^2) + 8\epsilon\overline{v}_R^3 v_R\right]}{\overline{v}_R}.
\end{aligned} \tag{2.43}$$

We calculate the contribution of the off-diagonal (M_{13}, M_{14}) entries in the mass-squared matrix to the lightest eigenvalue using the seesaw formula. For simplicity we

take the approximation $D_\epsilon = 0$ and we get the following result:

$$M^2_{h_{tree}} = 2M^2_W \cos^2 2\beta \left[1 - \frac{x}{2\left(\frac{g_R^4 x}{g_R^2 - g'^2} + y\right)}\right] \tag{2.44}$$

where

$$x = B_2\mu_2(v_R^2 - \overline{v}_R^2)^2 + 2\epsilon(v_R^2 + \overline{v}_R^2)\left[\mu_2(v_R^4 - 10v_R^2\overline{v}_R^2 + \overline{v}_R^4) - 24\epsilon v_R^3\overline{v}_R^3\right],$$

$$y = 8v_R\overline{v}_R\epsilon(B_2\mu_2^2(v_R^2 + \overline{v}_R^2) + \mu_2^2[3v_R^4 + 2v_R^2\overline{v}_R^2 + 3\overline{v}_R^4)\epsilon + 2\mu_2\overline{v}_R(7v_R^5 + 6v_R^3\overline{v}_R^2 + 7v_R\overline{v}_R^4)\epsilon^2$$
$$+ v_R\overline{v}_R\epsilon(3m_8^2(v_R^2 + \overline{v}_R^2) + 16v_R\overline{v}_R(v_R^4 + v_R^2\overline{v}_R^2 + \overline{v}_R^4)\epsilon^2],$$

$\tan\beta = \frac{v_1}{v_2}$ and $g_R = g_L$. This result shows that the lightest CP-even Higgs boson mass has an upper limit of $\sqrt{2}M_W$ in this case which can be realized if $x = 0$.[‡] So

$$M^2_{h_{tree}} = 2M^2_W \cos^2 2\beta. \tag{2.45}$$

Including the one and two loop corrections from the top quark and stop squark, we get:

$$M^2_{h_{max}} = (2M^2_W \cos^2 2\beta)\Delta_1 + \Delta_2, \tag{2.46}$$

where Δ_1 and Δ_2 are defined in Eq. (2.28).

The Higgs boson mass is plotted in Fig 2.2(a) as a function of $\tan\beta$. The red region in the figure represents the band where the mass is between 124 GeV and 126 GeV. The light blue region represents the area where the stop squark mixing is minimum i.e. $X_t = 0$ while the pink upper region is for maximal mixing where $X_t = 6$. The green region is for all values of Higgs mass greater than 126 GeV and it is overlapped by the blue and the pink region. Fig. 2.2(b) represents the Higgs mass and as a function M_S. Again the red band is where the Higgs boson mass is between 124 GeV and 126 GeV, green region is for $X_t = 0$, yellow region represents

[‡]If we consider $\overline{v}_R^2 - v_R^2 \sim M^2_{SUSY}$ and $v_R, \overline{v}_R >> M_{SUSY}$, we get an upper limit of M_Z for the lightest scalar Higgs boson mass.

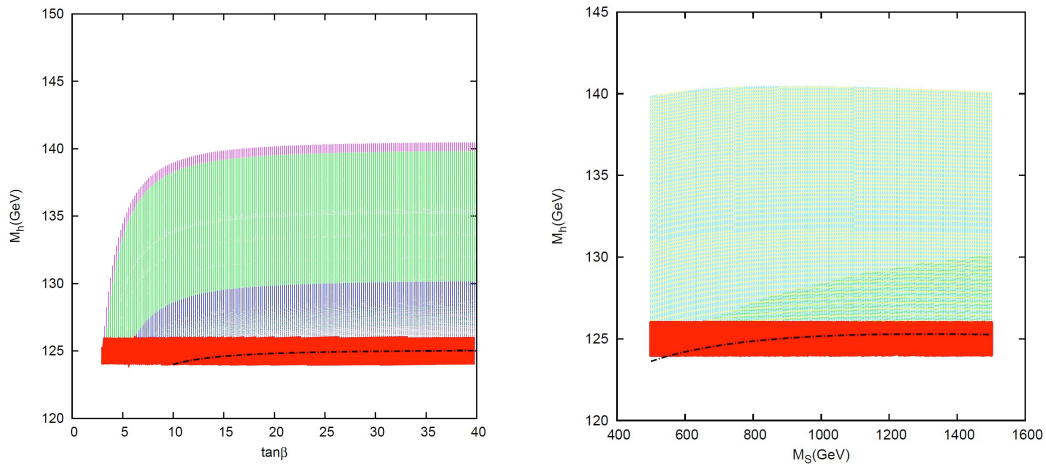

Figure 2.2: *(a) Variation of Higgs boson mass with* $\tan\beta$*, (b) Higgs boson mass as a function of* M_S

$X_t = 6$ and blue region is for all values of Higgs mass greater than 126 GeV which is overlapped by the green and the yellow regions. The black dotted line in each case represents the MSSM Higgs mass.

The pseudo-scalar mass-squared matrix is again two 2×2 blocks which can be obtained by putting all the singlet couplings to zero in Eq. (2.29) and Eq. (2.31).

The charged Higgs boson mass-squared matrix is exactly the same as in Eq. (2.35) with some extra terms which become zero when we take $D_\epsilon = 0$.

Chargino and Neutralino masses

We now look at the chargino and neutralino sector in this case. The chargino basis is exactly the same as in the case discussed in **section 3.1**. The chargino mass

matrix in this case is written as

$$M_{ch} = \begin{pmatrix} \mu_2 + \epsilon v_R \overline{v}_R & 0 & 0 & -\sqrt{2} g_R v_R & 0 \\ 0 & \mu_1 & 0 & 0 & 0 \\ 0 & 0 & \mu & g_R v_2 & g_L v_2 \\ \sqrt{2} g_R \overline{v}_R & 0 & g_R v_1 & M_R & 0 \\ 0 & 0 & g_L v_1 & 0 & M_L \end{pmatrix}, \tag{2.47}$$

and the neutralino mass matrix in the basis $\begin{pmatrix} \widetilde{\delta}^{c^0} & \widetilde{\overline{\delta}}^{c^0} & \widetilde{\delta}^0 & \widetilde{\overline{\delta}}^0 & \widetilde{\phi}_1^0 & \widetilde{\phi}_2^0 & \lambda_0 & \lambda_{R_3} & \lambda_{L_3} \end{pmatrix}$ is given as

$$M_n = \begin{pmatrix} \epsilon \overline{v}_R^2 & \mu_2 + \epsilon v_R \overline{v}_R & 0 & 0 & 0 & 0 & -\sqrt{2} g_V v_R & \sqrt{2} g_R v_R & 0 \\ \mu_2 + \epsilon v_R \overline{v}_R & \epsilon v_R^2 & 0 & 0 & 0 & 0 & \sqrt{2} g_V \overline{v}_R & -\sqrt{2} g_R \overline{v}_R & 0 \\ 0 & 0 & 0 & \mu_1 & 0 & 0 & 0 & 0 & 0 \\ 0 & 0 & \mu_1 & 0 & 0 & 0 & 0 & 0 & 0 \\ 0 & 0 & 0 & 0 & 0 & -\mu & 0 & -\frac{g_R v_1}{\sqrt{2}} & -\frac{g_L v_1}{\sqrt{2}} \\ 0 & 0 & 0 & 0 & -\mu & 0 & 0 & \frac{g_R v_2}{\sqrt{2}} & \frac{g_L v_2}{\sqrt{2}} \\ -\sqrt{2} g_V v_R & \sqrt{2} g_V \overline{v}_R & 0 & 0 & 0 & 0 & M_1 & 0 & 0 \\ \sqrt{2} g_R v_R & -\sqrt{2} g_R \overline{v}_R & 0 & 0 & -\frac{g_R v_1}{\sqrt{2}} & \frac{g_R v_2}{\sqrt{2}} & 0 & M_R & 0 \\ 0 & 0 & 0 & 0 & -\frac{g_L v_1}{\sqrt{2}} & \frac{g_L v_2}{\sqrt{2}} & 0 & 0 & M_L \end{pmatrix}. \tag{2.48}$$

2.3.3 Case with two pair of triplets and a bidoublet

This is a special case of the one discussed in **Section 2.3.1**. We don't have the singlet Higgs and as a result it will be seen that the lightest Higgs boson mass becomes the same as MSSM.

The most general superpotential relevant to our calculation is given by:

$$W = \mu_1 \mathrm{Tr}(\Delta \overline{\Delta}) + \mu_2 \mathrm{Tr}(\Delta^c \overline{\Delta}^c) + \frac{1}{2} \mu \mathrm{Tr}(\Phi^T \tau_2 \Phi \tau_2). \tag{2.49}$$

The D-term in the Higgs potential is exactly the same as given in Eq. (2.20), the F-term can be obtained from Eq. (2.19) by putting all the singlet couplings to zero.

The soft supersymmetry breaking terms are given by:

$$\begin{aligned} V_{Soft} &= m_1^2 \mathrm{Tr}(\Delta^{c\dagger}\Delta^c) + m_2^2 \mathrm{Tr}(\overline{\Delta}^{c\dagger}\overline{\Delta}^c) + m_3^2 \mathrm{Tr}(\Delta^\dagger \Delta) + m_4^2 \mathrm{Tr}(\overline{\Delta}^\dagger \overline{\Delta}) \\ &+ m_5^2 \mathrm{Tr}(\Phi^\dagger \Phi) + \left[B\mu \mathrm{Tr}(\Phi^T \tau_2 \Phi \tau_2) + h.c.\right] \\ &+ \left[B_1 \mu_1 \mathrm{Tr}(\Delta \overline{\Delta}) + h.c.\right] + \left[B_2 \mu_2 \mathrm{Tr}(\Delta^c \overline{\Delta}^c) + h.c.\right]. \end{aligned} \tag{2.50}$$

We use this potential to calculate the Higgs boson mass-squared matrices for the charged, neutral CP-even and neutral CP-odd Higgs bosons. To easily identify the field corresponding to the lightest eigenvalue, we redefine the Higgs fields. This redefinition is the same as in Eq. (2.23).

The minimization conditions and the Higgs mass-squared in this case can again be obtained by putting all the singlet couplings to zero in the model of **Section 2.3.1**.

Calculating the lightest eigenvalue for the CP-even Higgs boson mass-squared matrix we get:

$$M^2_{h_{tree}} = \frac{g_L^4 (g'^2 + g_R^2)(v_1^2 - v_2^2)^2}{2[g_L^2 g_R^2 + g'^2(g_L^2 - g_R^2)](v_1^2 + v_2^2)}. \tag{2.51}$$

If we assume that the $SU(2)_R$ gauge coupling (g_R) is equal to the $SU(2)_L$ gauge coupling (g_L), $\tan\beta = \frac{v_1}{v_2}$ and $v^2 = v_1^2 + v_2^2$, then

$$M^2_{h_{tree}} = \frac{(g_L^2 + g'^2)}{2} v^2 \cos^2 2\beta. \tag{2.52}$$

The mass of the Z boson in this model is $\sqrt{\frac{g_L^2 + g'^2}{2}} v$. So we see that the tree-level lightest CP-even Higgs mass has an upper limit of M_Z. This is same as the case of MSSM.

The charged mass-squared matrix is the same as in Eq. (2.35) while the pseudo-scalar mass-squared matrix is composed of two 2×2 block which can be obtained from Eq. (2.29) and Eq. (2.31) by putting all the singlet couplings to zero.

The chargino mass matrix in this case is a special limit of **Section 2.3.1** obtained by neglecting all the singlet couplings while the neutralino mass matrix is obtained from Eq. (2.48) by putting $\epsilon = 0$.

2.3.4 Case with two pair of triplets and two bidoublets

This case is a realistic model where, unlike previous cases, we can generate the CKM matrices for quarks and leptons. The calculation of the Higgs mass, though shows that the result is exactly the same as the case with only one bidoublet. Due to the complexity of the calculations, we only discuss the neutral CP-even Higgs boson mass in this case and see that it is the same as with one bidoublet. The particle content of the Higgs sector will be exactly as in Eq. (2.2) except in this case $a = 1, 2$.

The superpotential of the model is given as:

$$W = \mu_1 \mathrm{Tr}(\Delta\overline{\Delta}) + \mu_2 \mathrm{Tr}(\Delta^c\overline{\Delta}^c) + \frac{1}{2}\mu_{ab}\mathrm{Tr}(\Phi_a^T\tau_2\Phi_b\tau_2). \tag{2.53}$$

The relevant terms in the Higgs potential is given by:

$$\begin{aligned}
V_F &= |\mu_1|^2\mathrm{Tr}(\Delta^\dagger\Delta + \overline{\Delta}^\dagger\overline{\Delta}) + |\mu_2|^2\mathrm{Tr}(\Delta^{c\dagger}\Delta^c + \overline{\Delta}^{c\dagger}\overline{\Delta}^c) \\
&+ \sum_{a=1}^{2}\mathrm{Tr}|(\mu_{a1}\Phi_1 + \mu_{a2}\Phi_2)|^2, \qquad (2.54) \\
V_D &= \frac{g_L^2}{8}\sum_{a=1}^{3}\left|\mathrm{Tr}(2\Delta^\dagger\tau_a\Delta + 2\overline{\Delta}^\dagger\tau_a\overline{\Delta} + (\Phi_1^\dagger\tau_a\Phi_1) + (\Phi_2^\dagger\tau_a\Phi_2)\right|^2 \\
&+ \frac{g_R^2}{8}\sum_{a=1}^{3}\left|\mathrm{Tr}(2\Delta^{c\dagger}\tau_a\Delta^c + 2\overline{\Delta^c}^\dagger\tau_a\overline{\Delta}^c + (\Phi_1^\dagger\tau_a\Phi_1) + (\Phi_2^\dagger\tau_a\Phi_2)\right|^2 \\
&+ \frac{g_V^2}{2}\left|\mathrm{Tr}(\Delta^\dagger\Delta - \overline{\Delta}^\dagger\overline{\Delta} - \Delta^{c\dagger}\Delta^c + \overline{\Delta^c}^\dagger\overline{\Delta}^c)\right|^2, \qquad (2.55) \\
V_{Soft} &= m_{ab}^2\mathrm{Tr}(\Phi_a^\dagger\Phi_b) + \sum_{a,b=1}^{2}B_{ab}\mu_{ab}\left[\mathrm{Tr}(\Phi_a^T\tau_2\Phi_b\tau_2) + h.c.\right] + m_3^2\mathrm{Tr}(\Delta^\dagger\Delta) + m_4^2\mathrm{Tr}(\overline{\Delta}^\dagger\overline{\Delta}) \\
&+ m_5^2\mathrm{Tr}(\Delta^{c\dagger}\Delta^c) + m_6^2\mathrm{Tr}(\overline{\Delta}^{c\dagger}\overline{\Delta}^c) + [B_1\mu_1\mathrm{Tr}(\Delta\overline{\Delta}) + h.c.] \\
&+ [B_2\mu_2\mathrm{Tr}(\Delta^c\overline{\Delta}^c) + h.c.]. \qquad (2.56)
\end{aligned}$$

We use this Higgs potential for this variation of the LRSUSY model and calculate the mass-squared matrix for the neutral CP-even Higgs boson. The vacuum structure

for this model is given by:

$$\langle \Delta^c \rangle = \begin{pmatrix} 0 & v_R \\ 0 & 0 \end{pmatrix},\ \langle \overline{\Delta}^c \rangle = \begin{pmatrix} 0 & 0 \\ \overline{v}_R & 0 \end{pmatrix},\ \langle \Phi_1 \rangle = \begin{pmatrix} 0 & v_{d_1} \\ v_{u_1} & 0 \end{pmatrix},\ \langle \Phi \rangle = \begin{pmatrix} 0 & v_{d_2} \\ v_{u_2} & 0 \end{pmatrix}. \tag{2.57}$$

The left-handed triplet fields Δ and $\overline{\Delta}$ do not get any VEV. We do a field redefinition with the $\phi^0_{11}, \phi^0_{21}, \phi^0_{12}, \phi^0_{22}$ fields so that only one of the new fields get a non-zero vacuum expectation value. The transformation we use is given by:

$$\begin{aligned} \rho_1 &= \frac{v_{u_1}\phi^0_{11} + v_{d_1}\phi^0_{21} + v_{u_2}\phi^0_{12} + v_{d_2}\phi^0_{22}}{\sqrt{v^2_{u_1} + v^2_{d_1} + v^2_{u_2} + v^2_{d_2}}},\ \rho_2 = \frac{v_{d_1}\phi^0_{11} - v_{u_1}\phi^0_{21}}{\sqrt{v^2_{u_1} + v^2_{d_1}}},\ \rho_3 = \frac{v_{d_2}\phi^0_{21} - v_{u_2}\phi^0_{22}}{\sqrt{v^2_{u_2} + v^2_{d_2}}}, \\ \rho_4 &= \frac{v_{u_1}(v^2_{u_2} + v^2_{d_2})\phi^0_{11} + v_{d_1}(v^2_{u_2} + v^2_{d_2})\phi^0_{21} - v_{u_2}(v^2_{u_1} + v^2_{d_1})\phi^0_{12} - v_{d_2}(v^2_{u_1} + v^2_{d_1})\phi^0_{22}}{\sqrt{(v^2_{u_1} + v^2_{d_1})(v^2_{u_2} + v^2_{d_2})(v^2_{u_1} + v^2_{d_1} + v^2_{u_2} + v^2_{d_2})}}. \end{aligned}$$

The ρ_1 field gets a VEV of $\sqrt{v^2_{u_1} + v^2_{d_1} + v^2_{u_2} + v^2_{d_2}}$, the other fields do not get any VEV. The Δ and $\overline{\Delta}$ fields decouple and we get a 6×6 mass-square matrix in the basis $(\mathrm{Re}\rho_1, \mathrm{Re}\rho_2, \mathrm{Re}\rho_3, \mathrm{Re}\rho_4, \mathrm{Re}\delta^{c0}, \mathrm{Re}\overline{\delta}^{c0})$. The minimization conditions for this case are given in the Appendix. The matrix elements for this case are not quoted here as they are lengthy and this case is not very interesting in terms of the final result which comes out to be exactly as **section 2.3.3**.

Using the minimization conditions and the assumption that the right-handed symmetry breaking scale is much above the electroweak scale, we get the lightest eigenvalue to be:

$$M^2_{h_{tree}} = \frac{(g^2_L + g')\,(v^2_{u_2} - v^2_{d_2} + v^2_{u_1} - v^2_{d_1})^2}{2(v^2_{u_2} + v^2_{d_2} + v^2_{u_1} + v^2_{d_1})} = M^2_Z \cos^2 2\beta \tag{2.58}$$

where $\tan\beta = \frac{\sqrt{(v^2_{u_1} + v^2_{u_2})}}{\sqrt{(v^2_{d_1} + v^2_{d_2})}}$ and $v^2 = \sqrt{v^2_{u_1} + v^2_{d_1} + v^2_{u_2} + v^2_{d_2}}$. We have made the assumption that $g_R = g_L$.

This result is the same as the previous case and gives the tree-level mass of lightest CP-even neutral Higgs boson to be M_Z.

2.4 Inverse seesaw model

The Higgs spectrum of this model is given in Eq. (2.7). The most general superpotential terms needed for calculation of the Higgs boson mass are given as:

$$W = i\mu_1 H_L^T \tau_2 \overline{H}_L + i\mu_1 H_R^T \tau_2 \overline{H}_R + \lambda H_L^T \tau_2 \Phi \tau_2 H_R + \lambda \overline{H}_L^T \tau_2 \Phi \tau_2 \overline{H}_R + \mu \mathrm{Tr}\left[\Phi \tau_2 \Phi^T \tau_2\right]. \tag{2.59}$$

The relevant Higgs potential in this case is given as:

$$\begin{aligned}
V_F &= \mathrm{Tr}\Big[\left|i\mu_1\tau_2\overline{H}_L + \lambda\tau_2\Phi\tau_2 H_R\right|^2 + \left|i\mu_1\tau_2\overline{H}_R + \lambda\tau_2\Phi^T\tau_2 H_L\right|^2 \\
&+ \left|-i\mu_1\tau_2 H_L + \lambda\tau_2\Phi\tau_2\overline{H}_R\right|^2 + \left|-i\mu_1\tau_2 H_R + \lambda\tau_2\Phi^T\tau_2\overline{H}_L\right|^2 \\
&+ \left|\lambda H_R H_L^T + \lambda\overline{H}_R\overline{H}_L^T + 2\mu\phi^T\right|^2\Big], \qquad (2.60) \\
V_D &= \frac{g_L^2}{8}\sum_{a=1}^{3}\left|H_L^\dagger\tau_a H_L + \overline{H}_L^\dagger\tau_a\overline{H}_L + \mathrm{Tr}(\Phi^\dagger\tau_a\Phi)\right|^2 \\
&+ \frac{g_R^2}{8}\sum_{a=1}^{3}\left|H_R^\dagger\tau_a H_R + \overline{H}_R^\dagger\tau_a\overline{H}_R + \mathrm{Tr}(\Phi^\dagger\tau_a\Phi)\right|^2 \\
&+ \frac{g_V^2}{8}\left|H_R^\dagger H_R - \overline{H}_R^\dagger\overline{H}_R - H_L^\dagger H_L + \overline{H}_L^\dagger\overline{H}_L\right|^2, \qquad (2.61) \\
V_{Soft} &= \mathrm{Tr}\Big[m_1^2\left(H_L^\dagger H_L + H_R^\dagger H_L\right) + m_2^2\left(\overline{H}_L^\dagger\overline{H}_L + \overline{H}_R^\dagger\overline{H}_R\right) + m_3^2\Phi^\dagger\Phi \\
&+ \left(\lambda A_\lambda H_L^T\tau_2\Phi\tau_2 H_R + \lambda A_\lambda\overline{H}_L^T\tau_2\Phi\tau_2\overline{H}_R + h.c.\right) + \left(B\mu\Phi^T\tau_2\Phi\tau_2 + h.c.\right) \\
&+ \left(iB_1\mu_1 H_L^T\tau_2\overline{H}_L + iB_1\mu_1 H_R^T\tau_2\overline{H}_R + h.c\right)\Big]. \qquad (2.62)
\end{aligned}$$

The vacuum expectation values of the Higgs fields are given as:

$$\begin{aligned}
\langle H_L\rangle &= \begin{pmatrix} v_L \\ 0 \end{pmatrix}, \langle H_R\rangle = \begin{pmatrix} 0 \\ v_R \end{pmatrix}, \langle \overline{H}_L\rangle = \begin{pmatrix} 0 \\ \overline{v}_L \end{pmatrix}, \\
\langle \overline{H}_R\rangle &= \begin{pmatrix} \overline{v}_R \\ 0 \end{pmatrix}, \langle\Phi\rangle = \begin{pmatrix} 0 & v_2 \\ v_1 & 0 \end{pmatrix}. \qquad (2.63)
\end{aligned}$$

We again choose a rotated basis similar to **section 2.3.4** such that the four Higgs fields getting electroweak vev mix together. Only one of the newly defined fields

now gets a non-zero vacuum value. The right-handed doublets get vacuum values of right-handed symmetry breaking scale. The minimization conditions in this case are given as:

$$
\begin{aligned}
&2m_3^2 v_1 + \frac{v_1}{2}\left[g_L^2\left(v_1^2 - v_2^2 - v_L^2 + \overline{v}_L^2\right) + g_R^2\left(v_1^2 - v_2^2 + v_R^2 - \overline{v}_R^2\right) + 4\lambda^2\left(v_L^2 + v_R^2\right)\right] \\
&- 2\lambda A_\lambda v_L v_R + 2\lambda\mu_1\left(v_L\overline{v}_R - v_R\overline{v}_L\right) + 4\mu\left(\lambda\overline{v}_L\overline{v}_R - Bv_2 + 2\mu v_1\right) = 0, \\
&2m_3^2 v_2 + \frac{v_2}{2}\left[g_L^2\left(-v_1^2 + v_2^2 + v_L^2 - \overline{v}_L^2\right) - g_R^2\left(v_1^2 - v_2^2 + v_R^2 - \overline{v}_R^2\right) + 4\lambda^2\left(\overline{v}_L^2 + \overline{v}_R^2\right)\right] \\
&- 2\lambda A_\lambda \overline{v}_L\overline{v}_R - 2\lambda\mu_1\left(v_L\overline{v}_R - v_R\overline{v}_L\right) + 4\mu\left(\lambda v_L v_R - Bv_1 + 2\mu v_2\right) = 0, \\
&2m_1^2 v_L + \frac{v_L}{2}\left[g_L^2\left(-v_1^2 + v_2^2 + v_L^2 - \overline{v}_L^2\right) + g_V^2\left(v_L^2 - \overline{v}_L^2 - v_R^2 + \overline{v}_R^2\right) + 4\lambda^2\left(v_1^2 + v_R^2\right)\right] \\
&- 2\lambda A_\lambda v_1 v_R + 2\lambda\mu_1\overline{v}_R\left(v_1 - v_2\right) + 2\mu_1^2 v_L + 2B_1\mu_1\overline{v}_L + 4\mu\lambda v_2 v_R = 0, \\
&2m_1^2 v_R + \frac{v_R}{2}\left[g_R^2\left(v_1^2 - v_2^2 + v_R^2 - \overline{v}_R^2\right) + g_V^2\left(-v_L^2 + \overline{v}_L^2 + v_R^2 - \overline{v}_R^2\right) + 4\lambda^2\left(v_1^2 + v_L^2\right)\right] \\
&- 2\lambda A_\lambda v_1 v_L - 2\lambda\mu_1\overline{v}_L\left(v_1 - v_2\right) + 2\mu_1^2 v_R - 2B_1\mu_1\overline{v}_R + 4\mu\lambda v_2 v_L = 0, \\
&2m_2^2\overline{v}_L + \frac{\overline{v}_L}{2}\left[g_L^2\left(v_1^2 - v_2^2 - v_L^2 + \overline{v}_L^2\right) - g_V^2\left(v_L^2 - \overline{v}_L^2 - v_R^2 + \overline{v}_R^2\right) + 4\lambda^2\left(v_2^2 + \overline{v}_R^2\right)\right] \\
&- 2\lambda A_\lambda v_2\overline{v}_R - 2\lambda\mu_1 v_R\left(v_1 - v_2\right) + 2\mu_1^2\overline{v}_L + 2B_1\mu_1 v_L + 4\mu\lambda v_1\overline{v}_R = 0, \\
&2m_2^2\overline{v}_R + \frac{\overline{v}_R}{2}\left[g_R^2\left(-v_1^2 + v_2^2 - v_R^2 + \overline{v}_R^2\right) + g_V^2\left(v_L^2 - \overline{v}_L^2 - v_R^2 + \overline{v}_R^2\right) + 4\lambda^2\left(v_2^2 + \overline{v}_L^2\right)\right] \\
&- 2\lambda A_\lambda v_2\overline{v}_L + 2\lambda\mu_1 v_L\left(v_1 - v_2\right) + 2\mu_1^2\overline{v}_R - 2B_1\mu_1 v_R + 4\mu\lambda v_1\overline{v}_L = 0. \qquad (2.64)
\end{aligned}
$$

The relevant mass-matrix elements in this case are given as:

$$
\begin{aligned}
M_{11} &= \frac{g_R^2\left(v_1^2 - v_2^2\right)^2 + g_V^2\left(v_L^2 - \overline{v}_L^2\right)^2 + g_L^2\left(v_1^2 - v_2^2 - v_L^2 + \overline{v}_L^2\right)^2 + 8\lambda^2\left(v_1^2 v_L^2 + v_2^2\overline{v}_L^2\right)}{2\left(v_1^2 + v_2^2 + v_L^2 + \overline{v}_L^2\right)}, \\
M_{12} &= \frac{v_L\overline{v}_L\left(g_V^2\left(v_L^2 - \overline{v}_L^2\right) + g_L^2\left(-v_1^2 + v_2^2 + v_L^2 - \overline{v}_L^2\right) + 2\left(v_1^2 - v_2^2\right)\lambda^2\right)}{\sqrt{v_L^2 + \overline{v}_L^2}\sqrt{v_1^2 + v_2^2 + v_L^2 + \overline{v}_L^2}}, \\
M_{13} &= \left[v_1\left\{g_V^2 v_L^4 - 2g_V^2 v_L^2\overline{v}_L^2 + g_V^2\overline{v}_L^4 + 2g_L^2 v_L^2\left(-v_1^2 + v_2^2 + v_L^2 - \overline{v}_L^2\right)\right.\right. \\
&- \left.\left. g_R^2\left(v_1^2 - v_2^2\right)\left(v_L^2 + \overline{v}_L^2\right) + 4v_1^2 v_L^2\lambda^2 - 4v_L^4\lambda^2 + 4v_2^2\overline{v}_L^2\lambda^2 - 4v_L^2\overline{v}_L^2\lambda^2\right\}\right] \Big/ \\
&\quad \left(2\sqrt{\left(v_L^2 + \overline{v}_L^2\right)\left(v_1^2 + v_L^2 + \overline{v}_L^2\right)}\sqrt{v_1^2 + v_2^2 + v_L^2 + \overline{v}_L^2}\right), \\
M_{14} &= \left[v_2\left\{g_V^2 v_L^4 - 2g_V^2 v_L^2\overline{v}_L^2 + g_V^2\overline{v}_L^4 + 2g_L^2 v_L^2\left(-v_1^2 + v_2^2 + v_L^2 - \overline{v}_L^2\right)\right.\right. \\
&- \left.\left. g_R^2\left(v_1^2 - v_2^2\right)\left(v_L^2 + \overline{v}_L^2\right) + 4\lambda^2\left(2v_1^2 v_L^2 + v_1^2\overline{v}_L^2 + v_2^2\overline{v}_L^2 + v_L^2\overline{v}_L^2 + \overline{v}_L^4\right)\right\}\right] \Big/
\end{aligned}
$$

$$\left(2\sqrt{v_1^2+v_2^2+v_L^2+\overline{v}_L^2}\sqrt{\left(v_1^2+v_L^2+\overline{v}_L^2\right)\left(v_1^2+v_2^2+v_L^2+\overline{v}_L^2\right)}\right),$$

$$\begin{aligned}
M_{15} &= \left[g_R^2\left(v_1^2-v_2^2\right)v_R+g_V^2\left(-v_L^2+\overline{v}_L^2\right)v_R+4\lambda\left\{-A_\lambda v_1 v_L+\mu_1(-v_1+v_2)\overline{v}_L\right.\right. \\
&+ \left.\left. v_1^2 v_R\lambda+v_L^2 v_R\lambda+2v_2 v_L\mu\right\}\right]/\left(2\sqrt{v_1^2+v_2^2+v_L^2+\overline{v}_L^2}\right), \\
M_{16} &= \left[g_R^2\left(-v_1^2+v_2^2\right)\overline{v}_R+g_V^2\left(v_L^2-\overline{v}_L^2\right)\overline{v}_R+4\lambda\left\{\mu_1(v_1-v_2)v_L-A_\lambda v_2\overline{v}_L+\lambda v_2^2\overline{v}_R\right.\right. \\
&+ \left.\left.\lambda\overline{v}_L^2\overline{v}_R+2\mu v_1\overline{v}_L\right\}\right]/\left(2\sqrt{v_1^2+v_2^2+v_L^2+\overline{v}_L^2}\right). \qquad (2.65)
\end{aligned}$$

All the other elements in the mass matrix are of SUSY breaking scale or the right-handed symmetry breaking scale. The only matrix elements that can provide significant contributions to the lightest eigenvalue comes from M_{15} and M_{16}. We focus on the 3×3 sector formed by $M_{11}, M_{15}, M_{16}, M_{55}, M_{56}, M_{66}$. We choose some of the parameters such that the M_{15} and M_{16} terms become zero and check that we have enough freedom to consistently keep the other eigenvalues of the matrix to be positive. The smallest eigenvalue in this case is the lightest CP-even Higgs boson in the model and is given by:

$$M_{h_{tree}}^2=\frac{g_R^2\left(v_1^2-v_2^2\right)^2+g_V^2\left(v_L^2-\overline{v}_L^2\right)^2+g_L^2\left(v_1^2-v_2^2-v_L^2+\overline{v}_L^2\right)^2+8\lambda^2\left(v_1^2v_L^2+v_2^2\overline{v}_L^2\right)}{2\left(v_1^2+v_2^2+v_L^2+\overline{v}_L^2\right)}. \qquad (2.66)$$

We define $v_1 = v\sin\beta\cos\phi$, $v_2 = v\cos\beta\sin\psi$, $v_L = v\cos\beta\cos\psi$, $\overline{v}_L = v\sin\beta\sin\phi$ and $g_R = g_L$. Now maximizing this resulting expression with respect to ϕ and ψ gives

$$M_{h_{tree}}^2 = 2M_W^2\sin^4\beta+\frac{M_W^4}{2M_W^2-M_Z^2}\cos^4\beta-\frac{M_W^2}{2}\sin^2 2\beta+\lambda^2v^2\sin^2 2\beta. \qquad (2.67)$$

The Higgs boson mass including the one and two loop corrections from the top and stop sector is given as:

$$\begin{aligned}
M_{h_{max}}^2 &= \left(2M_W^2\sin^4\beta+\frac{M_W^4}{2M_W^2-M_Z^2}\cos^4\beta-\frac{M_W^2}{2}\sin^2 2\beta+\lambda^2v^2\sin^2 2\beta\right)\Delta_1 \\
&+ \Delta_2, \qquad (2.68)
\end{aligned}$$

where Δ_1 and Δ_2 are defined in Eq. (2.28).

The Higgs boson mass is plotted in Fig 2.3(a) as a function of $\tan\beta$.The red region in the figure represents the band where the mass is between 124 GeV and 126 GeV. The light blue region represents the area where the stop squark mixing is minimum

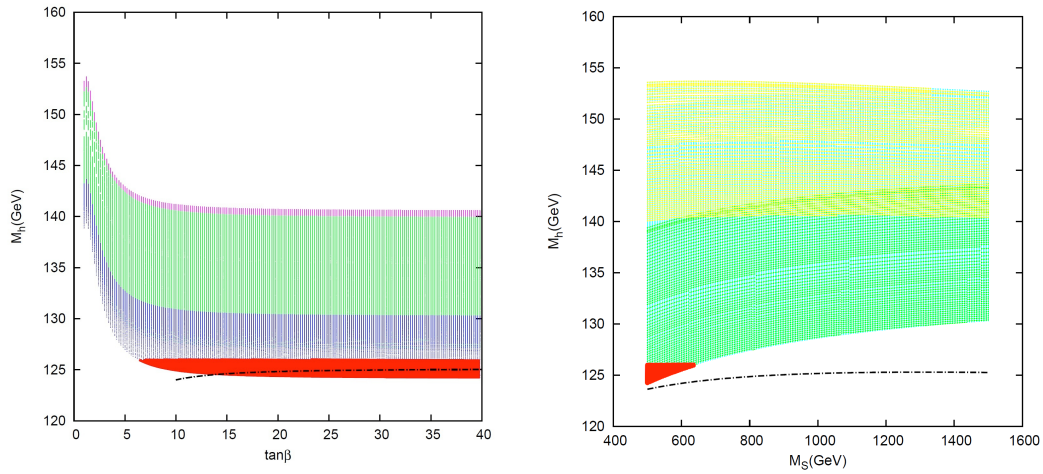

Figure 2.3: *(a) Variation of Higgs boson mass with* $\tan\beta$*, (b) Higgs boson mass as a function of* M_S

i.e. $X_t = 0$ while the pink upper region is for maximal mixing where $X - t = 6$. The green region is for all values of Higgs mass greater than 126 GeV and it is overlapped by the blue and the pink region. Fig. 2.3(b) represents the Higgs mass and as a function M_S. Again the red band is where the Higgs boson mass is between 124 GeV and 126 GeV, green region is for $X_t = 0$, yellow region represents $X_t = 6$ and blue region is for all values of Higgs mass greater than 126 GeV which is overlapped by the green and the yellow regions. The black dotted line in each case represents the MSSM Higgs mass.

The pseudo-scalar mass-squared matrix in this case is a 4×4 matrix. The matrix elements are given as:

$$
\begin{aligned}
M_{11} &= -\frac{(v_L^2+\overline{v}_L^2)\left[B_1\mu_1 v_L\overline{v}_L - \mu_1(v_1\overline{v}_L v_R + v_2 v_L\overline{v}_R)\lambda + 2\mu(\lambda v_2 v_L v_R + \lambda v_1\overline{v}_L\overline{v}_R - B v_1 v_2)\right]}{v_L^2\overline{v}_L^2} \\
M_{12} &= -\frac{2\mu\left(-B v_1 v_2 + \lambda v_2 v_L v_R + \lambda v_1\overline{v}_L\overline{v}_R\right)\sqrt{(v_L^2+\overline{v}_L^2)(v_R^2+\overline{v}_R^2)}}{v_L\overline{v}_L v_R\overline{v}_R} \\
M_{13} &= -\frac{(\lambda\mu_1\overline{v}_L v_R + 2B\mu v_2 - 2\lambda\mu\overline{v}_L\overline{v}_R)\sqrt{(v_L^2+\overline{v}_L^2)[v_L^2 v_R^2 + v_1^2(v_L^2+v_R^2)]}}{v_L^2\overline{v}_L v_R} \\
M_{14} &= -\frac{(\lambda\mu_1\overline{v}_R v_L + 2B\mu v_1 - 2\lambda\mu v_L v_R)\sqrt{(v_L^2+\overline{v}_L^2)[\overline{v}_L^2\overline{v}_R^2 + v_2^2(\overline{v}_L^2+\overline{v}_R^2)}}{v_L\overline{v}_L^2\overline{v}_R}
\end{aligned}
$$

$$
\begin{aligned}
M_{22} &= \frac{(v_R^2+\overline{v}_R^2)\left[B_1\mu_1 v_R\overline{v}_R-\mu_1(v_2\overline{v}_L v_R+v_1 v_L\overline{v}_R)\lambda-2\mu(\lambda v_2 v_L v_R+\lambda v_1\overline{v}_L\overline{v}_R-Bv_1v_2)\right]}{v_R^2\overline{v}_R^2}\\
M_{23} &= \frac{(\lambda\mu_1\overline{v}_R v_L-2B\mu v_2+2\lambda\mu\overline{v}_L\overline{v}_R)\sqrt{(v_R^2+\overline{v}_R^2)[v_L^2v_R^2+v_1^2(v_L^2+v_R^2)]}}{v_L\overline{v}_R v_R^2}\\
M_{24} &= -\frac{(\lambda\mu_1\overline{v}_L v_R-2B\mu v_1+2\lambda\mu v_L v_R)\sqrt{(v_R^2+\overline{v}_R^2)[\overline{v}_L^2\overline{v}_R^2+v_2^2(\overline{v}_L^2+\overline{v}_R^2)]}}{v_R\overline{v}_L\overline{v}_R^2}\\
M_{33} &= \frac{[v_L^2v_R^2+v_1^2(v_L^2+v_R^2)]\left[\lambda A_\lambda vLvR+\lambda\mu_1(\overline{v}_L v_R-v_L\overline{v}_R)+2B\mu v_2-2\lambda\mu\overline{v}_L\overline{v}_R\right]}{v_1v_L^2v_R^2}\\
M_{34} &= \frac{2\mu B\sqrt{v_L^2v_R^2+v_1^2(v_L^2+v_R^2)}\sqrt{\overline{v}_L^2+\overline{v}_R^2+v_2^2(\overline{v}_L^2+\overline{v}_R^2)}}{v_Lv_R\overline{v}_L\overline{v}_R}\\
M_{44} &= \frac{[\overline{v}_L^2\overline{v}_R^2+v_2^2(\overline{v}_L^2+\overline{v}_R^2)]\left[\lambda A_\lambda\overline{v}L\overline{v}R-\lambda\mu_1(\overline{v}_L v_R-v_L\overline{v}_R)+2B\mu v_1-2\lambda\mu v_L v_R\right]}{v_2\overline{v}_L^2\overline{v}_R^2}
\end{aligned}
\tag{2.69}
$$

Chargino and Neutralino masses

The chargino mass terms in this case is written as

$$
\mathcal{L}_{chargino}=-\frac{1}{2}\begin{pmatrix}\widetilde{H}_R^+ & \widetilde{\overline{H}}_L^+ & \widetilde{\phi}_1^+ & \lambda_R^+ & \lambda_L^+\end{pmatrix}\begin{pmatrix}\mu_1 & -\lambda v_2 & \lambda v_L & g_R v_R & 0\\ -\lambda v_1 & -\mu_1 & \lambda\overline{v}_R & 0 & g_l\overline{v}_L\\ \lambda\overline{v}_L & \lambda v_R & 2\mu & g_R v_1 & g_L v_1\\ g_R\overline{v}_R & 0 & g_R v_2 & M_R & 0\\ 0 & g_L v_L & g_L v_2 & 0 & M_L\end{pmatrix}\begin{pmatrix}\widetilde{\overline{H}}_R^- \\ \widetilde{H}_L^- \\ \widetilde{\phi}_2^- \\ \lambda_R^- \\ \lambda_L^-\end{pmatrix},
\tag{2.70}
$$

and the neutralino mass matrix in the basis $\begin{pmatrix}\widetilde{H}_R^0 & \widetilde{H}_L^0 & \widetilde{\overline{H}}_R^0 & \widetilde{\overline{H}}_L^0 & \widetilde{\phi}_1^0 & \widetilde{\phi}_2^0 & \lambda_0 & \lambda_{R_3} & \lambda_{L_3}\end{pmatrix}$

is given as

$$M_n = \begin{pmatrix} 0 & -\lambda v_1 & -\mu_1 & 0 & -\lambda v_L & 0 & \frac{g_V v_R}{\sqrt{2}} & -\frac{g_R v_R}{\sqrt{2}} & 0 \\ -\lambda v_1 & 0 & 0 & \mu_1 & -\lambda v_R & 0 & -\frac{g_V v_L}{\sqrt{2}} & 0 & \frac{g_L v_L}{\sqrt{2}} \\ -\mu_1 & 0 & 0 & -\lambda v_2 & 0 & -\lambda \overline{v}_L & -\frac{g_V \overline{v}_R}{\sqrt{2}} & \frac{g_R \overline{v}_R}{\sqrt{2}} & 0 \\ 0 & \mu_1 & -\lambda v_2 & 0 & 0 & -\lambda \overline{v_R} & \frac{g_V \overline{v}_L}{\sqrt{2}} & 0 & -\frac{g_L \overline{v}_L}{\sqrt{2}} \\ -\lambda v_L & -\lambda v_R & 0 & 0 & 0 & -2\mu & 0 & -\frac{g_R v_1}{\sqrt{2}} & -\frac{g_L v_1}{\sqrt{2}} \\ 0 & 0 & -\lambda \overline{v}_L & -\lambda \overline{v}_R & -2\mu & 0 & 0 & \frac{g_R v_2}{\sqrt{2}} & \frac{g_L v_2}{\sqrt{2}} \\ \frac{g_V v_R}{\sqrt{2}} & -\frac{g_V v_L}{\sqrt{2}} & -\frac{g_V \overline{v}_R}{\sqrt{2}} & \frac{g_V \overline{v}_L}{\sqrt{2}} & 0 & 0 & M_1 & 0 & 0 \\ -\frac{g_R v_R}{\sqrt{2}} & 0 & \frac{g_R \overline{v}_R}{\sqrt{2}} & 0 & -\frac{g_R v_1}{\sqrt{2}} & \frac{g_R v_2}{\sqrt{2}} & 0 & M_R & 0 \\ 0 & \frac{g_L v_L}{\sqrt{2}} & 0 & -\frac{g_L \overline{v}_L}{\sqrt{2}} & -\frac{g_L v_1}{\sqrt{2}} & \frac{g_L v_2}{\sqrt{2}} & 0 & 0 & M_L \end{pmatrix}, \tag{2.71}$$

where λ_R, λ_L and λ_0 are the superpartners of the right-handed gauge bosons, left-handed gauge bosons and the $U(1)_{B-L}$ gauge boson and M_R, M_L and M_1 are their soft masses respectively.

2.5 Universal Seesaw model

The particle spectrum for this case is given in Eq. (2.13) with an additional singlet Higgs field S. The superpotential is given as:

$$W = S(i\lambda H_L^T \tau_2 \overline{H}_L + i\lambda^c H_R^T \tau_2 \overline{H}_R - M^2), \tag{2.72}$$

where $\lambda^c = \lambda^*$ and M^2 is real from parity invariance.

The D-term, F-term and the soft supersymmetry breaking terms are given as:

$$\begin{aligned} V_F &= \left|\lambda \mathrm{Tr}[i H_L^T \tau_2 \overline{H}_L + i H_R^T \tau_2 \overline{H}_R] - M^2\right|^2 \\ &+ |\lambda S|^2 \mathrm{Tr}[H_L^\dagger H_L + \overline{H}_L{}^\dagger \overline{H}_L + H_R^\dagger H_R + \overline{H}_R{}^\dagger \overline{H}_R], \\ V_D &= \frac{g_L^2}{8} \sum_{a=1}^{3} |H_L^\dagger \tau_a H_L + \overline{H}_L^\dagger \tau_a \overline{H}_L|^2 \end{aligned} \tag{2.73}$$

$$
\begin{aligned}
&+ \quad \frac{g_R^2}{8}\sum_{a=1}^{3}|H_R^\dagger\tau_a H_R + \overline{H}_R^\dagger\tau_a\overline{H}_R|^2 \\
&+ \quad \frac{g_V^2}{8}|-H_L^\dagger H_L + \overline{H}_L^\dagger\overline{H}_L + H_R^\dagger H_R - \overline{H}_R^\dagger\overline{H}_R|^2, \qquad (2.74)\\
V_{Soft} &= m_3^2(H_L^\dagger H_L) + m_4^2(H_R{}^\dagger H_R) + m_5^2(\overline{H}_L{}^\dagger\overline{H}_L) + m_6^2(\overline{H}_R{}^\dagger\overline{H}_R) + m_S^2|S|^2 \\
&+ \quad \left[\lambda A_\lambda S(H_L^T\tau_2\overline{H}_L + H_R^T\tau_2\overline{H}) + h.c.\right] + (\lambda C_\lambda M^2 S + h.c.). \qquad (2.75)
\end{aligned}
$$

We choose a rotated basis which is exactly the same as in Eq. (2.23) with $\phi_1 \to H_L, \phi_2 \to \overline{H}_L, \delta^{c0} \to H_R, \overline{\delta}^{c0} \to \overline{H}_R, v_1 \to v_L, v_2 \to \overline{v}_L$. The minimization conditions are slightly modified form of Eq. (2.24) and are given by:

$$
\begin{aligned}
&v_L[4m_3^2 + g_L^2(-\overline{v}_L^2 + v_L^2) + g_V^2(-\overline{v}_L^2 + v_L^2 - v_R^2 + \overline{v}_R^2)] + 4\lambda A_\lambda\overline{v}_L v_S + 4\lambda^2 v_L v_S^2 \\
&+ 4\lambda\overline{v}_L(-M^2 + \lambda v_L\overline{v}_L - \lambda v_R\overline{v}_R) = 0, \\
&\overline{v}_L[4m_5^2 + g_L^2(-v_L^2 + \overline{v}_L^2) + g_V^2(-v_L^2 + \overline{v}_L^2 + v_R^2 - \overline{v}_R^2)] + 4\lambda A_\lambda v_L v_S + 4\lambda^2\overline{v}_L v_S^2 \\
&+ 4\lambda v_L(-M^2 + \lambda v_L\overline{v}_L - \lambda v_R\overline{v}_R) = 0, \\
&4m_4^2 v_R - g_V^2 v_R(-v_L^2 + \overline{v}_L^2 + v_R^2 - \overline{v}_R^2) + g_R^2 v_R(v_R^2 - \overline{v}_R^2) \\
&- 4\lambda A_\lambda\overline{v}_R v_S + 4\lambda\overline{v}_R(M^2 - \lambda v_L\overline{v}_L) + 4\lambda^2 v_R(\overline{v}_R^2 + v_S^2) = 0, \\
&4m_6^2\overline{v}_R + g_V^2\overline{v}_R(v_L^2 - \overline{v}_L^2 - v_R^2 + \overline{v}_R^2) + g_R^2\overline{v}_R(\overline{v}_R^2 - v_R^2) \\
&- 4\lambda A_\lambda v_R v_S + 4\lambda v_R(M^2 - \lambda v_L\overline{v}_L) + 4\lambda^2\overline{v}_R(v_R^2 + v_S^2) = 0, \\
&2m_S^2 v_S + 2C_\lambda M^2\lambda + 2\lambda A_\lambda(v_L\overline{v}_L - v_R\overline{v}_R) + \lambda^2(v_L^2 + \overline{v}_L^2 + v_R^2 + \overline{v}_R^2)v_S = 0. \qquad (2.76)
\end{aligned}
$$

Using this minimization and the basis $(\mathrm{Re}\rho_1, \mathrm{Re}\rho_2, \mathrm{Re}H_R{}^0, \mathrm{Re}\overline{H}_R{}^0)$, the relevant mass-squared matrix elements are given by:

$$
\begin{aligned}
M_{11} &= \frac{g_L^2(v_L^2 - \overline{v}_L^2)^2 + g_V^2(v_L^2 - \overline{v}_L^2)^2 + 8v_L^2\overline{v}_L^2\lambda^2}{2(v_L^2 + \overline{v}_L^2)}, \\
M_{12} &= \frac{v_L\overline{v}_L(v_L^2 - \overline{v}_L^2)(g_L^2 + g_V^2 - 2\lambda^2)}{(v_L^2 + \overline{v}_L^2)}, \\
M_{13} &= \frac{-g_V^2(v_L^2 - \overline{v}_L^2)(v_R^2 - \overline{v}_R^2) - 8\lambda^2 v_L\overline{v}_L v_R\overline{v}_R}{\sqrt{(v_L^2 + \overline{v}_L^2)(v_R^2 + \overline{v}_R^2)}}, \\
M_{14} &= \frac{-g_V^2(v_L^2 - \overline{v}_L^2)v_R\overline{v}_R + 2\lambda^2 v_L\overline{v}_L(v_R^2 - \overline{v}_R^2)}{\sqrt{(v_L^2 + \overline{v}_L^2)(v_R^2 + \overline{v}_R^2)}},
\end{aligned}
$$

$$
\begin{aligned}
M_{15} &= \frac{\lambda[2A_\lambda v_L \overline{v}_L + 2(v_L^2 + \overline{v}_L^2)v_S\lambda]}{\sqrt{v_L^2 + \overline{v}_L^2}}, \\
M_{55} &= m_S^2 + (v_L^2 + \overline{v}_L^2 + v_R^2 + \overline{v}_R^2)\lambda^2.
\end{aligned} \tag{2.77}
$$

The other terms in the mass matrix are given in the appendix. We choose the ratio between $\overline{v}_R$ and v_R such that the matrix element M_{13} vanishes and we choose the value of A_λ such that M_{15} becomes zero. Then we calculate the correction from the off-diagonal elements to the lightest eigenvalue of this mass-squared matrix. In the limit where the soft-supersymmetry breaking parameter m_6 is significantly larger v_R, we can show that this correction vanishes. Hence the tree-level mass of the lightest neutral Higgs boson in this case becomes:

$$
M_{h_{tree}}^2 = \frac{M_W^4}{(2M_W^2 - M_Z^2)} \cos^2 2\beta + \lambda^2 v^2 \sin^2 2\beta, \tag{2.78}
$$

where $\tan\beta = \frac{\overline{v}_L}{v_L}$ and $v^2 = v_L^2 + \overline{v}_L^2$. Including the loop corrections from the top and stop sector, the Higgs boson mass is:

$$
M_h^2 = \left(\frac{M_W^4}{2M_W^2 - M_Z^2} \cos^2 2\beta + \lambda^2 \sin^2 2\beta\right) \Delta_1 + \Delta_2, \tag{2.79}
$$

where Δ_1 and Δ_2 are defined in Eq. (2.28).

The Higgs boson mass is plotted in Fig 2.4(a) as a function of $\tan\beta$.The red region in the figure represents the band where the mass is between 124 GeV and 126 GeV. The light blue region represents the area where the stop squark mixing is minimum i.e. $X_t = 0$ while the pink upper region is for maximal mixing where $X - t = 6$. The green region is for all values of Higgs mass greater than 126 GeV and it is overlapped by the blue and the pink region. Fig. 2.4(b) represents the Higgs mass and as a function M_S. Again the red band is where the Higgs boson mass is between 124 GeV and 126 GeV, green region is for $X_t = 0$, yellow region represents $X_t = 6$ and blue region is for all values of Higgs mass greater than 126 GeV which is overlapped by the green and the yellow regions. The black dotted line in each case represents the MSSM Higgs mass.

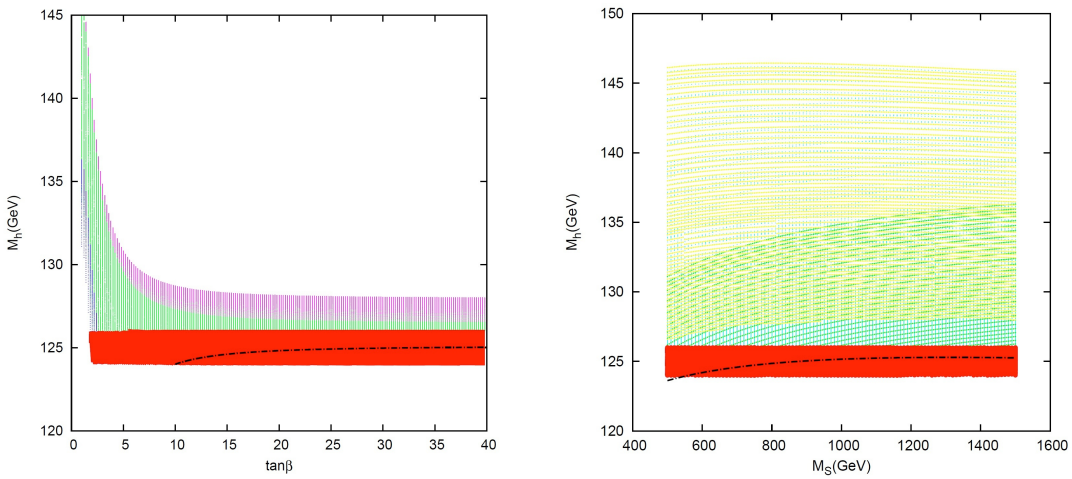

Figure 2.4: *(a) Variation of Higgs boson mass with* $\tan\beta$*, (b) Higgs boson mass as a function of* M_S

The eigenvalues of the 2×2 charged Higgs boson mass-squared matrix in this case are given by:

$$\begin{aligned} M^2_{h_1^+} &= m_4^2 + m_6^2 + \frac{1}{2}g_R^2(v_R^2+\overline{v}_R^2) + 2\lambda^2 v_S^2, \\ M^2_{h_2^+} &= m_3^2 + m_5^2 + \frac{1}{2}g_L^2(v_L^2+\overline{v}_L^2) + 2\lambda^2 v_S^2. \end{aligned} \tag{2.80}$$

The pseudo scalar mass-squared matrix is a 3×3 matrix whose elements are given as:

$$\begin{aligned} M_{11} &= m_4^2 + m_6^2 + \frac{\lambda^2}{2}(v_R^2+\overline{v}_R^2+2v_S^2), \\ M_{12} &= -\frac{\lambda^2}{2}\sqrt{(v_R^2+\overline{v}_R^2)(v_L^2+\overline{v}_L^2)} \\ M_{13} &= \frac{\lambda A_\lambda\sqrt{v_R^2+\overline{v}_R^2}}{\sqrt{2}} \\ M_{22} &= m_3^2 + m_5^2 + \frac{\lambda^2}{2}(v_L^2+\overline{v}_L^2+2v_S^2) \\ M_{23} &= -\frac{\lambda A_\lambda\sqrt{v_L^2+\overline{v}_L^2}}{\sqrt{2}} \\ M_{33} &= m_S^2 + \lambda^2(v_L^2+\overline{v}_L^2+v_R^2+\overline{v}_R^2) \end{aligned} \tag{2.81}$$

Here we use the minimization conditions given in Eq. (2.76) to eliminate m_4, m_5, m_6, M^2 and C_λ. Also while calculating the mass of the CP-even Higgs boson, we have

fixed the value of A_λ and the ratio between $\overline{v}_R$ and v_R. Using all these constraints on the aforementioned parameters, we numerically calculate the masses of the charged and pseudo-scalar Higgs boson. We choose a parameter space where $\lambda = 0.7$, $v_R = 1$ TeV, $m_3 = 2$ TeV, $v_S = 800$ GeV, $m_S = 2$ TeV, $v_L = 30$ GeV, $\overline{v}_L = 171$ GeV and g_R and g_V are 0.653 and 0.48 respectively. This choice of parameters gives us the mass of the charged Higgs bosons to be $M_{h_1^+} = 2.25$ TeV and $M_{h_2^+} = 2.41$ TeV while the masses of the pseudo-scalar Higgs boson are given as $M_{A_1} = 2.18$ TeV, $M_{A_2} = 3.5$ TeV and $M_{A_3} = 836$ GeV.

Chargino and Neutralino masses

The chargino mass terms in this case is written as

$$\mathcal{L}_{chargino} = -\frac{1}{2}\begin{pmatrix}\widetilde{H}_R^+ & \widetilde{\overline{H}}_L^+ & \lambda_R^+ & \lambda_L^+\end{pmatrix}\begin{pmatrix}\lambda^* v_S & 0 & g_R v_R & 0\\ 0 & -\lambda v_S & 0 & g_L \overline{v}_L\\ g_R \overline{v}_R & 0 & M_R & 0\\ 0 & g_L v_L & 0 & M_L\end{pmatrix}\begin{pmatrix}\widetilde{\overline{H}}_R^-\\ \widetilde{H}_L^-\\ \lambda_R^-\\ \lambda_L^-\end{pmatrix}, \quad (2.82)$$

and the neutralino mass matrix in the basis $\begin{pmatrix}\widetilde{H}_R^0 & \widetilde{H}_L^0 & \widetilde{\overline{H}}_R^0 & \widetilde{\overline{H}}_L^0 & \lambda_0 & \lambda_{R_3} & \lambda_{L_3} & \widetilde{S}\end{pmatrix}$ is given as

$$M_n = \begin{pmatrix}
0 & 0 & -\lambda^* v_S & 0 & \frac{g_V v_R}{\sqrt{2}} & -\frac{g_R v_R}{\sqrt{2}} & 0 & -\lambda^* \overline{v}_R\\
0 & 0 & 0 & \lambda v_S & -\frac{g_V v_L}{\sqrt{2}} & 0 & \frac{g_L v_L}{\sqrt{2}} & \lambda \overline{v}_L\\
-\lambda^* v_S & 0 & 0 & 0 & -\frac{g_V \overline{v}_R}{\sqrt{2}} & \frac{g_R \overline{v}_R}{\sqrt{2}} & 0 & -\lambda^* v_R\\
0 & \lambda v_S & 0 & 0 & \frac{g_V \overline{v}_L}{\sqrt{2}} & 0 & -\frac{g_L \overline{v}_L}{\sqrt{2}} & \lambda v_L\\
\frac{g_V v_R}{\sqrt{2}} & -\frac{g_V v_L}{\sqrt{2}} & -\frac{g_V \overline{v}_R}{\sqrt{2}} & \frac{g_V \overline{v}_L}{\sqrt{2}} & M_1 & 0 & 0 & 0\\
-\frac{g_R v_R}{\sqrt{2}} & 0 & \frac{g_R \overline{v}_R}{\sqrt{2}} & 0 & 0 & M_R & 0 & 0\\
0 & \frac{g_L v_L}{\sqrt{2}} & 0 & -\frac{g_L \overline{v}_L}{\sqrt{2}} & 0 & 0 & M_L & 0\\
-\lambda^* \overline{v}_R & \lambda \overline{v}_L & -\lambda^* v_R & \lambda v_L & 0 & 0 & 0 & 0
\end{pmatrix}. \quad (2.83)$$

Here λ_R, λ_L and λ_0 are the superpartners of the right-handed gauge bosons, left-handed gauge bosons and the $U(1)_{B-L}$ gauge boson and M_R, M_L and M_1 are their

soft masses respectively.

2.5.1 Case without singlet

The most general superpotential involving the Higgs fields in this case is given by:

$$W = i\mu_1 H_L^T \tau_2 \overline{H}_L + i\mu_2 H_R^T \tau_2 \overline{H}_R. \tag{2.84}$$

The D-term in the superpotential is the same as in Eq. (2.74). The F-term and the soft supersymmetry breaking terms in the Higgs potential are given by:

$$V_F = \mu_1^2(H_L^\dagger H_L + \overline{H}_L^\dagger \overline{H}_L) + \mu_2^2(H_R^\dagger H_R + \overline{H}_R^\dagger \overline{H}_R), \tag{2.85}$$

$$\begin{aligned} V_{Soft} &= B_1\mu_1(iH_L^T\tau_2\overline{H}_L + h.c.) + B_2\mu_2(iH_R\tau_2\overline{H}_R + h.c) \\ &+ m_3^2(H_L^\dagger H_L) + m_4^2(\overline{H}_L{}^\dagger \overline{H}_L) + m_5^2(H_R{}^\dagger H_R) + m_6^2(\overline{H}_R{}^\dagger \overline{H}_R). \end{aligned} \tag{2.86}$$

The vacuum structure in this case is given as:

$$\langle H_L \rangle = \begin{pmatrix} v_L \\ 0 \end{pmatrix}, \langle H_R \rangle = \begin{pmatrix} 0 \\ v_R \end{pmatrix}, \langle \overline{H}_L \rangle = \begin{pmatrix} 0 \\ \overline{v}_L \end{pmatrix}, \langle \overline{H}_R \rangle = \begin{pmatrix} \overline{v}_R \\ 0 \end{pmatrix}. \tag{2.87}$$

We take a rotated basis given by:

$$\rho_1 = \frac{v_L H_L{}^0 + \overline{v}_L \overline{H}_L{}^0}{\sqrt{v_L^2 + \overline{v}_L^2}},\ \rho_2 = \frac{\overline{v}_L H_L{}^0 - v_L \overline{v}_L^0}{\sqrt{v_L^2 + \overline{v}_L^2}}. \tag{2.88}$$

The minimization conditions are given by:

$$\begin{aligned} 0 &= 2\mu_2^2 v_R + 2m_4^2 v_R - 2B_2\mu_2\overline{v}_R + \frac{1}{2}v_R[g_R^2(v_R^2 - \overline{v}_R^2) - g_V^2(v_L^2 - \overline{v}_L^2 - v_R^2 + \overline{v}_R^2)], \\ 0 &= 2\mu_2^2 \overline{v}_R + 2m_6^2 \overline{v}_R - 2B_2\mu_2 v_R + \frac{1}{2}\overline{v}_R[g_R^2(-v_R^2 + \overline{v}_R^2) + g_V^2(v_L^2 - \overline{v}_L^2 - v_R^2 + \overline{v}_R^2)], \\ 0 &= 2\mu_1^2 v_L + 2m_3^2 v_L + 2B_1\mu_1\overline{v}_L + \frac{1}{2}v_L[g_L^2(v_L^2 - \overline{v}_L^2) + g_V^2(v_L^2 - \overline{v}_L^2 - v_R^2 + \overline{v}_R^2)], \\ 0 &= 2\mu_1^2 \overline{v}_L + 2m_5^2 \overline{v}_L + 2B_1\mu_1 v_L + \frac{1}{2}\overline{v}_L[g_L^2(-v_L^2 + \overline{v}_L^2) + g_V^2(\overline{v}_L^2 - v_L^2 + v_R^2 - \overline{v}_R^2)]. \end{aligned} \tag{2.89}$$

Using the potential and minimization equations, we calculate the mass-squared matrix in the basis $(\mathrm{Re}\rho_1, \mathrm{Re}\rho_2, \mathrm{Re}{H_R}^0, \mathrm{Re}{\overline{H}_R}^0)$. We get the following matrix:

$$\begin{bmatrix} \frac{(g_L^2+g_V^2)(v_L^2-\overline{v}_L^2)^2}{2(v_L^2+\overline{v}_L^2)} & \frac{(g_L^2+g_V^2)(v_L^2-\overline{v}_L^2)v_L\overline{v}_L}{(v_L^2+\overline{v}_L^2)} & \frac{g_V^2 v_R(v_L^2-\overline{v}_L^2)}{2\sqrt{(v_L^2+\overline{v}_L^2)}} & -\frac{g_V^2\overline{v}_R(v_L^2-\overline{v}_L^2)}{2\sqrt{(v_L^2+\overline{v}_L^2)}} \\ \frac{(g_L^2+g_V^2)(v_L^2+\overline{v}_L^2)v_L\overline{v}_L}{(v_L^2+\overline{v}_L^2)} & M_{22} & \frac{g_V^2 v_L\overline{v}_L v_R}{\sqrt{v_L^2+\overline{v}_L^2}} & -\frac{g_V^2 v_L\overline{v}_L\overline{v}_R}{\sqrt{v_L^2+\overline{v}_L^2}} \\ \frac{g_V^2 v_R(v_L^2-\overline{v}_L^2)}{2\sqrt{(v_L^2+\overline{v}_L^2)}} & \frac{g_V^2 v_L\overline{v}_L v_R}{\sqrt{v_L^2+\overline{v}_L^2}} & \frac{(g_R^2+g_V^2)v_R^3+2B_2\mu_2\overline{v}_R}{2v_R} & -B_2\mu_2 - \frac{1}{2}(g_R^2+g_V^2)v_R\overline{v}_R \\ -\frac{g_V^2\overline{v}_R(v_L^2-\overline{v}_L^2)}{2\sqrt{(v_L^2+\overline{v}_L^2)}} & -\frac{g_V^2 v_L\overline{v}_L\overline{v}_R}{\sqrt{v_L^2+\overline{v}_L^2}} & -B_2\mu_2 - \frac{1}{2}(g_R^2+g_V^2)v_R\overline{v}_R & \frac{(g_R^2+g_V^2)\overline{v}_R^3+2B_2\mu_2 v_R}{2\overline{v}_R} \end{bmatrix} \tag{2.90}$$

where $M_{22} = \frac{(g_L^2+g_V^2)(v_L^4-6v_L^2\overline{v}_L^2+\overline{v}_L^4)+8m_1^2 v_L\overline{v}_L+2(m_3^2-m_5^2)(v_L^2-\overline{v}_L^2)-g_v^2(v_L^2-\overline{v}_L^2)(v_R^2-\overline{v}_R^2)}{2(v_L^2+\overline{v}_L^2)}$.

Here we have assumed $v_R, \overline{v}_R \neq 0$ in obtaining the mass matrix. We calculate the contribution of the off-diagonal elements to the lightest eigenvalue using the seesaw formula and this gives us the result

$$M_{htree}^2 = M_Z^2 \cos^2 2\beta, \tag{2.91}$$

where we have also assumed that the $SU(2)_R$ gauge coupling (g_R) is equal to the $SU(2)_L$ gauge coupling (g_L), $\tan\beta = \frac{\overline{v}_L}{v_L}$ and $v^2 = v_L^2 + \overline{v}_L^2$.

The eigenvalues of the 2×2 charged Higgs boson mass-squared matrix in this case are given by:

$$\begin{aligned} M_{h_1^+}^2 &= m_4^2 + m_6^2 + \frac{1}{2}g_R^2(v_R^2+\overline{v}_R^2) + 2\mu_2^2, \\ M_{h_2^+}^2 &= m_3^2 + m_5^2 + \frac{1}{2}g_L^2(v_L^2+\overline{v}_L^2) + 2\mu_1^2. \end{aligned} \tag{2.92}$$

The pseudo scalar mass-squared matrix is also a 2×2 matrix whose eigenvalues are given as:

$$M_{A_1}^2 = m_4^2 + m_6^2 + 2\mu_2^2,\ M_{A_2}^2 = m_3^2 + m_5^2 + 2\mu_1^2. \tag{2.93}$$

Here we use the minimization conditions given in Eq. (2.89) to eliminate B_1, B_2, μ_1 and μ_2. We choose a parameter space where $v_R = 1.2$ TeV, $\overline{v}_R = 1$ TeV, $m_3 = 4$ TeV, $m_4 = 2$ TeV, $m_5 = 2$ TeV, $m_6 = 4$ TeV, $v_L = 10$ GeV, $\overline{v}_L = 173$ GeV and

g_R and g_V are 0.653 and 0.48 respectively. Using these values for the parameters we get the numerical values of the charged Higgs boson mass (denoted by $M_{h_i^+}$) to be $M_{h_1^+} = 8.14$ TeV and $M_{h_2^+} = 3.47$ TeV while the masses of the pseudo-scalar Higgs boson (denoted by H_{A_i}) are given as $M_{A_1} = 8.11$ TeV and $M_{A_2} = 3.47$ TeV.

Chargino and Neutralino masses

The chargino mass terms in this case is written as

$$\mathcal{L}_{chargino} = -\frac{1}{2}\begin{pmatrix} \widetilde{H}_R^+ & \widetilde{\overline{H}}_L^+ & \lambda_R^+ & \lambda_L^+ \end{pmatrix} \begin{pmatrix} \mu_2 & 0 & g_R v_R & 0 \\ 0 & -\mu_1 & 0 & g_L \overline{v}_L \\ g_R \overline{v}_R & 0 & M_R & 0 \\ 0 & g_L v_L & 0 & M_L \end{pmatrix} \begin{pmatrix} \widetilde{\overline{H}}_R^- \\ \widetilde{H}_L^- \\ \lambda_R^- \\ \lambda_L^- \end{pmatrix}, \quad (2.94)$$

and the neutralino mass matrix in the basis $\begin{pmatrix} \widetilde{H}_R^0 & \widetilde{H}_L^0 & \widetilde{\overline{H}}_R^0 & \widetilde{\overline{H}}_L^0 & \lambda_0 & \lambda_{R_3} & \lambda_{L_3} \end{pmatrix}$ is given as

$$M_n = \begin{pmatrix} 0 & 0 & -\mu_2 & 0 & \frac{g_V v_R}{\sqrt{2}} & -\frac{g_R v_R}{\sqrt{2}} & 0 \\ 0 & 0 & 0 & \mu_1 & -\frac{g_V v_L}{\sqrt{2}} & 0 & \frac{g_L v_L}{\sqrt{2}} \\ -\mu_2 & 0 & 0 & 0 & -\frac{g_V \overline{v}_R}{\sqrt{2}} & \frac{g_R \overline{v}_R}{\sqrt{2}} & 0 \\ 0 & \mu_1 & 0 & 0 & \frac{g_V \overline{v}_L}{\sqrt{2}} & 0 & -\frac{g_L \overline{v}_L}{\sqrt{2}} \\ \frac{g_V v_R}{\sqrt{2}} & -\frac{g_V v_L}{\sqrt{2}} & -\frac{g_V \overline{v}_R}{\sqrt{2}} & \frac{g_V \overline{v}_L}{\sqrt{2}} & M_1 & 0 & 0 \\ -\frac{g_R v_R}{\sqrt{2}} & 0 & \frac{g_R \overline{v}_R}{\sqrt{2}} & 0 & 0 & M_R & 0 \\ 0 & \frac{g_L v_L}{\sqrt{2}} & 0 & -\frac{g_L \overline{v}_L}{\sqrt{2}} & 0 & 0 & M_L \end{pmatrix}. \quad (2.95)$$

Here λ_R, λ_L and λ_0 are the superpartners of the right-handed gauge bosons, left-handed gauge bosons and the $U(1)_{B-L}$ gauge boson and M_R, M_L and M_1 are their soft masses respectively.

2.6 E_6 Inspired Left-right Supersymmetric model

The Higgs spectrum for this model is discussed in Eq. (2.16). The relevant terms in the superpotential involving the H_L, H_R and Φ fields are given as:

$$W = \lambda {H_L}^T \tau_2 \Phi \tau_2 H_R + \mu \mathrm{Tr}\left[\Phi \tau_2 \Phi^T \tau_2\right], \tag{2.96}$$

where the parameter λ and μ must be real for the superpotential to be invariant under parity transformation.

The Higgs potential consisting of the V_F, V_D and V_{Soft} terms will be given as:

$$\begin{aligned}
V_F &= \mathrm{Tr}(|\lambda H_R^T \tau_2 \Phi \tau_2|^2 + |\lambda H_L^T \tau_2 \Phi \tau_2|^2) + \mathrm{Tr}(|\lambda H_L H_R^T + 2\mu\Phi|^2), && (2.97)\\
V_D &= \frac{g_L^2}{8}\sum_{a=1}^{3} |H_L^\dagger \tau_a H_L + \mathrm{Tr}(\Phi^\dagger \tau_a \Phi)|^2 + \frac{g_R^2}{8}\sum_{a=1}^{3} |H_R^\dagger \tau_a H_R + \mathrm{Tr}(\Phi^\dagger \tau_a \Phi)|^2 \\
&+ \frac{g_V^2}{8}|H_R^\dagger H_R - H_L^\dagger H_L|^2, && (2.98)\\
V_{Soft} &= m_1^2 \mathrm{Tr}(\Phi^\dagger \Phi) + \left[B\mu \mathrm{Tr}(\Phi^T \tau_2 \Phi \tau_2) + h.c.\right] + m_3^2 (H_R^\dagger H_R + H_L^\dagger H_L) \\
&+ (A_\lambda \lambda H_L^T \tau_2 \Phi \tau_2 H_R + h.c.). && (2.99)
\end{aligned}$$

Using this potential we calculate the Higgs boson mass-squared matrix. We choose the following vacuum structure for the Higgs fields:

$$\langle H_L \rangle = \begin{pmatrix} v_L \\ 0 \end{pmatrix}, \langle H_R \rangle = \begin{pmatrix} 0 \\ v_R \end{pmatrix}, \langle \Phi \rangle = \begin{pmatrix} 0 & v_2 \\ v_1 & 0 \end{pmatrix} \tag{2.100}$$

To easily identify the field corresponding to the lightest eigenvalue, we take a linear combination of the ${H_L}^0, \phi_1^0$ and ϕ_2^0 fields. We make sure that only one of the newly defined fields get a non-zero vacuum expectation value(or VEV). The field redefinition that we used is:

$$\begin{aligned}
\rho_1 &= \frac{v_L {H_L}^0 + v_1 \phi_1^0 + v_2 \phi_2^0}{\sqrt{v_L^2 + v_1^2 + v_2^2}}, \rho_2 = \frac{v_L \phi_1^0 - v_1 {H_L}^0}{\sqrt{v_1^2 + v_L^2}}, \\
\rho_3 &= \frac{v_L v_2 {H_L}^0 + v_1 v_2 \phi_1^0 - (v_1^2 + v_L^2)\phi_2^0}{\sqrt{(v_1^2 + v_2^2)(v_1^2 + v_2^2 + v_L^2)}}. && (2.101)
\end{aligned}$$

One can verify that only the ρ_1 field gets a non-zero vacuum expectation value of $\sqrt{v_1^2 + v_2^2 + v_L^2}$. We calculate the 4×4 mass-squared matrix for the neutral CP-even Higgs boson in the basis $(\mathrm{Re}\rho_1, \mathrm{Re}{H_R}^0, \mathrm{Re}\rho_2, \mathrm{Re}\rho_3)$. It is easy to identify the lightest mass eigenvalue in this new basis. We use the minimization condition for the potential to express the soft SUSY breaking masses and the coefficient μ in terms of the other parameters in the model. The minimization conditions and mass-squared matrix is given in Appendix. We assume that $v_R >> v_1, v_2, v_L$ and using this assumption we can get he lightest eigenvalue of the mass-squared matrix. It turns out that we can neglect the corrections from two of the off-diagonal matrix elements as they are of order of $\sim \frac{v_1^4}{v_R^2}$. So we effectively have a 2×2 matrix. Diagonalizing this matrix, we get the lightest neutral CP-even Higgs mass given by:

$$M_{h_{tree}}^2 = [g_R^2(v_1^2 - v_2^2)^2 + g_V^2 v_L^4 + g_L^2(-v_1^2 + v_2^2 + v_L^2)^2 + 8v_1^2 v_L^2 \lambda^2 \\ - (g_V^2 v_L^2 + g_R^2(-v_1^2 + v_2^2 + v_L^2) + 4v_1^2\lambda^2)^2/(g_R^2 + g_V^2)]/(2(v_1^2 + v_2^2 + v_L^2)). \tag{2.102}$$

We then choose $v_1 = v \sin\beta$, $v_2 = v \cos\beta \cos\phi$ and $v_L = v \cos\beta \cos\phi$. Maximizing the resulting expression with respect to λ and ϕ and choosing $g_R = g_L$, we get:

$$M_{h_{tree}}^2 = 2M_W^2 \cos^2 2\beta. \tag{2.103}$$

This result is exactly the same as in **Section 2.3.2** and has been discussed in details in that section.

Chargino and Neutralino masses

The higgsino and the gauginos mix to form the charginos and the neutralinos.

The chargino mass term in this case is written as

$$\mathcal{L}_{chargino} = -\frac{1}{2}\begin{pmatrix}\widetilde{H}_R^+ & \widetilde{\phi}_1^+ & \lambda_R^+ & \lambda_L^+\end{pmatrix}\begin{pmatrix}-\lambda v_2 & \lambda v_L & g_R v_R & 0\\ \lambda v_R & 2\mu & g_R v_1 & g_L v_1\\ 0 & g_R v_2 & M_R & 0\\ g_L v_L & g_L v_2 & 0 & M_L\end{pmatrix}\begin{pmatrix}\widetilde{H}_L^-\\ \widetilde{\phi}_2^-\\ \lambda_R^-\\ \lambda_L^-\end{pmatrix}, \quad (2.104)$$

and the neutralino mass matrix in the basis $\begin{pmatrix}\widetilde{H}_R^0 & \widetilde{H}_L^0 & \widetilde{\phi}_1^0 & \widetilde{\phi}_2^0 & \lambda_0 & \lambda_{R_3} & \lambda_{L_3}\end{pmatrix}$ is given as

$$M_n = \begin{pmatrix}0 & -\lambda v_1 & -\lambda v_L & 0 & \frac{g_V v_R}{\sqrt{2}} & -\frac{g_R v_R}{\sqrt{2}} & 0\\ -\lambda v_1 & 0 & -\lambda v_R & 0 & -\frac{g_V v_L}{\sqrt{2}} & 0 & \frac{g_L v_L}{\sqrt{2}}\\ -\lambda v_L & -\lambda v_R & 0 & -2\mu & 0 & -\frac{g_R v_1}{\sqrt{2}} & -\frac{g_L v_1}{\sqrt{2}}\\ 0 & 0 & -2\mu & 0 & 0 & \frac{g_R v_2}{\sqrt{2}} & \frac{g_L v_2}{\sqrt{2}}\\ \frac{g_V v_R}{\sqrt{2}} & -\frac{g_V v_L}{\sqrt{2}} & 0 & 0 & M_1 & 0 & 0\\ -\frac{g_R v_R}{\sqrt{2}} & 0 & -\frac{g_R v_1}{\sqrt{2}} & \frac{g_R v_2}{\sqrt{2}} & 0 & M_R & 0\\ 0 & \frac{g_L v_L}{\sqrt{2}} & -\frac{g_L v_1}{\sqrt{2}} & \frac{g_L v_2}{\sqrt{2}} & 0 & 0 & M_L\end{pmatrix}. \quad (2.105)$$

Here λ_R, λ_L and λ_0 are the superpartners of the right-handed gauge bosons, left-handed gauge bosons and the $U(1)_{B-L}$ gauge boson and M_R, M_L and M_1 are their soft masses respectively.

2.7 Doubly-charged Higgs Mass

In the models discussed under section 2.3, the right-handed symmetry breaking was achieved by triplet Higgs bosons. Each triplet Higgs boson has a doubly-charged particle which should be relatively easy to detect experimentally if they can be produced at the colliders. These doubly-charged particles, if seen, can tell us a lot about the symmetry breaking pattern and their properties can help identify the underlying model.

Let us take a closer look at a fully realistic left-right supersymmetric model where the $SU(2)_R \times U(1)_{B-L}$ symmetry is broken into $U(1)_Y$ by triplet Higgs boson field

Δ^c, and then the $SU(2)_L \times U(1)_Y$ symmetry breaking is achieved via bidoublet field Φ.

The chiral matter sector of this model is given in Eq. (2.1). Being left-right symmetric, the lepton and quark left-handed doublets L and Q have accompanying right-handed doublets given by L^c and Q^c. A right-handed neutrino is quite naturally present in this model and can generate a light neutrino mass.

The Higgs boson sector is given in Eq. (2.2). Although a single right-handed triplet field Δ^c is enough for the right-handed symmetry breaking, the model being supersymmetric, we need another triplet Higgs field $\overline{\Delta}^c$ for anomaly cancellation and to prevent R-parity violating couplings. For parity conservation these right-handed triplet fields must be accompanied by left-handed triplet fields Δ and $\overline{\Delta}$ as well. Two bidoublets Φ_1 and Φ_2 are needed for the generation of lepton and quark masses and the CKM mixing. A singlet field S is introduced so that the $SU(2)_R \times U(1)_{B_L}$ symmetry breaking can be achieved in the supersymmetric limit.

The superpotential of the model is given as:

$$\begin{aligned} W &= Y_u Q^T \tau_2 \Phi_1 \tau_2 Q^c + Y_d Q^T \tau_2 \Phi_2 \tau_2 Q^c + Y_\nu L^T \tau_2 \Phi_1 \tau_2 L^c + Y_l L^T \tau_2 \Phi_2 \tau_2 L^c \\ &+ i(f^* L^T \tau_2 \Delta L + f L^{c^T} \tau_2 \Delta^c L^c) \\ &+ S[Tr(\lambda^* \Delta \overline{\Delta} + \lambda \Delta^c \overline{\Delta}^c) + \lambda'_{ab} Tr(\Phi_a^T \tau_2 \Phi_b \tau_2) - M_R^2] + W' \end{aligned} \tag{2.106}$$

where

$$W' = \left[M_\Delta Tr(\Delta \overline{\Delta}) + M_\Delta^* Tr(\Delta^c \overline{\Delta}^c)\right] + \mu_{ab} Tr\left(\Phi_a^T \tau_2 \Phi_b \tau_2\right) + M_S S^2 + \lambda_S S^3. \tag{2.107}$$

Here $Y_{u,d}$ and $Y_{\nu,l}$ are the Yukawa couplings for quarks and leptons respectively and f is the Majorana neutrino Yukawa coupling matrix. This is the most general superpotential. R-parity is automatically preserved in this case. Putting $W' = 0$ gives an enhanced $U(1)$ R-symmetry in the theory. Under this R-symmetry, Q, Q^C, L, L^C fields have a charge of $+1$, S has charge $+2$ and all other fields have charge zero with

W carrying a charge +2. Putting $W' = 0$ also helps in understanding the μ-problem and makes the doubly-charged left-handed and right-handed Higgsinos degenerate in mass.

We will look at the case where $W' = 0$. The left-handed triplets do not get any vev and hence the masses of their doubly-charged particles are heavy. Thus we will concentrate on the right-handed Higgs boson triplet sector from here on. The Higgs potential consists of F term, D term and soft supersymmetry breaking terms which in this case are then given as

$$\begin{aligned}
V_F &= \left|\lambda \mathrm{Tr}(\Delta^c \overline{\Delta}^c) + \lambda'_{ab} \mathrm{Tr}\left(\Phi_a^T \tau_2 \Phi_b \tau_2\right) - \mathcal{M}_R^2\right|^2 + |\lambda|^2 |S|^2 \left|\mathrm{Tr}(\Delta^c \Delta^{c\dagger}) + \mathrm{Tr}(\overline{\Delta}^c\ \overline{\Delta}^{c\dagger})\right| \\
V_{\mathrm{soft}} &= M_1^2 \mathrm{Tr}(\Delta^{c\dagger} \Delta^c) + M_2^2 \mathrm{Tr}(\overline{\Delta}^{c\dagger} \overline{\Delta}^c) + M_S^2 |S|^2 \\
&+ \{A_\lambda \lambda S \mathrm{Tr}(\Delta^c \Delta^{c\dagger}) - C_\lambda \mathcal{M}_R^2 S + h.c.\} \\
V_D &= \frac{g_R^2}{8} \sum_a \left|\mathrm{Tr}(2\Delta^{c\dagger} \tau_a \Delta^c + 2\overline{\Delta}^{c\dagger} \tau_a \overline{\Delta}^c + \Phi_a \tau_a^T \Phi_a^\dagger)\right|^2 \\
&+ \frac{g'^2}{8} \left|\mathrm{Tr}(2\Delta^{c\dagger} \Delta^c + 2\overline{\Delta}^{c\dagger} \overline{\Delta}^c)\right|^2 \ . \qquad (2.108)
\end{aligned}$$

If we consider a charged breaking vacuum structure for the Δ^c and $\overline{\Delta}^c$ fields given as

$$\langle \Delta^c \rangle = \begin{pmatrix} 0 & v_R \\ v_R & 0 \end{pmatrix}, \ \langle \overline{\Delta}^c \rangle = \begin{pmatrix} 0 & \overline{v}_R \\ \overline{v}_R & 0 \end{pmatrix}, \qquad (2.109)$$

it can be shown that the Higgs potential is lower compared to the charge conserving vacuum given in Eq. (2.22). The F term and the soft SUSY breaking terms will be the same for both vacuua whereas the D term of the potential will vanish for the charged breaking vacuum while being positive definite for the charge conserving one. This would lead to a charge breaking vacuum to be the stable one which is unphysical. The solution to this problem lies in the calculation of the loop correction to the Higgs potential and then the total potential can be shown to be lower for the physically acceptable charge conserving vacuum.

The doubly-charged Higgs mass-squared matrix in the basis $(\delta^{c^{--^*}}, \overline{\delta}^{c^{++}})$ is given as

$$M^2_{\delta^{++}} = \begin{pmatrix} -2g_R^2(|v_R|^2 - |\overline{v}_R|^2) - \frac{\overline{v}_R^*}{v_R} Y^* & Y \\ Y^* & 2g_R^2(|v_R|^2 - |\overline{v}_R|^2) - \frac{v_R}{\overline{v}_R^*} Y \end{pmatrix} \tag{2.110}$$

where $Y = \lambda A_\lambda S + |\lambda|^2 \left(v_R \overline{v}_R - \frac{M_R^2}{\lambda} \right)$ and the electroweak vev has been neglected. It can be easily seen that if the gauge couplings are neglected, then this matrix will have a massless mode. Thus in this limit, the loop corrections to this massless mode should remain finite [**?**]. Such a Goldstone boson cannot remain in the theory and hence we calculate the one-loop corrections to this massless doubly-charged Higgs boson in this limit and show that it gets a positive mass. We look at the Yukawa interaction of the doubly-charged Higgs boson and calculate the corresponding one-loop corrections.

We first identify the eigenstate corresponding to the Goldstone state. It is given as

$$G^{++} = \frac{v_R^* \delta^{c^{--^*}} + \overline{v}_R \overline{\delta}^{c^{++}}}{\sqrt{v_R^2 + \overline{v}_R^2}}. \tag{2.111}$$

The couplings that we would need to consider include the direct coupling of the doubly-charged particles to the electron and selectron fields, doubly-charged Higgs coupling to the neutral Higgs triplet and singlet Higgs bosons and the coupling of these neutral fields to the neutrino and sneutrino fields. We also need to calculate the masses of each of these particles.

The right-handed leptons and sleptons are the ones that are running inside the loops in the one-loop corrections to the Goldstone state. It consists of an almost massless electron, a heavy right-handed neutrino, two degenerate selectrons and two sneutrinos. If we denote

$$\widetilde{\nu}^c = \frac{n_1 + i n_2}{\sqrt{2}}, \ \widetilde{\nu}^{c^*} = \frac{n_1 - i n_2}{\sqrt{2}}, \tag{2.112}$$

then the masses of all the particles are then given as

$$M_{e^c} \approx 0,\ M^2_{\tilde{e}^c_{1,2}} = m^2_{L^c},\ M_{\nu^c} = f v_R,$$
$$M^2_{n_{1,2}} = m^2_{L^c} + \left[f^2 v_R^2 \pm (f\lambda \overline{v}_R v_S + f A_f v_R)\right] \tag{2.113}$$

where $m^2_{L^c}$ is the soft mass for the sleptons and A_f is the trilinear coupling.

The neutral Higgs sector relevant for our calculation would include the $\delta^{c^0}, \overline{\delta}^{c^0}$ and S fields. Let us write them as

$$\delta^{c^0} = \frac{X_1 + iY_1}{\sqrt{2}},\ \overline{\delta}^{c^0} = \frac{X_2 + iY_2}{\sqrt{2}},\ S = \frac{X_3 + iY_3}{\sqrt{2}}. \tag{2.114}$$

If we choose all the couplings and the vevs to be real, then we will get two 3×3 mass-squared matrices for these fields– one for the real part and another for the imaginary part. We only need to consider the real fields as the imaginary fields will have no relevant cubic couplings to the Goldstone field. We will look at this mass-squared matrix a little later but first we give the relevant interaction terms in the Lagrangian which would be necessary for our calculation. These are given as

$$\begin{aligned}
-\mathcal{L}_{int} &= G^{++}G^{--}\left[(|\tilde{e}^c_1|^2 + |\tilde{e}^c_2|^2)\frac{f^2 v_R^2}{v_R^2 + \overline{v}_R^2} + \sqrt{2}\frac{\lambda^2 v_R \overline{v}_R^2}{v_R^2 + \overline{v}_R^2} X_1 + \sqrt{2}\frac{\lambda^2 v_R^2 \overline{v}_R}{v_R^2 + \overline{v}_R^2} X_2\right. \\
&+ \left.\sqrt{2}\left(\lambda^2 v_S + \frac{\lambda A_\lambda v_R \overline{v}_R}{v_R^2 + \overline{v}_R^2}\right) X_3\right] - \left[\frac{f A_f v_R + f\lambda \overline{v}_R v_S}{2\sqrt{v_R^2 + \overline{v}_R^2}}(\tilde{e}^c_1 \tilde{e}^c_1 + \tilde{e}^c_2 \tilde{e}^c_2) G^{--}\right] \\
&+ \left[\frac{f A_f}{2\sqrt{2}}(n_1^2 - n_2^2) + \frac{f^2 v_R}{\sqrt{2}}(n_1^2 + n_2^2)\right] X_1 \\
&+ \frac{f\lambda v_S}{2\sqrt{2}}(n_1^2 - n_2^2) X_2 + \frac{f\lambda \overline{v}_R}{2\sqrt{2}}(n_1^2 - n_2^2) X_3.
\end{aligned} \tag{2.115}$$

The mass-squared matrix for the neutral scalar Higgs bosons is given as

$$M_h^2 = \begin{pmatrix}
M_1^2 + \lambda^2(v_S^2 + \overline{v}_R^2) & \lambda^2 v_R \overline{v}_R + \lambda A_\lambda v_S - \lambda^2 M_R^2 & 2\lambda^2 v_S v_R + \lambda A_\lambda \overline{v}_R \\
\lambda^2 v_R \overline{v}_R + \lambda A_\lambda v_S - \lambda^2 M_R^2 & M_2^2 + \lambda^2(v_S^2 + v_R^2) & 2\lambda^2 v_S \overline{v}_R + \lambda A_\lambda v_R \\
2\lambda^2 v_S v_R + \lambda A_\lambda \overline{v}_R & 2\lambda^2 v_S \overline{v}_R + \lambda A_\lambda v_R & M_S^2 + \lambda^2(v_R^2 + \overline{v}_R^2)
\end{pmatrix}. \tag{2.116}$$

Usually one would need to diagonalize this mass-squared matrix and identify the mass eigenstates. Fortunately that is not the case here. Let us choose a basis given as

$$\hat{X} = V^T X \tag{2.117}$$

where $X = \begin{pmatrix} X_1 & X_2 & X_3 \end{pmatrix}^T$, V is an orthogonal transformation matrix and $\hat{X}$ represent the mass eigenbasis. Then the diagonal mass-squared matrix is given as

$$D^2 = V^T M_h^2 V. \tag{2.118}$$

All the couplings of the neutral Higgs bosons can now be written as

$$-\mathcal{L}_{\hat{X}} = P_i V_{ij} \hat{X}_j G^{++} G^{--} + Q_i V_{ij} \hat{X}_j n_1^2 + R_i V_{ij} \hat{X}_j n_2^2 + T_i V_{ij} \hat{X}_j \nu^c \nu^c \tag{2.119}$$

where P, Q, R and T are vectors given as

$$\begin{aligned}
P &= \left[\sqrt{2} \tfrac{\lambda^2 v_R \overline{v}_R^2}{v_R^2 + \overline{v}_R^2} \quad \sqrt{2} \tfrac{\lambda^2 v_R^2 \overline{v}_R}{v_R^2 + \overline{v}_R^2} \quad \sqrt{2} \left(\lambda^2 v_S + \tfrac{\lambda A_\lambda v_R \overline{v}_R}{v_R^2 + \overline{v}_R^2} \right) \right], \\
Q &= \left[\tfrac{f A_f}{2\sqrt{2}} + \tfrac{f^2 v_R}{\sqrt{2}} \quad \tfrac{f \lambda v_S}{2\sqrt{2}} \quad \tfrac{f \lambda \overline{v}_R}{2\sqrt{2}} \right], \\
R &= \left[\tfrac{-f A_f}{2\sqrt{2}} + \tfrac{f^2 v_R}{\sqrt{2}} \quad -\tfrac{f \lambda v_S}{2\sqrt{2}} \quad -\tfrac{f \lambda \overline{v}_R}{2\sqrt{2}} \right], \\
T &= \left[\tfrac{f}{\sqrt{2}} \quad 0 \quad 0 \right].
\end{aligned} \tag{2.120}$$

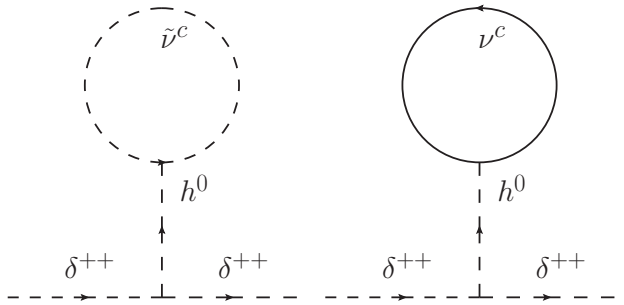

Figure 2.5: Feynman diagrams for neutrino and sneutrino one-loop correction

We can now calculate the one-loop corrections to the doubly-charged Higgs boson mass. The corrections coming from the right-handed neutrino and sneutrino sector

are given by the Feynman diagrams in Fig. 2.5. The corresponding amplitudes are given as

$$\begin{aligned} M_1 &= -\frac{i}{2}\left[P^T M_h^{-2} Q \int \frac{d^4k}{(2\pi)^4}\frac{1}{k^2-m_{n_1}^2} + P^T M_h^{-2} R \int \frac{d^4k}{(2\pi)^4}\frac{1}{k^2-m_{n_2}^2}\right], \\ M_2 &= 2iM_{\nu^c} P^T M_h^{-2} T \int \frac{d^4k}{(2\pi)^4}\mathrm{Tr}\left(\frac{\not{k}+M_{\nu^c}}{k^2-M_{\nu^c}^2}\right). \end{aligned} \tag{2.121}$$

The Feynman diagrams for the electron and selectron corrections are given in Fig. 2.6

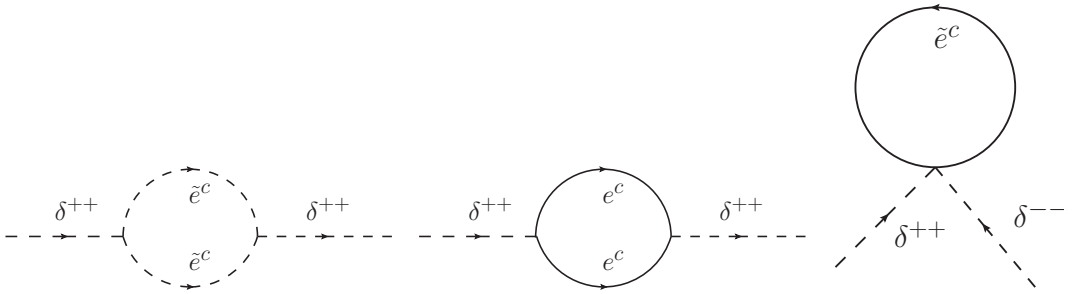

Figure 2.6: Feynman diagrams for electron and selectron one-loop correction

and the corresponding amplitudes are given as

$$\begin{aligned} M_3 &= -\frac{i}{2}\frac{\left(fA_f v_R + f\lambda \overline{v}_R v_S\right)^2}{v_R^2+\overline{v}_R^2}\int \frac{d^4k}{(2\pi)^4}\frac{1}{k^2-m_{\tilde{e}^c}^2}, \\ M_4 &= -\frac{if^2 v_R^2}{v_R^2+\overline{v}_R^2}\int \frac{d^4k}{(2\pi)^4}\frac{1}{k^2}, \\ M_5 &= \frac{if^2 v_R^2}{v_R^2+\overline{v}_R^2}\int \frac{d^4k}{(2\pi)^4}\frac{1}{k^2-m_{\tilde{e}^c}^2} \end{aligned} \tag{2.122}$$

Summing over all the correction to the doubly-charged Higgs boson mass coming from these diagrams we get

$$\begin{aligned} \Delta M_{G^{++}}^2 &= \frac{1}{16\pi^2\left(v_R^2+\overline{v}_R^2\right)}\left[f^2 v_R^2 m_{\tilde{e}^c}^2 \ln\left(\frac{m_{\tilde{e}^c}^2}{M_{\nu^c}^2}\right) + \frac{f^2}{2}\left(\lambda\overline{v}_R v_S + A_f v_R\right)^2 \ln\left(\frac{m_{\tilde{e}^c}^2}{M_{\nu^c}^2}+1\right)\right. \\ &- \frac{f}{4}\left(A_f v_R + 2f v_R^2 + \lambda\overline{v}_R v_S\right) m_{n_1}^2 \ln\left(\frac{m_{n_1}^2}{M_{\nu^c}^2}\right) \\ &- \left.\frac{f}{4}\left(-A_f v_R + 2f v_R^2 - \lambda\overline{v}_R v_S\right) m_{n_2}^2 \ln\left(\frac{m_{n_2}^2}{M_{\nu^c}^2}\right)\right]. \end{aligned} \tag{2.123}$$

Choosing an appropriate set of parameters this correction can be made positive and hence the Goldstone boson would become a light doubly-charged Higgs boson.

2.8 Summary

The tree level Higgs boson mass in the Standard Model and MSSM is bounded by the mass of the Z boson while the Standard Model-like Higgs boson observed at the LHC has a mass of around 125 GeV. For a TeV scale supersymmeytric model, the loop corrections to the Higgs boson mass is not particularly big and to achieve a Higgs boson mass of 125 GeV, either the tri-linear couplings must be really big or the stop mass must be large. This problems can be solved if the tree level Higgs boson mass can be made larger. In this chapter we show that for the models we have described in the previous sections, we can push the tree level mass of the lightest Standard Model-like Higgs boson to a much higher value eliminating the need for large trilinear couplings or very heavy stop masses.

CHAPTER 3

NEW SIGNALS OF DOUBLY-CHARGED SCALARS AND FERMIONS AT THE LARGE HADRON COLLIDER

3.1 Introduction

Several extensions of the Standard Model (SM) predict the existence of doubly-charged Higgs bosons. In some cases these particles remain light, which motivates searches for them in high energy collider experiments. The minimal left-right supersymmetric model with automatic R-parity conservation is an example, where a light doubly-charged Higgs boson arises as a pseudo-Goldstone boson of the $SU(2)_R$ gauge symmetry breaking [28–31]. Models with radiative neutrino mass generation [32], Type-II see-saw mechanism [33] for small neutrino masses, and the 3-3-1 model [**?**] are some other examples of SM extensions which have doubly-charged Higgs bosons. Supersymmetric versions of these models also have doubly-charged Higgsinos, which are the fermionic partners of the Higgs bosons. If the doubly-charged Higgs boson is light, its Higgsino partner cannot be much heavier and must have mass of the order a few hundred GeV to a few TeV, in the context of low energy supersymmetry (SUSY).

In this chapter we study a new signal for the doubly-charged Higgs bosons and Higgsinos in SUSY models which arises through the pair-production of the doubly-charged Higgsinos. Each Higgsino decays into a doubly-charged Higgs boson and the lightest supersymmetric particle (LSP) which escapes detection. Thus the final state would have four leptons and missing transverse energy, with the same-sign dileptons originating from the decays of the doubly-charged Higgs bosons showing characteristic peaks in the invariant mass distribution. We show by detailed calculations in the

context of left-right supersymmetric model that the reach at the LHC for both these doubly-charged particles can be enhanced by studying this mode. While we focus on the minimal supersymmetric left-right model, these new signals should also be present in other SUSY models with a light doubly-charged Higgsino and a lighter doubly-charged Higgs boson.

The focus of our analysis will be the minimal supersymmetric left-right gauge model. Left-right symmetric models [13] have a number of attractive features which are not naturally present in the Standard Model. Firstly, it explains the small neutrino masses through the see-saw mechanism [35] in a compelling manner – unlike the SM, existence of right-handed neutrinos is required by gauge symmetry here. Secondly, it provides a natural understanding of the origin of parity violation as a spontaneous phenomenon [13]. Thirdly, with the inclusion of supersymmetry, this model solves the gauge hierarchy problem and in its simplest version, also provides an automatic R-parity. This symmetry arises as remnant of the $(B - L)$ gauge symmetry [36] and leads to a stable light supersymmetric particle which can be a candidate for dark matter. With supersymmetry these models also provide natural solutions to the strong CP problem and the SUSY CP problem [37].

In the minimal left-right supersymmetric model, the gauge group is extended to $G_{3221} = SU(3)_c \times SU(2)_L \times SU(2)_R \times U(1)_{B-L}$. The $SU(2)_R \times U(1)_{B-L}$ symmetry breaks at a high scale resulting in most of the new particles getting very heavy masses. The right-handed neutrino mass is at this scale and facilitates the generation of the light neutrino mass via the see-saw mechanism. The doubly-charged Higgs supermultiplet, on the other hand, remains light and can produce new signals which is the focus of our analysis in this chapter.

To understand why the doubly-charged Higgs boson remains light in the minimal model, we need to look at the symmetry breaking sector. To spontaneously break the $SU(2)_R$ gauge symmetry and to generate large Majorana mass for the right-

handed neutrino, we need to introduce a Higgs multiplet with quantum numbers $(1, 1, 3, -2)$ under the group G_{3221}. This right-handed triplet contains three complex fields: a doubly-charged, a singly-charged and a neutral field denoted by $\delta^{c^{--}}, \delta^{c^{-}}, \delta^{c^{0}}$ respectively. The $\delta^{c^{-}}$ and the phase of $\delta^{c^{0}}$ are absorbed by the gauge fields via the super-Higgs mechanism to generate masses for the $W_R^{\pm}$ and Z_R gauge bosons. The real part of $\delta^{c^{0}}$ gets a mass through the Higgs potential. The $\delta^{c^{--}}$ field, on the other hand, is not absorbed by any gauge bosons, nor does it acquire a mass from the superpotential of the minimal model. Thus it behaves like pseudo-Goldstone boson, acquiring its mass only after supersymmetry breaking.* As a result, the right-handed doubly-charged Higgs bosons and the doubly-charged Higgsinos remain light in this model.

The doubly-charged Higgs bosons decay to two same charge leptons, which can be seen relatively easily in collider experiments via the invariant mass peak in the dilepton mass spectrum. LHC has been looking for signals of doubly-charged Higgs boson in the four lepton final states [38,39]. The experimental lower limit inferred on the mass of such Higgs bosons would depend on the assumed branching ratios into leptons of definite flavors. For example, CMS experiment quotes a 95% CL lower limit of 355 GeV for the mass of a doubly-charged Higgs boson arising from an $SU(2)_L$ triplet, if it decays with equal branching ratios of 33% into e^+e^+, $\mu^+\mu^+$ and $\tau^+\tau^+$. The 95% CL lower limit on such a Higgs particle from the ATLAS experiment is 318 GeV. These limits are somewhat weaker for an $SU(2)_L$ singlet doubly-charged Higgs boson, since its production cross section is smaller compared to the case when it is a

*The superpotential of the model, which only has quadratic mass terms, has an enhanced global $U(3, c)$ (complexified $U(3)$) symmetry which is broken to an $U(2, c)$ by the VEV of this Higgs multiplet. This leads to five massless superfields of which three are absorbed to give mass to the heavy gauge bosons and the remaining are the two doubly-charged Higgs bosons. Since SUSY is unbroken at this stage, the doubly-charged Higgsino is degenerate with the doubly-charged Higgs boson.

$SU(2)_L$ triplet. For example, ATLAS collaboration quotes a lower limit on the mass of an $SU(2)_L$ singlet doubly-charged scalar that decays with a 33% BR into $\mu^+\mu^+$ of about 220 GeV, while the limit is about 210 GeV if it decays into e^+e^+ with the same branching ratio. We anticipate that the lower limit, when both modes are combined, would be somewhat smaller than 300 GeV, for an $SU(2)_L$ singlet, as in our case.[†]

The decay of doubly-charged Higgsino ($\widetilde{\delta}^{c^{\pm\pm}}$) through a doubly-charged Higgs boson ($\delta^{c^{\pm\pm}}$) can produce new signals through the following process:

$$\widetilde{\delta}^{c^{\pm\pm}} \to \delta^{c^{\pm\pm}} \tilde{\chi}_1^0 \to l^{\pm} l^{\pm} \tilde{\chi}_1^0 \ .$$

So the pair production of doubly-charged Higgsinos yields a final state consisting of four leptons and missing transverse energy due to the LSP escaping the detector. This process, which has not been explored before to the best of our knowledge, gives a unique collider signature which can help improve the discovery reach of doubly-charged particles. The invariant mass plot would show a peak at the doubly-charged Higgs mass for the same-sign lepton while there would be no such peak for opposite-sign leptons. The angular distributions for the final state leptons also show a peak at a low value of ΔR (defined later in the chapter) for same-sign leptons while the opposite-sign leptons have a peak at a much higher value. Using these distributions we can probe deeper into the model than one could just by looking at the pair production of the doubly-charged Higgs bosons. The cross section for pair production of doubly-charged Higgsinos is larger compared to the cross section for the pair production of doubly-charged Higgs bosons of the same mass. From the current data at the LHC, we expect around 30 events for the process discussed in this chapter, if the doubly-charged Higgs boson has a mass of about 500 GeV, and if it decays into a doubly-charged Higgs boson of mass around 300 GeV.

In section 3.2 we describe the model and the Lagrangian needed for our analysis.

[†]When an $SU(2)_L$ singlet doubly-charged Higgs boson decays 100% of the time into $\mu^+\mu^+$ (or e^+e^+), the ATLAS lower limit on its mass is about 310 (or 320) GeV [39].

We also explain the origin of masses of the doubly-charged Higgs boson and the Higgsino and show that they remain light. In section 3.3, we present our analysis of the production and decay of the doubly-charged scalars and fermions and give the collider signatures which can be observed at the LHC. Section 3.4 gives a discussion of the results that we have obtained and how we can distinguish our signal against the background.

3.2 A brief review of the Left-Right Supersymmetric Model

In this section, we briefly review the relevant features of the minimal supersymmetric left-right model (LRSUSY) necessary for the analysis which follows in the later sections [28, 31].[‡] The chiral matter for this model is given in Eq. (2.1) while the Higgs sector is the same as in Eq. (2.2).

The superpotential of the model is given as

$$\begin{aligned} W &= Y_u Q^T \tau_2 \Phi_1 \tau_2 Q^c + Y_d Q^T \tau_2 \Phi_2 \tau_2 Q^c + Y_\nu L^T \tau_2 \Phi_1 \tau_2 L^c + Y_l L^T \tau_2 \Phi_2 \tau_2 L^c \\ &+ i(f^* L^T \tau_2 \Delta L + f L^{c^T} \tau_2 \Delta^c L^c) \\ &+ S[Tr(\lambda^* \Delta \overline{\Delta} + \lambda \Delta^c \overline{\Delta}^c) + \lambda_{ab}^{'} Tr(\Phi_a^T \tau_2 \Phi_b \tau_2) - M_R^2] + W' \end{aligned} \tag{3.1}$$

where

$$W' = \left[M_\Delta Tr(\Delta \overline{\Delta}) + M_\Delta^* Tr(\Delta^c \overline{\Delta}^c)\right] + \mu_{ab} Tr\left(\Phi_a^T \tau_2 \Phi_b \tau_2\right) + M_S S^2 + \lambda_S S^3 \tag{3.2}$$

Here $Y_{u,d}$ and $Y_{\nu,l}$ are the Yukawa couplings for quarks and leptons respectively and f is the Majorana neutrino Yukawa coupling matrix. This is the most general superpotential. R-parity is automatically preserved in this case, which is a consequence of $(B-L)$ being part of the gauge symmetry. Putting $W'=0$ gives an enhanced $U(1)$ R-symmetry in the theory. Under this R-symmetry, Q, Q^C, L, L^C fields have a charge of $+1$, S has charge $+2$ and all other fields have charge zero with W carrying

[‡]For alternative versions of SUSY left-right model, see Ref. [40].

a charge of +2. Putting $W' = 0$ also helps in understanding the μ-parameter of MSSM since it is induced as $\mu \sim \lambda' \langle S \rangle$ from Eq. (3.1), which is of the scale of SUSY breaking, as necessary. Setting $W' = 0$ would make the doubly-charged left-handed and right-handed Higgsinos degenerate in mass since both masses are given by $\lambda \langle S \rangle$, see Eq. (3.1).[§]

The $SU(2)_R \times U(1)_{B-L}$ symmetry is broken at a large scale by giving a large vacuum expectation value to the right-handed triplet Higgs boson fields Δ^c and $\overline{\Delta}^c$. This generates a large right-handed neutrino mass, $M_{\nu^c} = 2fv_R$, where v_R is the vacuum expectation value of the δ^{c^0} field which breaks the $SU(2)_R$ symmetry. This helps generate a small Majorana mass for the left-handed neutrino via the see-saw mechanism [35]. The bidoublets get VEVs of the order of electroweak symmetry breaking scale and generate the masses of the quarks and leptons. The singlet S gets a VEV of order the SUSY breaking scale, and helps solve the μ-problem of the MSSM, assuming that $W' = 0$.

The terms in the Lagrangian which will be most essential for our calculation later are the gauge kinetic terms for the triplet superfields and the quarks and leptons. These terms will give us the interaction vertices between the Higgs boson fields and the gauge bosons as well as the the fermions and the gauge bosons [41]. The kinetic terms for the triplet scalar fields and the fermions are given by:

$$L = i \sum Tr[\overline{q}_i \not{D} q_i] + Tr[(D^\mu \Phi_i)^\dagger (D_\mu \Phi_i)] \tag{3.3}$$

where $q_i = Q, Q^c, \widetilde{\Delta}, \widetilde{\overline{\Delta}}, \widetilde{\Delta^c}, \widetilde{\overline{\Delta}^c}$ and $\Phi_i = \Delta, \overline{\Delta}, \Delta^c, \overline{\Delta}^c$. The covariant derivatives are defined as

$$D_\mu Q \;\; = \;\; [\partial_\mu - i\frac{g_L}{2}\vec{\tau} \cdot \vec{W}_{\mu L} - i\frac{g_V}{6} V_\mu] Q$$

[§]Keeping a non-zero W' term does not affect the right-handed particle spectrum, but the left-handed Higgsino becomes very heavy in this case and will not contribute to our new signal. We present results of our analysis with and without the left-handed doubly-charge Higgsino in the light spectrum, so this effect can be disentangled.

$$
\begin{aligned}
D_\mu Q^c &= [\partial_\mu + i\frac{g_R}{2}\vec{\tau}\cdot\vec{W}_{\mu R} + i\frac{g_V}{6}V_\mu]Q^c \\
D_\mu \Delta &= \partial_\mu \Delta - i\frac{g_L}{2}[\vec{\tau}\cdot\vec{W}_{\mu L}, \Delta] - ig_V V_\mu \Delta \\
D_\mu \overline{\Delta} &= \partial_\mu \overline{\Delta} - i\frac{g_L}{2}[\vec{\tau}\cdot\vec{W}_{\mu L}, \overline{\Delta}] + ig_V V_\mu \overline{\Delta} \\
D_\mu \Delta^c &= \partial_\mu \Delta^c + i\frac{g_R}{2}[\vec{\tau}\cdot\vec{W}_{\mu R}, \Delta^c] + ig_V V_\mu \Delta^c \\
D_\mu \overline{\Delta^c} &= \partial_\mu \overline{\Delta^c} + i\frac{g_R}{2}[\vec{\tau}\cdot\vec{W}_{\mu R}, \overline{\Delta^c}] - ig_V V_\mu \overline{\Delta^c}\ . \qquad (3.4)
\end{aligned}
$$

The covariant derivatives for $\widetilde{\Delta}$,$\widetilde{\overline{\Delta}}$,$\widetilde{\Delta^c}$,$\widetilde{\overline{\Delta}^c}$ have similar form as Δ,$\overline{\Delta}$,Δ^c,$\overline{\Delta}^c$ respectively.

We now turn to some details of the calculation of the masses of doubly-charged Higgs boson [30, 31, 42, 43] and the Higgsinos. This will show that these particles are indeed light and will help us in our analysis later on. In the context of type-II seesaw mechanism without supersymmetry, signatures of doubly-charged Higgs bosons at the LHC has been studied in Ref. [44] and in Ref. [45] recently. The main difference in our study is the inclusion of doubly-charged Higgsino, which helps enhance the multi-lepton signals.

3.2.1 Doubly-charged Higgs boson

The doubly-charged Higgs boson mass has been studied in details in Section 2.7. Here we briefly review some of the important results. The right-handed doubly-charged Higgs boson mass-squared matrix is given at tree-level as:

$$
M^2_{\delta^{++}} = \begin{pmatrix} -2g_R^2(|v_R|^2 - |\overline{v_R}|^2) - \frac{\overline{v_R}}{v_R}Y & Y^* \\ Y & 2g_R^2(|v_R|^2 - |\overline{v_R}|^2) - \frac{v_R}{\overline{v_R}}Y \end{pmatrix} \qquad (3.5)
$$

where

$$
Y = \lambda A_\lambda S + |\lambda|^2(v_R\overline{v}_R - \frac{M_R^2}{\lambda})\ .
$$

Solving for the squared mass, it can be seen that one of the eigenvalues is negative. Including the contribution from the one-loop correction to the mass the eigenvalues become [31]

$$
M^2_{\delta^{\pm\pm}} = \frac{-Y(|v_R|^2 + |\overline{v_R}|^2) \pm \sqrt{(|v_R|^2 + |\overline{v_R}|^2)^2|4g_R^2 v_R\overline{v_R} - Y|^2 + 4|v_R|^2|\overline{v_R}|^2|Y|^2}}{2|v_R||\overline{v_R}|}
$$

$$+ \quad \mathcal{O}(\frac{M_{SUSY}^2}{16\pi^2}) \tag{3.6}$$

where M_{SUSY} is the mass scale for the supersymmetry breaking which we assume to be $\sim$ 1 TeV. The factor of $1/(16\pi^2)$ factor comes from the one loop corrections as can be seen in Eq. (2.123). Explicit calculation of the effective potential utilizing the Majorana Yukawa couplings of the right-handed neutrino shows that the eigenvalue which is negative at the tree-level can be made positive, thus making the symmetry breaking consistent. This makes the mass of the right-handed doubly-charged Higgs boson to be of the electroweak scale, of order few hundred GeV. It is naturally lighter than the doubly-charged Higgsino, since there is no loop suppression for its mass. This light doubly-charged Higgs boson will be denoted as $\delta_R^{\pm\pm}$ in this chapter.

A light doubly-charged Higgs boson can also be obtained in left-right supersymmetric models which include non-renormalizable operators in the superpotential [29]. Terms in the superpotential of the type $(\Delta^c\bar{\Delta}^c)^2/M_{\rm Pl}$ will give mass to the doubly-charged Higgs bosons and Higgsinos of order few hundred GeV without resort to the Coleman-Weinberg effective potential, provided that the $SU(2)_R$ breaking scale is in the range of $v_R \sim (10^{11} - 10^{12})$ GeV. Our analysis will also be valid for these models with light doubly-charged particles.

The left-handed doubly-charged Higgs boson mass-squared matrix looks very similar to the right-handed case except that the VEVs of the right-handed neutral Higgs boson fields are now replaced by the VEVs of the left-handed fields which we assume to be negligible. Hence the mass of the left-handed doubly-charged Higgs boson become of the order of M_R, which is of the scale of the $SU(2)_R$ symmetry breaking and hence large. This happens because in the Higgs boson potential, there is a cancellation between the terms $|\lambda|^2(v_R\overline{v}_R)$ and $\frac{M_R^2}{\lambda}$, arising from the vanishing of the F-terms, which is not present for the left-handed doubly-charged Higgs boson mass-squared matrix. We denote the left-handed doubly charged Higgs boson as $\delta_L^{\pm\pm}$.

3.2.2 Doubly-charged Higgsino

The right-handed doubly-charged Higgsino gets its mass only from the superpotential Eq. (3.1) and has the form $\lambda \langle S \rangle$. In the supersymmetric limit, $\langle v_R \rangle = \langle \overline{v}_R \rangle$ (which arises from the vanishing of the D terms) and $\langle S \rangle = 0$ (which arises from the vanishing of the F terms), and thus the Higgsino mass is zero in this limit. After supersymmetry breaking, the singlet S gets a VEV which is of the order of M_{SUSY}. Taking λ to be of order one, we see that its mass is at the SUSY breaking scale. Thus the Higgsino has to be relatively light if we consider supersymmetry to be broken at a scale of $\sim$ 1 TeV.

The left-handed doubly-charged Higgsino would become heavy if we turn on the W' term in the superpotential. In this chapter we will consider $W' = 0$ and hence the left-handed and the right-handed doubly-charged Higgsinos remain degenerate. However, the case of left-handed Higgsino being heavy can be inferred from our results, since we separate out its contribution to the four lepton plus missing $\not{E}_T$ final states.

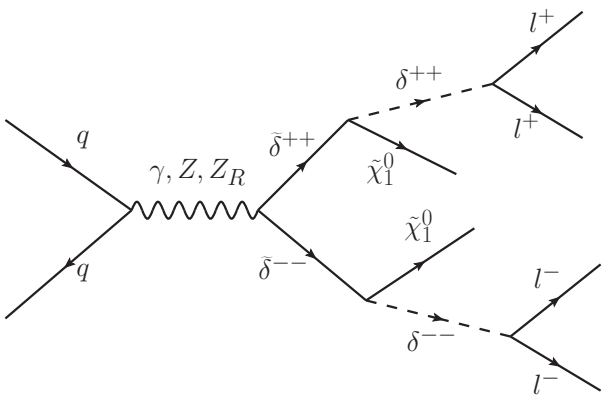

Figure 3.1: *Direct production of $\widetilde{\delta}_R^{\pm\pm}$ pair at the LHC. Subsequent decays of $\widetilde{\delta}_R^{\pm\pm}$ give rise to two leptons plus missing energy signal, if $M_{\delta_R^{\pm\pm}} < M_{\widetilde{\delta}_R^{\pm\pm}}$.*

3.3 Signals of doubly-charged scalars and fermions at LHC

In this section we discuss the signal for doubly charged Higgsinos at LHC and analyze the final states coming from the pair-production of the doubly-charged Higgsinos and their subsequent decay.[¶] The doubly charged Higgsinos are pair-produced at the LHC through the process

$$p\,p \longrightarrow \widetilde{\delta}^{++}_{L,R}\widetilde{\delta}^{--}_{L,R} \text{ (illustrated in Fig. 3.1)}$$

which proceeds through s-channel γ and $Z_{L,R}$ exchanges [46]. As the mass of Z_R is dependent on the scale at which the $SU(2)_R$ is broken, its contribution will vary depending upon its allowed values. In the minimal left-right supersymmetric model, there is a relation between the W_R and the Z_R mass where $M_{Z_R} \sim 1.7 M_{W_R}$. Therefore the current limit on the W_R mass of about 2.5 TeV [47] requires the Z_R to be rather heavy. This heavy Z_R has very small contributions to the pair-production cross section of the doubly charged Higgsinos. In our analysis we have fixed the Z_R mass at 5 TeV and find that the contributions from Z_R exchange only become comparable to the electroweak gauge boson exchanges for large values of the doubly charged Higgsino mass, where the overall signal is quite suppressed.

We focus on a natural scenario where the only "light" states beyond the SM are the doubly-charged Higgs boson, doubly-charged Higgsino and the lightest neutralino, which is the LSP. The left-handed doubly-charged Higgsino is degenerate with the right-handed doubly-charged Higgsino (in the case where $W' = 0$). All other SUSY particles are assumed to be much heavier. We further assume that the doubly-charged Higgsino is heavier than the right-handed doubly charged Higgs boson and the lightest neutralino. Then the dominant decay channel for the doubly-charged Higgsino is to the light doubly-charged Higgs boson and the LSP neutralino, which we assume is allowed by kinematics. The branching ratio for this process is almost 1 in this scenario

[¶]The relevant Feynman rules are listed in the Appendix.

as the next leading decay mode is into a lepton and an off-shell slepton which is highly suppressed. The right-handed doubly-charged Higgs boson now decays almost entirely into two same sign leptons giving rise to a final signal of 4 leptons and missing energy. Other decay modes of the right-handed doubly-charged Higgs boson would be into two real or virtual W_R bosons or a W_R and a single-charged Higgs boson. Both the W_R and the single-charged Higgs boson are very heavy in this model and hence those decays will be forbidden or highly suppressed. The entire decay chain is then,

- $\widetilde{\delta}_R^{\pm\pm} \to \delta_R^{\pm\pm}\widetilde{\chi}_1^0$
- $\delta_R^{\pm\pm} \to \ell^\pm\ell^\pm$

Though the right-handed doubly-charged Higgsino decays almost always into a right-handed doubly-charged Higgs boson and a neutralino, the left-handed doubly-charged Higgsino which is degenerate with the right-handed doubly-charged Higgsino cannot decay through this channel as the left-handed doubly-charged Higgs boson is much heavier. The main decay channel for the left-handed Higgsino is then given by the three-body decay through an off-shell slepton and a lepton, where the off-shell slepton mediates the decay into a lepton and a neutralino [46]. This produces the same final state product as our signal and is therefore a source of background if we consider the signal coming only from the right-handed doubly charged Higgsinos. The left-handed doubly-charged Higgsino production cross-section is larger than the right-handed Higgsino due to the Z-boson coupling strength being larger to the left-handed particles and hence we also need to analyze the decay of the left-handed Higgsino and include its contributions. We must however note that both the right-handed and left-handed Higgsino pair production leads to a four-lepton final state with large missing transverse momenta because of the presence of the undetected LSP passing through the detector. Another source for the four-lepton final state would come from the pair production of the light doubly-charged Higgs boson present in the model. Presence

of such doubly-charged Higgs bosons have been looked for by experimentalists in the context of various other models at Tevatron as well as LHC [51] which put strong limits on the masses of such particles.

In Fig. 3.2 we plot the production cross-sections for the pair production of doubly-charged Higgsinos (both chirality) as well as for the right-handed doubly-charged Higgs boson. Note that the production cross section for the left-handed doubly-charged Higgsino is much larger than the right-handed one. This is due to the bigger Z boson coupling with the left-handed doubly-charged Higgsino. However for larger values of the mass, the required center of mass energy to produce the particles in pair also increases and therefore an s-channel suppression would appear in the case of the left-handed doubly-charged Higgsino as the center of mass energy moves away from the Z boson pole mass, i.e. $\frac{1}{\hat{s}-M_Z^2} \to \frac{1}{\hat{s}}$ ($\hat{s} >> M_Z^2$). In comparison the Z_R contribution would increase as the center of mass energy starts approaching the Z_R boson pole mass, i.e. $\frac{1}{\hat{s}} \to \frac{1}{\hat{s}-M_{Z_R}^2}$ ($\hat{s} \sim M_{Z_R}^2$) which also has larger coupling to the right-handed doubly-charged Higgsino. This effect is visible for very large values of the Higgsino mass (although not shown in the Fig. 3.2) where we find that the production cross section for the left-handed Higgsino actually falls below the production cross section

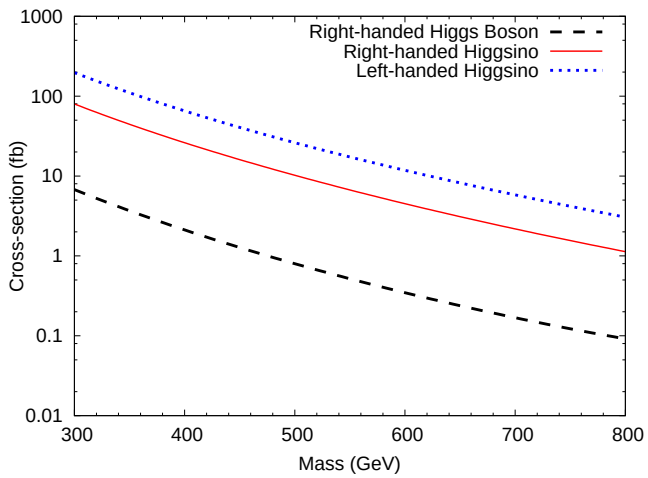

Figure 3.2: *Production cross sections for $\widetilde{\delta}_{L,R}^{\pm\pm}$ pair and $\delta_R^{\pm\pm}$ at the LHC at 14 TeV*

.

of the right-handed Higgsino. It can also be seen that the Higgsino production cross-sections are much larger than the doubly-charged Higgs boson production rate (for the same mass) and hence they effectively help in enhancing the 4-lepton signal at colliders. In general, from spin arguments we might expect the production cross-section of the fermion to be four times that of the scalar, but this is only true in the massless limit. One can think that since the center of mass energy is much higher than the masses of the particles the massless limit should be a good approximation, but turning on the parton distribution function produces partons of all energies and hence we get a cross-section ratio which is much higher. The Higgsino process also gives a unique signal with $4\ell + \not{E}_T$ which is not present for the doubly-charged Higgs boson pair-production process.

Considering the decays of the doubly-charged particles discussed before, we find that the final states coming from the pair production and subsequent decays of the doubly-charged Higgsinos are two pairs of same-sign leptons of same or different flavor (i.e., e or μ) and missing energy. We want to focus on all the possibilities with the final states consisting of same flavor or different flavor leptons, with and without missing energy.

As we have no hint of SUSY signals yet at the LHC, it can be safely assumed that the SUSY particles are heavy and difficult to produce at the current energies at which LHC was run. We therefore restrict ourselves to the low lying mass spectrum of some of the SUSY particles and their decay probabilities to study its signals. Since the model in study naturally accommodates light doubly-charged particles, we assume all other SUSY partners as well as the Higgs scalars to be much heavier than the doubly-charged Higgsinos and the doubly charged Higgs boson (from the right-handed sector). The only other particle which is assumed to be lighter is the lightest neutralino, which is the LSP. With this choice of the spectrum, the decay patterns for the doubly charged particles are known and have already been discussed earlier.

To highlight the signal we have considered two representative points :

- The first choice, which we call **BP1** (Benchmark Point 1), we consider a doubly-charged Higgs boson with mass 300 GeV, an LSP neutralino with a mass of 80 GeV, charged sleptons with mass of 1 TeV and doubly-charged Higgsinos with a mass of 500 GeV. With this choice we focus our attention on two particular scenarios. First, we analyze the situation where all the finals state leptons coming from the decay are of the same flavor (e.g all the final state leptons are either electrons or muons) while the other case is when each doubly-charged particle decays to a different flavor pair (e.g. two same sign electrons and two same sign muons).

- The second choice, which we call **BP2**, we consider a lower value for the mass of doubly-charged Higgsino as 400 GeV while the other mass choices remain the same. Note that this choice gives a larger production rate for the doubly-charged Higgsinos, but also affects the kinematics of the final state decay products because of smaller mass splitting between the doubly-charged Higgsino and the doubly-charged Higgs boson.

In our analysis, for the charged lepton final states we have considered the signal consisting of either electrons or muons only and neglected the tau lepton. Nevertheless the decay of the doubly-charged Higgs boson to tau lepton pair will be very similar to the decay into muons and electrons and is only considered less relevant due to the limited tau-tagging efficiency at experiments. However, the signal will also be dictated by the decay probabilities of the doubly-charged scalar into the charged lepton pairs, and in models where the Yukawa structure demands that the decays are maximally to a pair of same sign taus, then one needs to consider the tau final states.

We now turn our focus to analyzing the final state signal consisting of the four charged leptons with or without missing transverse energy. Note that when we do not

demand any criterion for the missing transverse momenta in the final state, our signal contributions come from three different sources, *i.e.* pair production of the doubly-charged Higgsinos (both chirality) as well as the pair production of the doubly-charged scalars. This would not only enhance the four-lepton signal when compared to individual contributions but also help in identifying the nature of additional contributions to such multi-lepton final states. To study the signal we demand that the final state particles satisfy the following kinematic cuts:

- Each charged lepton must carry a minimum transverse momentum given by $p_T > 15$ GeV.
- The charged leptons must lie in the central rapidity region of $|\eta_\ell| < 2.5$.
- For proper resolution to detect the final state particles we set $\Delta R_{\ell\ell} > 0.2$ between the final state charged leptons, where $\Delta R = \sqrt{(\Delta\phi)^2 + (\Delta\eta)^2}$ defines the resolution of a pair of particles in the (η, ϕ) plane.
- We also specify an invariant mass cut between the opposite sign same flavor leptons such that $M_{\ell^+\ell^-} > 10\ GeV$ and a further cut of $80\ GeV > M_{\ell^+\ell^-} > 100\ GeV$, where the latter one is aimed at removing the SM contributions coming from resonant Z boson decays.

With the above set of kinematic selections we perform a detailed numerical analysis of the final state events of the multilepton signal as well as the SM background. For our numerical analysis, we have included the model description into the event generator `CalcHEP` [48] and generated the event files for the production and decays of the doubly-charged Higgsinos. These event files were then passed through the `CalcHEP+Pythia` [49] interface where we include the effects of both initial and final state radiations using Pythia switches to smear the final states. We have used the leading order CTEQ6L [50] parton distribution functions (PDF) for our analysis.

So there are three major processes that contribute to out signal.

- The direct pair-production of the right-handed doubly-charged Higgs bosons. Each Higgs boson then decays into a pair of same sign leptons producing a final state signal of 4 leptons. We call this ($\mathcal{C}1$)

$$p\ p \to \delta_R^{++}\delta_R^{--} \to \ell_i^+\ell_i^+\ell_j^-\ell_j^-$$

- Pair-production of right-handed doubly-charged Higgsino. Each Higgsino decays into a right-handed doubly-charged Higgs boson and a neutralino. The doubly-charged Higgs boson then decays into a pair of same-sign leptons giving a final state signal of 4 leptons and $\not{E}_T$. We call this ($\mathcal{C}2$)

$$p\ p \to \widetilde{\delta}_R^{++}\widetilde{\delta}_R^{--} \to \delta_R^{++}\delta_R^{--}\widetilde{\chi}_1^0\widetilde{\chi}_1^0 \to \ell_i^+\ell_i^+\ell_j^-\ell_j^-\not{E}_T$$

- Pair-production of left-handed doubly-charged Higgsino. The Higgsino decays through an off-shell slepton to a same sign lepton pair and a neutralino. This process also gives a final state signal with 4 leptons and $\not{E}_T$. We call this ($\mathcal{C}3$)

$$p\ p \to \widetilde{\delta}_L^{++}\widetilde{\delta}_L^{--} \to (\widetilde{\ell}_i^{*+}\ell_i^+)\ (\widetilde{\ell}_j^{*-}\ell_j^-) \to \ell_i^+\ell_i^+\ell_j^-\ell_j^-\widetilde{\chi}_1^0\widetilde{\chi}_1^0$$

All the three subprocesses mentioned above lead to a signal with four charged leptons in the final state which is a very clean signal at a hadron machine such as the LHC, with very little SM background, and therefore should be an interesting test for the model. Significantly one should note that the signal described by ($\mathcal{C}1$) is an important channel for the search of doubly charged particle resonances such as double charged scalars [51] or bileptons [52] and can appear even in R-parity violating supersymmetric models [53]. The highlight of course is that there is no source for missing transverse momenta in the signal. However, the other two signals described by ($\mathcal{C}2$) and ($\mathcal{C}3$) not only lead to four charged leptons in the final states but is also accompanied by large missing transverse momenta due to the LSP present in the final state. There could be numerous new physics scenarios where such a signal can be common and

so it would be interesting to be able to identify the signal associated with our model in a unique way. We find that our signal can in general be classified into two types,

LHC Energy	$\mathcal{C}1$		$\mathcal{C}2$		$\mathcal{C}3$	
	$\not{E}_T$ (GeV)		$\not{E}_T$ (GeV)		$\not{E}_T$ (GeV)	
	> 0	> 100	> 0	> 100	> 0	> 100
7 TeV	0.266 fb	0.033 fb	0.275 fb	0.226 fb	0.642 fb	0.568 fb
8 TeV	0.368 fb	0.048 fb	0.430 fb	0.359 fb	0.992 fb	0.927 fb
14 TeV	1.153 fb	0.228 fb	1.859 fb	1.649 fb	4.208 fb	3.667 fb

Table 3.1: *Cross-section table for a final state of* $\ell_i^+\ell_i^+\ell_i^-\ell_i^- + X$ *with* $M_{\tilde{\delta}^{\pm\pm}_{L,R}} = 500$ *GeV,*$M_{\delta_R^{\pm\pm}} = 300$ *GeV,* $M_{\tilde{\chi}_1^0} = 80$ *GeV and* $M_{\tilde{l}^\pm} = 1$ *TeV*

one where we only demand four charged leptons in the final state and do not put any requirement on the missing transverse momenta. The other type would be to demand a minimum missing transverse momenta in the final state in addition to the four tagged charged leptons. We list the cross-sections for the three subprocesses ($\mathcal{C}1$–$\mathcal{C}3$) at different LHC energies in Table 3.1 which gives the cross section for a final state consisting of same-sign pairs and all four of same-flavor (SF) charged leptons in our model for **BP1** where the doubly-charged Higgsino mass is taken as 500 GeV, doubly-charged Higgs boson mass of 300 GeV, slepton mass of 1 TeV and a neutralino mass of 80 GeV. Note that the signal cross sections are invariably larger for the ($\mathcal{C}3$) as it comes from the pair production of the left-handed doubly charged Higgsinos which has the greater production rate. We can see that without any missing E_T requirement on the final state, a somewhat lower cross section for the signal coming from the pair production of doubly charged scalar is found to be enhanced considerably by including contributions from the pair production of the doubly charged Higgsinos. This enhances the sensitivity of the experiment to exotic doubly charged particles through the four charged lepton final state. With a minimum

missing E_T requirement of 100 GeV on the events, it is found that the signal coming from the pair production of the doubly charged scalars is reduced drastically while the events from the pair production of the doubly charged Higgsinos are not affected much. This is expected because the doubly charged Higgsinos decay to final states consisting of the undetected LSP which carries off substantial missing energy and therefore satisfies the large $\not{E}_T$ cut-off. In Table 3.2 we show the cross-section for

LHC Energy	$\mathcal{C}1$		$\mathcal{C}2$		$\mathcal{C}3$	
	$\not{E}_T$ (GeV)		$\not{E}_T$ (GeV)		$\not{E}_T$ (GeV)	
	> 0	> 100	> 0	> 100	> 0	> 100
7 TeV	0.302 fb	0.032 fb	0.314 fb	0.257 fb	0.753 fb	0.672 fb
8 TeV	0.418 fb	0.047 fb	0.480 fb	0.402 fb	1.152 fb	1.078 fb
14 TeV	1.266 fb	0.216 fb	1.989 fb	1.749 fb	4.655 fb	4.051 fb

Table 3.2: *Cross-section table for a final state of* $\ell_i^+\ell_i^+\ell_j^-\ell_j^- + X$ *with* $M_{\tilde{\delta}^{\pm\pm}_{L,R}} = 500$ *GeV,*$M_{\delta^{\pm\pm}_R} = 300$ *GeV,* $M_{\tilde{\chi}^0_1} = 80$ *GeV and* $M_{\tilde{l}^\pm} = 1$ *TeV*

a final state consisting of same-sign pairs where each pair is of different-flavor (DF) leptons for **BP1**. Here we assume that one of the doubly-charged particle decays to one particular flavor of the charged leptons while the other decays to a different flavor. So the final states would have four charged leptons of the type $e^\pm e^\pm \mu^\mp \mu^\mp$. Note that such a combination of final state would have practically no SM background as it requires at least four W bosons to give such a combination of charged leptons in the final state. We neglect the τ lepton as discussed before. The cross sections are slightly greater than those listed in Table 3.1 because we have removed the additional kinematic cut on the invariant mass on the opposite-sign same flavor leptons given by $80\ GeV > M_{\ell^+\ell^-} > 100\ GeV$. As our estimates rely on the assumption that the branching fractions for the doubly charged particles decay to each flavor of charged lepton is 1/3, we must point out that this final state will be relevant only when the

decay rates to either $e^{\pm}e^{\pm}$ or $\mu^{\pm}\mu^{\pm}$ are not too suppressed.

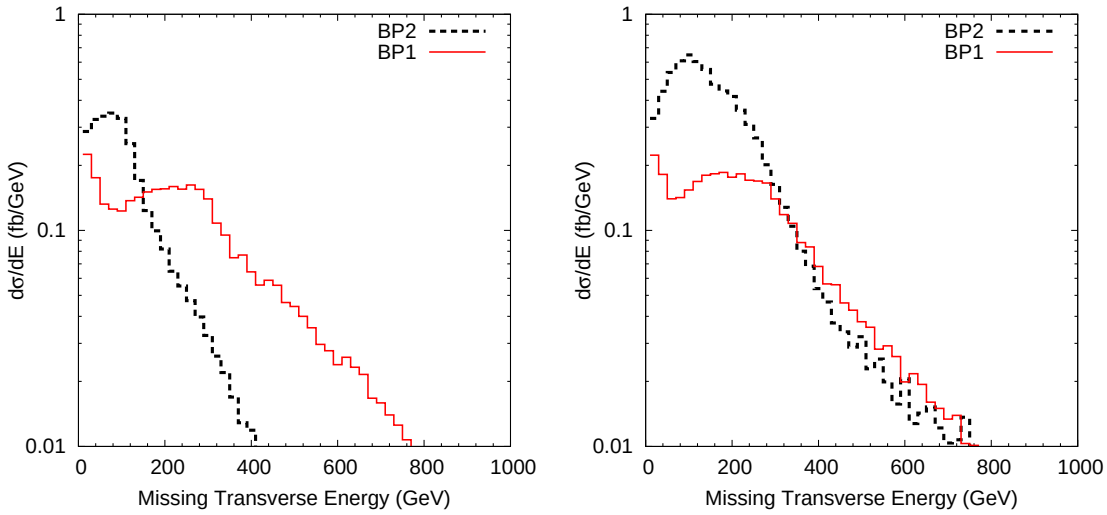

Figure 3.3: *(a) $\not{E}_T$ for doubly-charged Right-handed Higgsino and Higgs boson, (b) $\not{E}_T$ for doubly-charged Right-handed and Left-handed Higgsinos and Right-handed Higgs boson.*

We now consider a case where the doubly charged Higgsinos are slightly lighter (400 GeV) while the other particles have the same mass as before (**BP2**). This choice enhances the production rates for the doubly-charged Higgsinos but also gives a compressed spectrum for its decays. Note that a bigger mass difference between the parent particle and its decay products would lead to greater energy for the decay products. In this case, one expects that as the LSP mass and the doubly charged Higgs mass add up very close to the doubly-charged Higgsino mass, the missing transverse momenta in the events due to the LSP will be less compared to the previous case. This can be seen in Fig. 3.3 where we show the distribution for the differential cross section as a function of the missing transverse energy. In Fig. 3.3(a) we show the $\not{E}_T$ distribution in the signal events coming from the contributions of the right-handed doubly-charged Higgsino and Higgs while Fig. 3.3(b) shows $\not{E}_T$ distribution for contributions from both the right-handed and left-handed doubly-charged Higgsino including the doubly charged Higgs boson. We see that differential cross section in

Fig. 3.3(a) has a higher fraction of events at very small $\not{E}_T$. This is because of the contribution from the direct pair production of the doubly-charged Higgs boson which will have very little missing energy which might originate due to mismeasurements of the final state particles, as there is no other source of missing energy in the form of the neutralino in the final state. In Fig. 3.3(b) this effect is washed away because the number of events from the left handed doubly-charged Higgsino pair-production

LHC Energy	$\mathcal{C}1$		$\mathcal{C}2$		$\mathcal{C}3$	
	$\not{E}_T$ (GeV)		$\not{E}_T$ (GeV)		$\not{E}_T$ (GeV)	
	> 0	> 20	> 0	> 20	> 0	> 20
7 TeV	0.266 fb	0.143 fb	0.871 fb	0.823 fb	1.797 fb	1.774 fb
8 TeV	0.368 fb	0.203 fb	1.248 fb	1.183 fb	2.576 fb	2.550 fb
14 TeV	1.153 fb	0.737 fb	4.467 fb	4.309 fb	8.892 fb	8.806 fb

Table 3.3: *Cross-section table for a final state of* $\ell_i^+\ell_i^+\ell_i^-\ell_i^- + X$ *with* $M_{\widetilde{\delta}^{\pm\pm}_{L,R}} = 400$ *GeV,*$M_{\delta_R^{\pm\pm}} = 300$ *GeV,* $M_{\widetilde{\chi}_1^0} = 80$ *GeV and* $M_{\widetilde{l}^{\pm}} = 1$ *TeV*

is now much larger compared to both the doubly-charged Higgs boson and Higgsino pair-production and hence their contribution is suppressed.

In Table 3.3 we give the cross sections for a final state consisting of the same-flavored charged leptons for **BP2**. Note that we have a slightly weaker requirement on the missing transverse energy of 20 GeV for the events corresponding to **BP2**. This is to avoid large suppression of the signal which can happen due to the smaller mass splittings.

In Table 3.4 we give the cross sections for a final state consisting of different-flavored charged lepton pairs for **BP2**. Again the kinematic characteristics for the events remain the same as before but the cross section is slightly greater than that for SF events because of the removal of the kinematic cut corresponding to the invariant mass removing the Z peak for opposite sign same flavor charged lepton pairs.

LHC Energy	$\mathcal{C}1$		$\mathcal{C}2$		$\mathcal{C}3$	
	$\not{E}_T$ (GeV)		$\not{E}_T$ (GeV)		$\not{E}_T$ (GeV)	
	> 0	> 20	> 0	> 20	> 0	> 20
7 TeV	0.302 fb	0.149 fb	1.009 fb	0.949 fb	2.332 fb	2.308 fb
8 TeV	0.418 fb	0.213 fb	1.451 fb	1.358 fb	3.327 fb	3.288 fb
14 TeV	1.266 fb	0.721 fb	4.804 fb	4.610 fb	10.886 fb	10.767 fb

Table 3.4: *Cross-section table for a final state of* $\ell_i^+\ell_i^+\ell_j^-\ell_j^- + X$ *with* $M_{\widetilde{\delta}^{\pm\pm}_{L,R}} = 400$ *GeV,*$M_{\delta^{\pm\pm}_R} = 300$ *GeV,* $M_{\widetilde{\chi}^0_1} = 80$ *GeV and* $M_{\widetilde{l}^{\pm}} = 1$ *TeV*

We must point out here that the corresponding SM background for the four charged lepton final state with our selection cuts on the kinematic variables is found to be completely negligible and therefore has not been shown or considered in our analysis. The most dominant background which one expects for the SF charged lepton signal will be from the pair production of Z bosons which we have suppressed using the invariant mass cut on the opposite-sign same flavor lepton pairs. However, as we have a light doubly-charged Higgs in the spectrum, we expect to see a resonance in the invariant mass distributions of like-signed charge lepton pairs. We have already shown that there are three different subprocesses for the signal contributions for the $4\ell + X$ final state and the cross-section for ($\mathcal{C}3$) is much larger than ($\mathcal{C}1$) and ($\mathcal{C}2$). Note that ($\mathcal{C}3$) corresponds to the signal where the left-handed doubly-charged Higgsino is pair produced and decays through an off-shell slepton. Therefore one does not expect any resonance behavior in the invariant mass distributions of the charged lepton pairs but a kinematic edge is expected [46]. This would mean that a part of the signal itself acts as a background to smear out the resonant signal for the doubly charged Higgs boson. This is in fact the highlight of our analysis where we show that our signal actually stands out as a resonance and is also enhanced because of the additional contributions coming from the heavy doubly charged fermion production.

To show some kinematic characteristics of the events for the SF signal we take the case of $e^+e^+e^-e^-$ in the final state and for the DF signal we take $\mu^-\mu^-e^+e^+$. We put the aforementioned cuts and simulate the events using CalcHEP and Pythia and look at the ΔR_{ll} and invariant mass M_{ll} of the final state leptons.

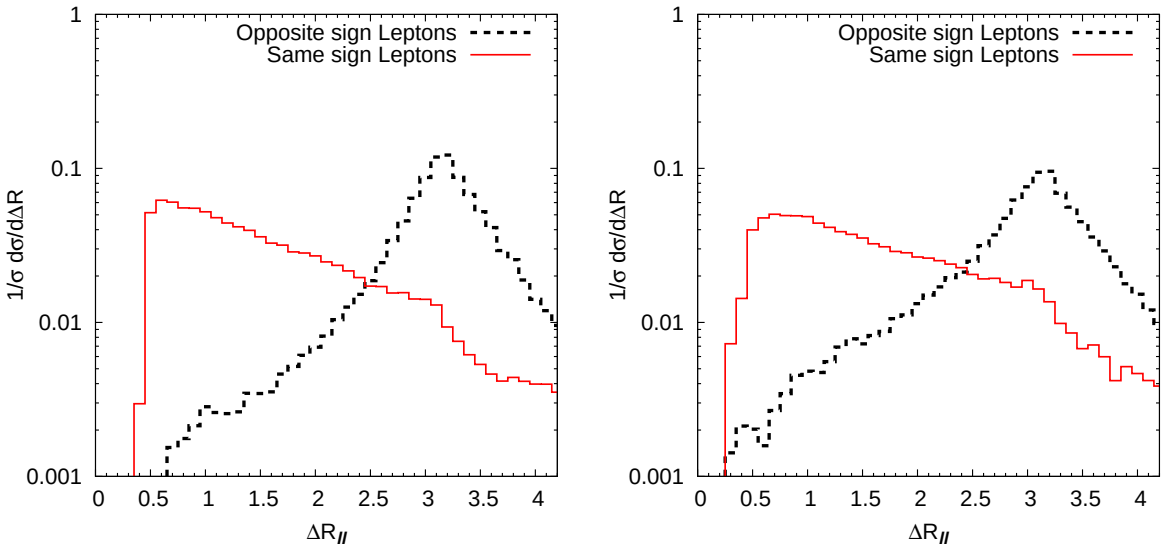

Figure 3.4: *(a) Illustrating the ΔR_{ll} distribution for events coming from the doubly-charged right-handed Higgsino and Higgs boson pair production and, (b) ΔR_{ll} distribution for events when the contributions from the pair production of the left-handed Higgsinos is also included for* **BP1**.

The ΔR_{ll} for the same-sign and opposite-sign final state charged leptons of same flavor for **BP1** are shown in Fig. 3.4. Fig. 3.4(a) includes only the contribution of the right-handed doubly-charged Higgsino and Higgs ($\mathcal{C}1 + C2$) while Fig. 3.4(b) denotes the contribution from the doubly-charged Higgs as well as both the right-handed and left-handed doubly-charged Higgsino ($\mathcal{C}1 + C2 + C3$). It is worth noting that in each plot there is a marked difference between the same-sign lepton and the opposite-sign leptonic final states. It can be seen that for the same-sign charged leptons the distribution is peaked at low values of ΔR while the opposite-sign charged leptons have a ΔR which is peaked at a much higher value. This is what is expected since

the same-sign pair of leptons arise from the decay of a single doubly-charged Higgs boson while the opposite-sign leptons arise from two different particles and hence are much further apart. The measurement of ΔR at the LHC for a four lepton final state can thus give a definite indication of the existence of a doubly-charged particle if the distribution is similar to what we get in our analysis. Note that the ΔR distributions are also very sensitive to the boost of the mother particle as larger boost will make the decay products come out more closer to each other.

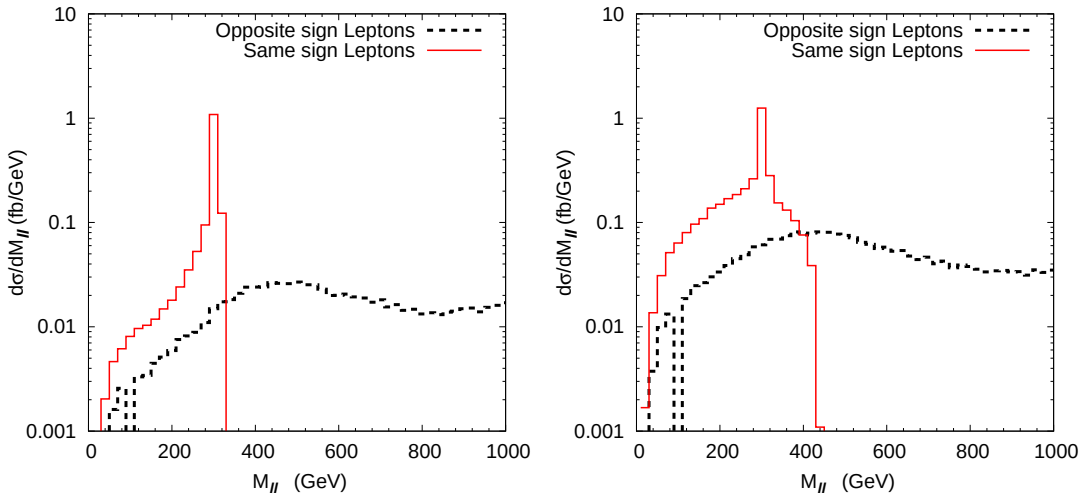

Figure 3.5: *Illustrating the (a) invariant mass distribution for events coming from the doubly-charged right-handed Higgsino and Higgs boson pair production and, (b) invariant mass distribution for events when the contributions from the pair production of the left-handed Higgsinos is also included for* **BP1**.

In Fig. 3.5 we show the invariant mass distributions for the same-sign and opposite-sign final state leptons of same flavor for **BP1**. Note that for the opposite-sign lepton pair invariant mass there are no events between 80 GeV and 100 GeV. This is due to the cut that we applied to get rid of the Z peak for the SM background. The invariant mass for the opposite-sign leptons do not show any resonant behavior. For the same-sign lepton pairs, we see a pronounced peak at an invariant mass of 300 GeV which is the doubly-charged Higgs boson mass. As we include the contributions

coming from the pair production of the left-handed doubly-charged Higgsino, the resonant peak is seen to broaden a little but is still very significant. Such a peak, though very difficult to see without a priori knowledge of the Higgs boson mass, would be a definite proof of a doubly-charged particle if seen in the detector. It is also worth noting the distinct kinematic edge seen in the invariant mass distribution of the like-sign charged lepton pair in both Fig. 3.5(a) and (b). The edge in Fig. 3.5(a) is at a different M_{ll} when compared to that in Fig. 3.5(b). Note that in Fig. 3.5(a) the resonant peak is because of the doubly-charged Higgs decaying to two same-sign leptons while the sharp cut-off in the distribution is because of the maximum invariant mass allowed for the lepton pair that comes from $\delta_R^{\pm\pm} \to \ell^\pm\ell^\pm$. This would mean that the distribution will fall rapidly beyond the resonance which is the $\delta_R^{\pm\pm}$ mass. On the other hand, the signal in Fig. 3.5(b) is completely dominated by the contributions coming from the left-handed doubly-charged Higgsino production and therefore it washes away the kinematic edge from the other subprocesses. The sharp cut-off in Fig. 3.5(b) then appears because of $\widetilde{\delta}_L^\pm \to (\widetilde{\ell}_i^{*\pm}\ell_i^\pm) \to \ell_i^\pm\ell_i^\pm\widetilde{\chi}_1^0$ and is given by (in the rest frame of the decaying particle) $M_{l^\pm l^\pm}^{max} = \sqrt{M^2_{\widetilde{\delta}_L^{\pm\pm}} + M^2_{\widetilde{\chi}_1^0} - 2M_{\widetilde{\delta}_L^{\pm\pm}}E_{\widetilde{\chi}_1^0}}$, where $E_{\widetilde{\chi}_1^0}$ is the energy of the LSP. This yields an edge in the invariant mass distribution of the same-sign same flavor charged lepton pairs at the bin around $M_{l^\pm l^\pm} = M_{\widetilde{\delta}_L^{\pm\pm}} - M_{\widetilde{\chi}_1^0} \simeq 420$ GeV. It is interesting to observe that we find a distinct resonance in the invariant mass distribution as well as a sharp kinematic edge due to the off-shell decay of the left-handed doubly-charged Higgsino which clearly highlights an additional contribution to the resonant signal of doubly-charged scalar production leading to four charged lepton final states.

We can also consider the case where the right-handed doubly-charged Higgsino too decays via off-shell doubly charged scalar which can be realized when the right-handed doubly-charged Higgsino is not much heavier than the right-handed doubly-charged Higgs boson such that $M_{\widetilde{\delta}_R^{\pm\pm}} < M_{\delta_R^{\pm\pm}} + M_{\widetilde{\chi}_1^0}$. In this case the Higgsino will decay

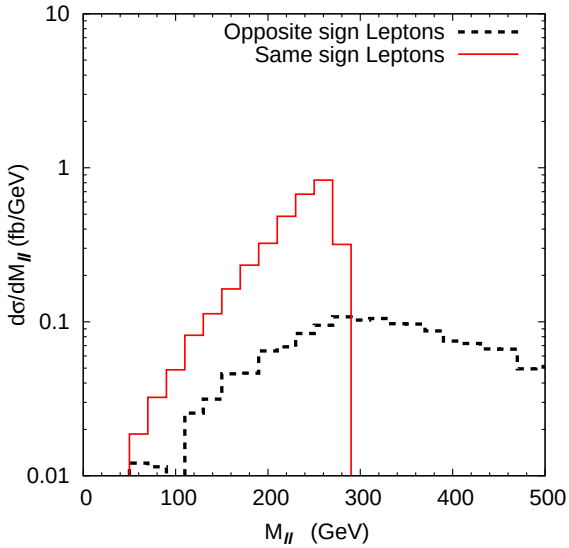

Figure 3.6: *Invariant mass distribution in M_{ll} for a doubly-charged right-handed Higgsino which decays through an off-shell doubly-charged Higgs boson.*

into the LSP and two same sign leptons through an off-shell doubly-charged Higgs boson. In Fig. 3.6 we show the invariant mass distribution for the charged lepton pairs, where the doubly-charged Higgsino mass is 350 GeV, the doubly-charged Higgs boson mass is 300 GeV and the LSP mass is 80 GeV. We see that in such a case the resonant peak in the same-sign charged lepton pair is lost but a kinematic edge exists at around 270 GeV. Note that we still expect a narrow resonance from the direct pair production of the doubly-charged scalar and an enhanced signal rate but we do not see any new enhancement at the resonance.

Experiments at the LHC are looking for doubly-charged Higgs bosons by analyzing final states with four high p_T charged leptons. Our model gives a resonant multi-lepton signal with large missing energy depending on the mass difference between the doubly-charged Higgs boson and the Higgsino. Such a signal accompanied by a peak in the same-sign lepton invariant mass distribution of the same-sign charged lepton pair. This will clearly suggest an alternative signal not restricted to the direct production of doubly charged scalars. This can definitely be a possible channel for

the discovery of the doubly-charged Higgsinos which might be worth looking for.

3.4 Summary

In this work we have studied the pair-production and decay of the doubly-charged Higgsinos in the left-right supersymmetric model and looked at the possible collider signatures at the LHC. The four lepton plus missing energy signal has a variety of distinct features which can easily distinguish itself from other signals, arising especially from the minimal supersymmetric standard model.

We have studied the multi-lepton final state $2\ell^+2\ell^- + \not{E}_T$ arising in the left-right SUSY model. We find that there are three distinct sub-processes that contribute to the signal. We have shown through two representative points in the model how each sub-process dominates the signal depending on the kinematic requirements on the missing transverse momenta. We also show through various kinematic distributions the highlight of the four lepton signal in this model. Using specific cuts on the final states we find that there is very little background from SM. The major background at the LHC where two Z bosons decay into four charged leptons is minimized by putting an invariant mass cut which neglects events at the Z boson peak. Thus, the signal produced by our model at the colliders would be clean and very easy to distinguish from other competing models. Large missing transverse momenta in the final state can be triggered upon to rule out contributions coming from the direct production of doubly-charged scalars and therefore would give a strong hint of a supersymmetric model with doubly-charged particles. The data collected by the LHC experiments should already provide significant constraints on the masses of the doubly charged Higgsino and Higgs boson through the process outlined here. Dedicated searches for these doubly charged particles in the channel proposed here by the experimental collaborations will be highly desirable.

CHAPTER 4

HIGGS BOSON DECAY CONSTRAINTS ON A MODEL WITH A UNIVERSAL EXTRA DIMENSION

4.1 Introduction

The discovery of the 125-126 GeV Higgs boson — or its close lookalike — at CERN, Geneva, in the previous year [54], has proved to be a game-changing moment in phenomenological studies of electroweak interactions. Gone are speculations about Higgsless models [55], strongly-coupled Higgs sectors [56] and fears that the Higgs boson self-coupling may hit a Landau pole at some large energy scale [57]. Instead, today's theoretical studies have other concerns, such as stability of the electroweak vacuum, fine-tuning constraints and the requirement that the measured Higgs boson mass and branching ratios be correctly explained in whatever model happens to be the subject of the study. At the present instance, there is no compelling reason, beyond certain theoretical prejudices (like grand unification), to believe that we require anything other than the Standard Model (SM) to explain all the known phenomena on a terrestrial scale. Destabilisation of the SM vacuum at some energy scale below the Planck scale could be one of the strongest hints of new physics [58], but at the moment this issue is mired in uncertainties of the top quark mass measurement [59].

Nevertheless, we do require physics beyond the Standard Model, and this requirement arises as soon as we look outside the confines of our Earth into the cosmos beyond. Here it is well known that the SM fails to provide explanations for (*i*) the composition of dark matter [60], (*ii*) the nature of dark energy [61] and (*iii*) the amount of CP-violation required for baryogenesis [62]. Of these, perhaps the most

tractable problem is the first one, viz. the generation of a model for dark matter, for all that is required is a model for a stable, weakly-interacting massive particle (WIMP). The most famous model which provides this is, of course, supersymmetry with conservation of R-parity, where the lightest supersymmetric particle is the WIMP in question [63]. An alternative model, which was proposed about a decade ago, is one with a so-called Universal Extra Dimension [64]. In the minimal model of this kind (mUED), each five-dimensional SM field is replaced by a tower of Kaluza-Klein (KK) modes, each labelled by a KK number n, and having masses given (at tree-level) by $M_n = (M_0^2 + n^2 R^{-2})^{1/2}$. Here, the lightest of the $n = 1$ particles is stable and weakly-interacting due to a Z_2 symmetry called KK parity, defined in terms of KK number by $(-1)^n$. This lightest KK particle, called the LKP, is an excellent candidate for dark matter [65].

At a high energy collider, the behaviour of the mUED models is very similar to that of supersymmetric models [66]. The $n = 1$ states form analogues of the supersymmetric particles, exhibiting cascade decays ending in the LKP, which is then a source of missing energy and momentum. A major difference from supersymmetry is the presence of $n = 2$ and higher KK modes, which could perhaps be produced as resonances in a high energy machine like the LHC [67]. However, a more significant difference arises when we consider the ultraviolet behaviour of the mUED model (or any model with KK modes), as was pointed out in a pioneering paper by Dienes *et al* [68]. This is the fact that when we allow the SM coupling constants to run in this model, we encounter repeated KK thresholds at every scale n/R, so that, when considered over a large range of energies, the coupling constant exhibits a piecewise logarithmic running closely mimicking a power law dependence. As a result, it has been shown that (a) the electromagnetic coupling hits a Landau pole at as low a scale as $\Lambda \approx 40R^{-1}$, and (b) there is approximate (but not exact) unification of the three gauge coupling constants at an even lower scale $\Lambda \approx 20R^{-1}$. One therefore assumes

that the low energy theory has a cutoff at either of these values, and phenomenological studies are made accordingly. This has been the standard practice in mUED studies over the past decade.

Of course, it is not only the gauge couplings that run faster in this model, but also the scalar self coupling λ. It has been shown [69] that if the self-coupling $\lambda = M_H^2/2v^2$ is less than 0.18 at the electroweak scale, then its renormalisation group evolution will inexorably drive it to zero at some high scale, at which point the electroweak vacuum will become unstable. Taking the experimental range 122 GeV $\leq M_H \leq$127 GeV for the Higgs boson mass, we obtain $0.123 \leq \lambda \leq 0.133$, which is clearly below 0.180. It follows that the electroweak vacuum in this model will indeed destabilise at some high scale, as, in fact, happens in the Standard Model itself at very high scales. The surprise lies in that fact that the 'power law' running of λ in the mUED model is so fast that the destabilisation takes place at a scale which is always below $6R^{-1}$. At this surprisingly low scale, new physics must come to the rescue, and hence the destabilisation scale can be treated as a cutoff for the mUED model.

The exact value of the cutoff scale is determined by evaluating the running coupling constant λ and determining where it vanishes [69]. The most important input parameters which determine this running are the mass of the Higgs boson (M_H) and the size parameter (R^{-1}), which is nothing but the inverse of the compactification radius of the extra dimension. The solid (red) lines in Figure 4.1 show the variation of the cutoff scale Λ, in units of R^{-1}, as a function of this size parameter R^{-1}, for two values of Higgs boson mass $M_H = 122, 127$ GeV (which represent the 3σ experimental limits). The (red) hatching, therefore, represents all the intermediate values of M_H. Horizontal (blue) lines represent the different KK levels n/R, for $n = 1, 2, \ldots, 6$. Our results shown here correspond closely to similar results shown in Ref. [70].

Obviously, assuming tree-level masses, the number of KK modes with mass $M_n \approx n/R$ which can participate in any process will be given by the nearest integer lower

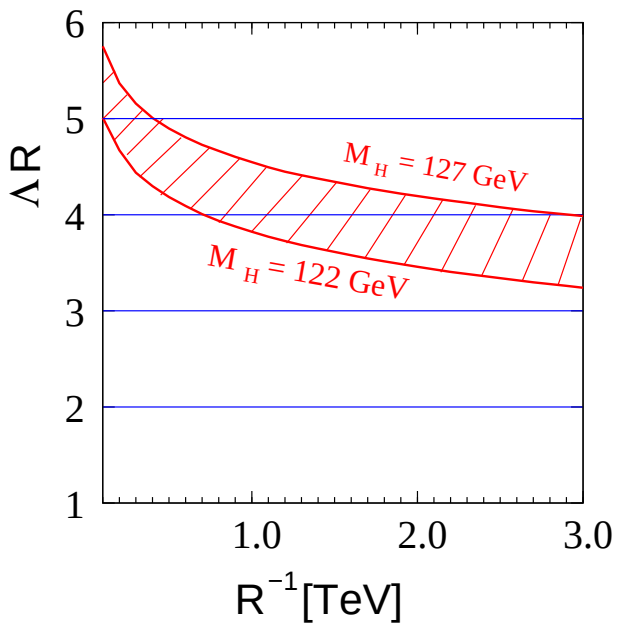

Figure 4.1: *Variation of Λ/R^{-1}, where Λ is the cutoff induced by destabilisation of the electroweak vacuum, as a function of size parameter R^{-1}. The (red) hatched band represents variations in the Higgs boson mass from 122 – 127 GeV, and horizontal (blue) lines represent KK levels.*

than the solid (red) curve for a given value of R^{-1}. It is clear that this number can only vary between 3 and 5, and can never reach higher values such as 20 and 40 which used to be assumed earlier. Note that in generating Figure 4.1, and subsequently, we have fixed the top quark mass at $m_t = 172.3$ GeV. Variation of the top quark mass between its experimentally allowed limits [71] does result in some distortion of the curves, as the related Yukawa coupling plays a role in the running of the self-coupling λ. However, these distortions have very minor effects on the final conclusions of this article, and hence are not shown here.

In an earlier article [75], written at a stage when the new boson discovered at the CERN LHC had not yet been identified with any certainty as the Higgs boson, two of the present authors had shown that this low value of cutoff (i.e. small number of KK modes to sum over) leads to a compressed spectrum of KK modes of SM fields at any level $n \geq 1$, which presents serious difficulties for detection at the Tevatron and LHC. However, it was not possible to impose constraints on the model from the Higgs boson decay branching ratios, which were very imperfectly measured [54] at that stage. Now,

however, we have better experimental results on these branching ratios [72,73], which, though not as precise or consistent between separate experiments as we would have liked them to be, have nevertheless reached a level where they are accurate enough to begin to constrain the mUED model [74]. These constraints form the subject of the present study.

Before we go on to actually study the Higgs boson decay widths, however, it may be noted that bounds on the size parameter R^{-1} quoted from hadron collider studies [78] are generally based on expanded spectra arising when we sum KK levels up to $N = 20$ or even $N = 40$, which, as we have shown, is incompatible with stability of the electroweak vacuum. *We should set aside such hadron collider bounds on the mUED model.* The LEP bound $R^{-1} > 260$ GeV, obtained at 3σ from precision electroweak tests [75], may, however, be taken as a certainty. In a recent work [76], it has been shown that even if we sum up to 5 KK levels, a lower bound of $R^{-1} > 720$ GeV at 95% C.L. can be obtained by noting the non-observation by the CMS Collaboration of dilepton signals [77] arising from the decay of $n = 2$ resonances of the mUED model in the 7-8 TeV runs of the LHC. The purpose of the present study is, therefore, to ascertain if the existing data on the Higgs boson decay channels can provide even better constraints.

4.2 Higgs boson decay signal strengths at LHC

In the Higgs boson decays, the actual experimentally-measured quantities are the so-called *signal strengths* [72, 73]. For a decay $H \to X\bar{X}$, the signal strength is defined by

$$\mu_{X\bar{X}} = \frac{\sigma(pp \to H^0) \times \mathcal{B}(H^0 \to X\bar{X})}{\sigma^{(\mathrm{SM})}((pp \to H^0) \times \mathcal{B}^{(\mathrm{SM})}(H^0 \to X\bar{X})} \tag{4.1}$$

where $\mathcal{B}(H^0 \to X\bar{X})$ is the branching ratio of the Higgs boson to an $X\bar{X}$ pair, and $\sigma(pp \to H^0)$ is the cross-section for single Higgs production at the LHC. The

superscript (SM) denotes the SM prediction. Obviously, if the SM is the correct theory, then the experimental data will eventually converge on the results $\mu_{X\bar{X}} \simeq 1$ for all the channels X. On the other hand, deviations from unity will indicate new physics. As of now, the ATLAS and CMS Collaborations at CERN have measured signal strengths for $X\bar{X} = WW^*, ZZ^*, b\bar{b}, \tau^-\tau^+, \gamma\gamma$. Of these, the case $X\bar{X} = b\bar{b}$ is not very viable yet because of large errors. The other four have been measured with a better degree of precision. The results are given in Table 4.1 below.

	μ_{WW}	μ_{ZZ}	$\mu_{\tau\tau}$	$\mu_{\gamma\gamma}$
ATLAS	$0.99^{+0.31}_{-0.28}$	$1.43^{+0.40}_{-0.35}$	0.8 ± 0.7	$1.55^{+0.33}_{-0.28}$
CMS	0.68 ± 0.20	0.92 ± 0.28	1.10 ± 0.41	0.77 ± 0.27

Table 4.1: *ATLAS [72] and CMS [73] data on Higgs boson signal strengths, as reported in the summer of 2013. For $\mu_{\tau\tau}$ we use the March 2013 results of ATLAS [79].*

4.3 Calculation of Higgs boson decay strength and comparison with experiments

We now discuss how to predict the values of $\mu_{X\bar{X}}$ in the mUED model. Using the fact that the parton-level cross-section for gluon fusion $gg \to H^0$ is related to the decay width of $H^- \to gg$ by the linear relation

$$\sigma(gg \to H^0) = \frac{\pi^2}{8M_H^3}\Gamma(H^0 \to gg) \ , \tag{4.2}$$

we can rewrite the signal strength entirely in terms of decay widths as

$$\mu_{X\bar{X}} \ = \ \frac{\Gamma(H^0 \to gg)}{\Gamma^{(\mathrm{SM})}((H^0 \to gg)} \times \frac{\Gamma(H^0 \to X\bar{X})}{\Gamma^{(\mathrm{SM})}(H^0 \to X\bar{X})} \times \frac{\Gamma_H^{(\mathrm{SM})}}{\Gamma_H} \tag{4.3}$$

where

$$\Gamma_H = \sum_X \Gamma(H^0 \to X\bar{X}) \tag{4.4}$$

and all PDF-related effects (to leading order) in the cross-section may be expected to cancel in the ratio. All we have to do, therefore, is to calculate the decay widths of the Higgs boson in the mUED model and the SM, and take the appropriate ratios. All the formulae relevant for these are available in the literature, but, for the sake of completeness and having a consistent notation, we list the most important formulae below.

In the SM, the decay width of the Higgs boson to a pair of leptons is given by [80]

$$\Gamma(H^0 \to \ell^+\ell^-) = \frac{\alpha(M_H)}{8\sin^2\theta_W}\frac{m_\ell^2}{M_W^2}M_H\left(1-\frac{4m_\ell^2}{M_H^2}\right)^{3/2} \tag{4.5}$$

where $\alpha(Q)$ is the running QED coupling at the mass scale Q. The corresponding decay width to a pair of quarks is given by [80]

$$\Gamma(H^0 \to q\bar{q}) = \frac{3\alpha(M_H)}{8\sin^2\theta_W}\frac{m_q^2(M_H)}{M_W^2}M_H\left(1-\frac{4m_q^2}{M_H^2}\right)^{3/2}\left\{1+5.67\frac{\alpha_s(M_H)}{\pi}\right\} \tag{4.6}$$

where the last factor represents the QCD corrections to the decay width [81], and the running quark mass is given by [82]

$$m_q^2(M_H) = m_q^2\left\{\frac{\alpha_s(M_H)}{\alpha_s(m_q)}\right\}^{24/23} \tag{4.7}$$

where $\alpha_s(Q)$ is the running QCD coupling at the mass scale Q.

The SM decay width of the Higgs boson to a WW^* pair is given by [83]

$$\Gamma(H^0 \to WW^*) = \frac{3\alpha^2(M_H)}{32\pi\sin^4\theta_W M_H}F(M_W) \tag{4.8}$$

and that to a ZZ^* pair by [83]

$$\Gamma(H^0 \to ZZ^*) = \frac{\alpha^2(M_H)}{72\pi\sin^4 2\theta_W M_H}\left(63-120\sin^2\theta_W+160\sin^4\theta_W\right)F(M_Z) \tag{4.9}$$

where

$$\begin{aligned} F(M) = & -\frac{1}{2}\left(1-\frac{M^2}{M_H^2}\right)\left(47M^2-13M_H^2+\frac{2M_H^4}{M^2}\right) \\ & -3\left(M_H^2-6M^2+\frac{4M^4}{M_H^2}\right)\ln\frac{M^2}{M_H^2} \end{aligned}$$

$$+ \quad 3\left(M_H^2 - 8M^2 + \frac{20M^4}{M_H^2}\right)\frac{M_H}{\sqrt{4M^2 - M_H^2}}\cos^{-1}\frac{M_H}{2M}\left(3 - \frac{M_H^2}{M^2}\right) \tag{4.10}$$

It is important to note that QCD corrections are significant only in the decay widths of the Higgs boson to quarks and can be neglected for all other decay modes. Likewise, the mUED contributions to the above decay modes is negligible, arising, as they do, from higher order effects which are severely suppressed by the heavy masses of the KK modes.

The decay modes which will be of most interest in the present work, are however, those that occur at the one-loop level in the SM, viz. the decays of the Higgs boson to a pair of gluons ($H^0 \to gg$) or a pair of photons ($H^0 \to \gamma\gamma$). Formulae for the partial decay widths in the SM are given in Ref. [80], and the extra contributions in the mUED, which occur at the same level in perturbation theory, are given in Ref. [84]. We list, below, these formulae in a common notation, with a couple of modifications to the formulae of Ref. [84], which will be mentioned at the appropriate juncture.

The partial decay width of the Higgs boson to a pair of gluons is given by

$$\begin{aligned}\Gamma(H^0 \to gg) &= \frac{\alpha(M_H)\alpha_s^2(M_H)}{72\pi^2\sin^2\theta_W}\frac{1}{M_H^5 M_W^2} \mid \Omega_{gg}^{(\mathrm{SM})} + \Omega_{gg}^{(\mathrm{KK})} \mid^2 \\ &\quad \times\left\{1 + 17.92\frac{\alpha_s(M_H)}{\pi} + 156.8\frac{\alpha_s^2(M_H)}{\pi^2} + 467.7\frac{\alpha_s^3(M_H)}{\pi^3}\right\}\end{aligned} \tag{4.11}$$

where the second line indicates the QCD corrections [81] and the loop integral functions are given by

$$\Omega_{gg}^{(\mathrm{SM})} = \sum_q 3m_q^2\left\{2M_H^2 - (M_H^2 - 4m_q^2)f(m_q)\right\} \tag{4.12}$$

$$\Omega_{gg}^{(\mathrm{KK})} = \sum_q\sum_{n=1}^{N} 3m_q^2\left\{4M_H^2 - (M_H^2 - 4m_{q,n,1}^2)f(m_{q,n,1}) - (M_H^2 - 4m_{q,n,2}^2)f(m_{q,n,2})\right\}$$

where $m_{q,n,1}$ and $m_{q,n,2}$ are the two eigenvalues of the mass matrix

$$\mathcal{M}_q^{(n)} = \begin{pmatrix} m_{qL}^{(n)} & m_q \\ m_q & -m_{qR}^{(n)} \end{pmatrix} \tag{4.13}$$

for the n'th level KK modes of the quarks, where

$$\left[m_{qL}^{(n)}\right]^2 = \frac{n^2}{R^2} + m_q^2 + \delta_{qL}^{(n)} \qquad \left[m_{qR}^{(n)}\right]^2 = \frac{n^2}{R^2} + m_q^2 + \delta_{qR}^{(n)} \tag{4.14}$$

in terms of the radiative corrections $\delta_{qL}^{(n)}$ and $\delta_{qR}^{(n)}$ [66]. The function $f(m)$ is the usual loop integral [80]

$$f(m) = \begin{cases} -2\left(\sin^{-1}\frac{M_H}{2m}\right)^2 & \text{for } m > \frac{M_H}{2} \\ -\frac{\pi^2}{2} & \text{for } m = \frac{M_H}{2} \\ \frac{1}{2}\left(\ln\frac{M_H+\sqrt{M_H^2-4m^2}}{M_H-\sqrt{M_H^2-4m^2}} - i\pi\right)^2 & \text{for } m < \frac{M_H}{2} \end{cases} \tag{4.15}$$

In using these formulae, we differ from Ref. [84] in two ways:

1. we consider the sum over KK modes to terminate at N, which is the largest integer smaller than ΛR as given in Fig. 4.1, instead of summing to infinity, as was done in Ref. [84]; and

2. we consider the splitting between mass eigenstates of KK modes of quarks at the level n, whereas Ref. [84] assumed them to be degenerate. Of course, the fact that the off-diagonal terms in the mass matrix of Eqn. 4.13 are m_q indicates that such splitting between these states as does occur will be perceptible only in the third generation.

In a similar vein, the partial decay width of the Higgs boson to a pair of photons is given by

$$\Gamma(H^0 \to \gamma\gamma) = \frac{\alpha^3(M_H)}{16\pi^2 \sin^2\theta_W} \frac{1}{M_H^5 M_W^2} \mid \Omega_{\gamma\gamma}^{(\mathrm{SM})} + \Omega_{\gamma\gamma}^{(\mathrm{KK})} \mid^2 \tag{4.16}$$

where the loop integral functions are given by

$$\begin{aligned} \Omega_{\gamma\gamma}^{(\mathrm{SM})} &= \sum_q e_q^2 \omega_q^{(\mathrm{SM})} + \sum_\ell e_\ell^2 \omega_\ell^{(\mathrm{SM})} + \omega_W^{(\mathrm{SM})} \\ \Omega_{\gamma\gamma}^{(\mathrm{KK})} &= \sum_{n=1}^{N} \left[\sum_q e_q^2 \omega_q^{(n)} + \sum_\ell e_\ell^2 \omega_\ell^{(n)} + \omega_W^{(n)} \right] \end{aligned} \tag{4.17}$$

in terms of [80]

$$\begin{aligned}
\omega_q^{(\mathrm{SM})} &= 3m_q^2\left\{2M_H^2-(M_H^2-4m_q^2)f(m_q)\right\} \\
\omega_\ell^{(\mathrm{SM})} &= m_\ell^2\left\{2M_H^2-(M_H^2-4m_\ell^2)f(m_\ell)\right\} \\
\omega_W^{(\mathrm{SM})} &= -3M_W^2\left\{M_H^2-(M_H^2-2M_W^2)f(M_W)\right\}-\frac{1}{2}M_H^4
\end{aligned} \tag{4.18}$$

and [84]

$$\begin{aligned}
\omega_q^{(n)} &= 3m_q^2\left\{4M_H^2-(M_H^2-4m_{q,n,1}^2)f(m_{q,n,1})-(M_H^2-4m_{q,n,2}^2)f(m_{q,n,2})\right\} \\
\omega_\ell^{(n)} &= m_\ell^2\left\{4M_H^2-(M_H^2-4m_{\ell,n,1}^2)f(m_{\ell,n,1})-(M_H^2-4m_{\ell,n,2}^2)f(m_{\ell,n,2})\right\} \\
\omega_W^{(n)} &= -4M_W^2M_H^2+\left\{4M_W^2\left(M_H^2-2M_{W,n}^2\right)-M_{W,n}^2M_H^2\right\}f(M_{W,n})-\frac{1}{2}M_H^4
\end{aligned} \tag{4.19}$$

where the lepton mass eigenvalues $m_{\ell,n,1}$ and $m_{\ell,n,2}$ are, for all practical purposes, degenerate.

Using these formulae, we can now find the signal strengths predicted in the mUED model as a function of the size parameter. To understand this behaviour, let us note the conclusion of Ref. [84], which remain qualitatively – though not quantitatively – true in our analysis as well. These may be summed up as follows.

- The tree-level decay widths of the Higgs boson are practically the same in the SM and the mUED model.

- The decay width of the Higgs boson to a pair of gluons is considerably enhanced in the mUED model, especially when R is taken close to its lower experimental bound (see Figure 4.2).

- The decay width of the Higgs boson to a pair of photons is suppressed in the mUED model, especially when R is taken close to its lower experimental bound (see Figure 4.2).

In our analysis, we obtain numerically different results from Ref. [84] because of two reasons. In the first place, we note that the sum over KK modes in our case is truncated at values of n between 3 and 5, whereas Ref. [84] took the sum to infinity.

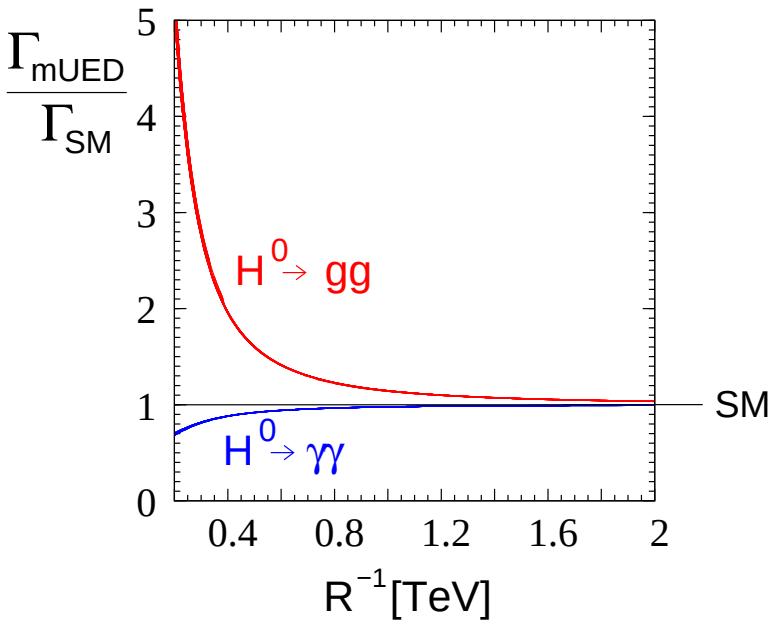

Figure 4.2: *Illustrating the effect of KK modes on the partial decay widths of* $H^0 \to gg$ *and* $H^0 \to \gamma\gamma$*. The former is always enhanced, while the latter is always suppressed, compared to the SM prediction.*

As a result, we obtain significantly smaller mUED contributions. The second point is that because of this low cutoff, we are able to take R^{-1} somewhat lower than what the earlier collider-based bounds permit us, and these lower values could then lead to larger mUED contributions.

If we take a closer look at Eqn. (4.3), however, we see that there are more conflicting effects. The three channels with $X\bar{X} = WW^*, ZZ^*$ and $\tau\tau$ will all receive enhancements in the mUED model through the first factor on the right of Eqn. (4.3). The second factor will be practically unity, as we have explained above. The third factor, however, will suppress the signal strength if there are large enough mUED contributions in the first factor. Owing to these opposed effects, the enhancement in signal strength is not as large as it might have been otherwise.

A curious fact worth noting is that the variation in the last factor arises only because we do not yet have an accurate measurement of the total decay width of the Higgs boson. If the Higgs boson decay width could be accurately determined from a

line shape analysis, as was done for the W and Z bosons at LEP and Tevatron, then that result alone could have been used to constrain any new physics model. In the case of the $\gamma\gamma$ channel, the second factor on the right of Eqn. (4.3) will be somewhat smaller than unity, as a result of which the signal strength will be somewhat more suppressed than in the other cases. It is therefore difficult, in the mUED model, to predict large excesses in the partial width of $H^0 \to \gamma\gamma$. We reiterate, therefore, that the mUED enhancement in $H^0 \to gg$ and the suppression of $H^0 \to \gamma\gamma$ are both in agreement with the results of Ref. [84], though the actual deviations are much more modest in the present case — a consequence of the small number of KK modes which contribute to these deviations.

These diverse effects together contribute to the numerical results exhibited in Figure 4.3. The four panels in this figure correspond to the four decays $H^0 \to WW^*, ZZ^*, \tau^+\tau^-$ and $\gamma\gamma$, as marked on each respective panel. The solid (black) lines represent the mUED predictions, and, as expected, these fall rapidly to the SM expectation $\mu_{X\bar{X}} = 1$ as R^{-1} increases, in every case. The thickness of these lines indicates the effect of varying $M_H = 122 - 127$ GeV. It is clear from the figure that this is not a very significant effect*. In fact, the solid (black) curves for μ_{WW}, μ_{ZZ} and $\mu_{\tau\tau}$ are identical, since the only effect of introducing mUED lies in the first and last factors of Eqn. 4.3, which depend mainly on $\Gamma(H^0 \to gg)$. The solid (black) curve for $\mu_{\gamma\gamma}$ is clearly different, as one would expect. However, the reason for showing each signal strength separately lies in the fact that the experimental constraints are significantly different in each of these channels. For both the ATLAS and CMS data, the strongest constraints come, in fact, from the WW^* channel. For a 125-126 GeV Higgs boson, these come out as $R^{-1} > 463$ GeV (1.3 TeV) for the ATLAS (CMS) results, which are far more restrictive than anything we can get from precision tests,

*The effect of varying the top quark Yukawa coupling is sub-leading to this variation, which is why we do not show it at all in the present work.

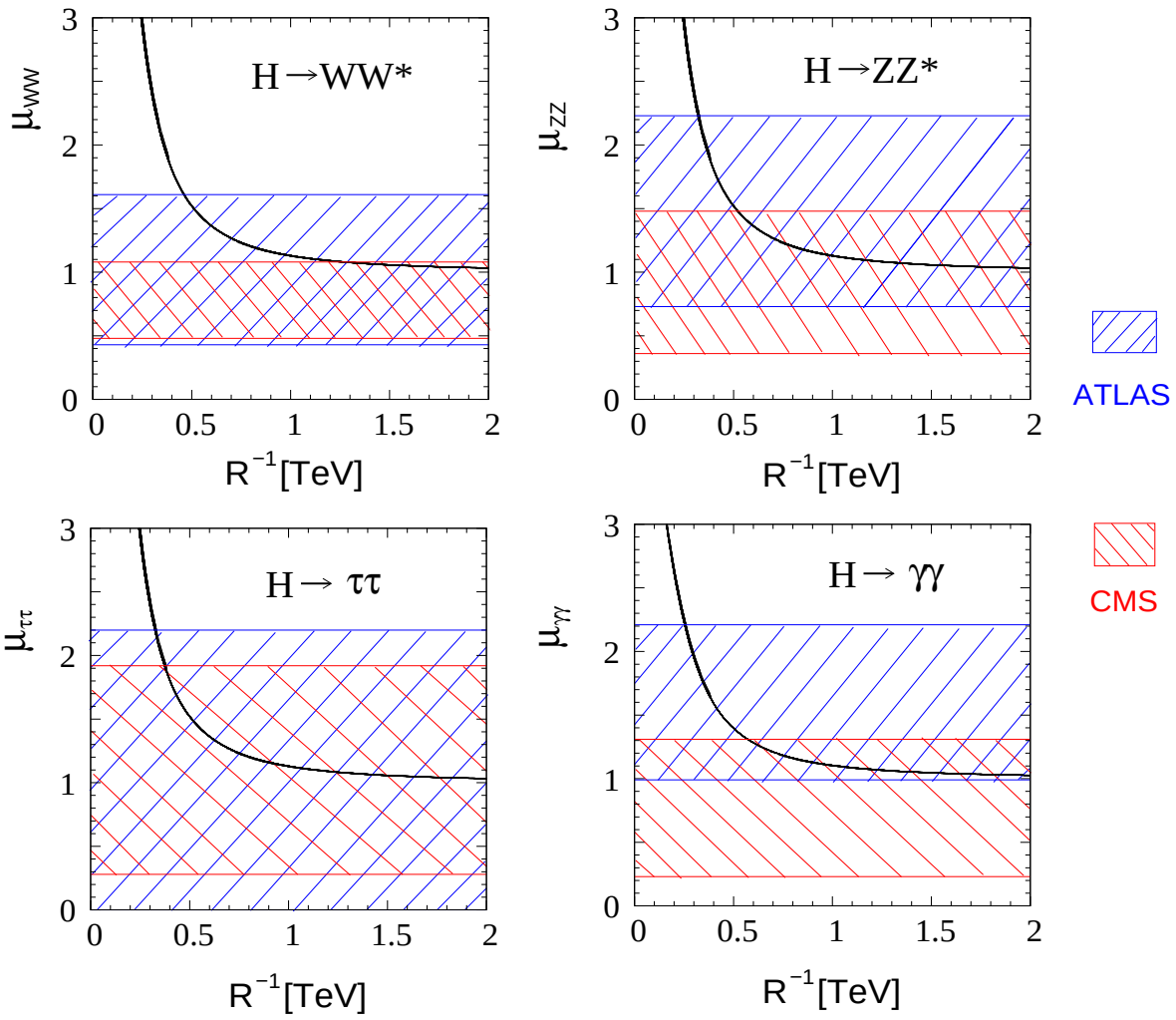

Figure 4.3: *Illustrating the variation with R^{-1} of the signal strengths μ_{WW}, μ_{ZZ}, $\mu_{\tau\tau}$ and $\mu_{\gamma\gamma}$, as marked on the respective panels. The solid (black) lines show the mUED prediction, with their thickness representing the effect of varying the Higgs boson mass M_H from $122 - 127$ GeV. The oppositely-hatched regions (blue and red) denote, as indicated in the key on the right, the 95% C.L. limits from the ATLAS and CMS Collaborations quoted in Table 4.1.*

and – at least for the CMS data – surpass the bounds from dilepton channels [76] by a factor close to 2.

95% C.L. constraints from the other channels are illustrated, together with the WW^* channel, in Figure 4.4, in the form of a bar graph. It is apparent, even from Figure 4.3, that the CMS data provide significantly stronger constraints, at this level, than the ATLAS data. In particular, if we consider the ATLAS data for $H^0 \to \gamma\gamma$,

where there appears to be an excess at the 1σ level over the SM prediction, this appears to hint at lower values of R^{-1}, though – as the graph shows – large values of R^{-1} are perfectly consistent with the 95% C.L. limits. In view of the substantial differences between the two experimental results, it may be premature to read too much into these constraints, but it is clear that for the WW^* channel, at least, we do find a reasonable level of consistency. Since this is the channel which provides the most stringent bounds on R^{-1}, these are perhaps the most acceptable among the four sets of constraints, at least at the present time.

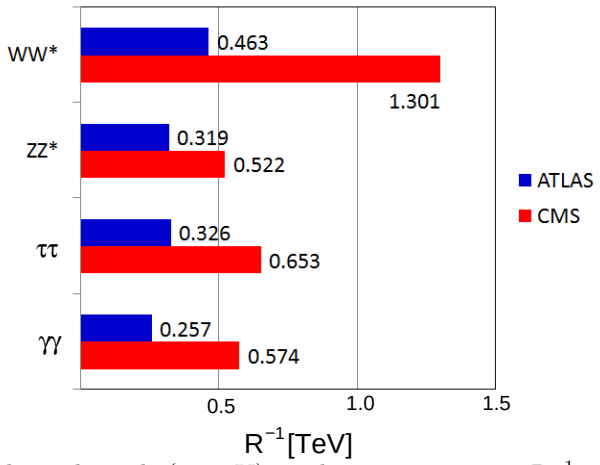

Figure 4.4: *95% C.L. lower bounds (in TeV) on the size parameter R^{-1} arising from four different Higgs boson decay channels. Numbers juxtaposed with the bars are the numerical value of the bounds.*

In Figure 4.4, as mentioned above, we have shown a bar graph illustrating the individual 95% C.L. constraints on R^{-1} from each of these four channels. The upper (blue) and lower (red) bars represent bounds arising from the ATLAS and CMS data respectively. For the ATLAS data, the strongest constraint is from the WW^* channel, but even the ZZ^* and $\tau\tau$ channels are more restrictive than the LEP constraints. So far as the ATLAS data is concerned, obviously no useful constraint can be expected to arise from the $\gamma\gamma$ channel, but if the excess in this channel turns out to be a genuine feature, it will favour the mUED model (among other rival models) with a somewhat smaller value of R^{-1}. The CMS data, on the other hand, are much more

restrictive. While the WW^* channel pushes the lower bound to as high as 1.3 TeV, none of the other channels permit a value of R^{-1} as low as 500 GeV, which is a substantial improvement over the LEP bound of 260 GeV, but is not as restrictive as the dilepton bound obtained in Ref. [76].

The lower bound of $R^{-1} > 1.3$ TeV obtained from our computations represents a very strong constraint for the mUED model and would severely impact the direct searches planned for the 14 TeV run of the LHC. It is interesting, therefore, to ask how far these bounds can be relaxed if we consider the ATLAS and CMS data at the 3σ level rather than at 95% confidence level. These bounds are presented in Table 4.2 below, and are naturally weaker, with the strongest bound lying at $R^{-1} > 685$ GeV, which is still a significant improvement over the precision tests[†].

	μ_{WW}	μ_{ZZ}	$\mu_{\tau\tau}$	$\mu_{\gamma\gamma}$
ATLAS	369	278	248	207
CMS	685	413	306	402

Table 4.2: *3σ lower bounds (in GeV) on R^{-1} using the ATLAS and CMS data from Table 4.1 and the signal strengths from Figure 4.3.*

If we further relax the constraints to the 5σ level, we find that the WW^* channel data imply bounds on $R^{-1} > 280$ (432) GeV from the ATLAS (CMS) data. Even with this very loose constraint, the lower bound of 432 GeV from the CMS data is still stronger than the LEP constraint. However, if we go by the conventional wisdom that 2σ deviations constitute a hint, 3σ deviations – or the lack thereof – constitute a bound, and 5σ is required for a discovery, then the stronger constraint $R^{-1} > 1.3$ TeV may be quite credible.

It is amusing to speculate on how these bounds might improve in the 14 TeV run of the LHC — under the somewhat pessimistic assumption that no deviations

[†]This is also definitely stronger than the 3σ bounds obtainable from dilepton signals, which would certainly lie around 600 GeV or below, if we go by the results quoted in Fig. 4 of Ref. [76].

from the SM will be discovered. Estimates [85] of the cross-section for $pp \to H^0$ at 8 TeV and 14 TeV indicate an enhancement in the cross-section by a factor around 2.5. Assuming that the integrated luminosity in the 14 TeV run will be as high as 1.5 ab^{-1}, this represents an enhancement of 100 times over the statistics collected at 8 TeV. Thus, the number of Higgs boson events in the 14 TeV run will be around 250 times the number collected at the 8 TeV run. If we concentrate on the WW^* signal and assume that the errors will scale as the inverse square root of the number of Higgs boson decay events, then the error on the CMS measurement of μ_{WW} could go down as low as 0.012. This is certainly an overestimate, since it does not take into account systematic effects, but it is probably safe to assume [86] that the error could be as low as 5%. Assuming, therefore, that we have a measured value $\mu_{WW} = 1.00 \pm 0.05$ (from either experiment, or from both combined), we immediately predict a 95% C.L. limit $R^{-1} > 1.58$ TeV, which would increase to 1.90 TeV if the integrated luminosity is doubled to 3 ab^{-1}. For such large values of R^{-1}, it is more or less sure that direct searches for mUED signals will fail, and even the LKP may become too heavy to explain the observed relic density of dark matter. In this admittedly pessimistic scenario, there will be no real motivation to study the mUED model any further.

Of course, we do not have any compelling reason to think that the above scenario is a true picture of the future. In fact, given the urgency with which an explanation of the composition of dark matter is required, we may well hope for just the reverse of this scenario, i.e. the observation of deviations in some of the Higgs boson partial decay widths in the 14 TeV run. In that case, we can reverse some of the arguments of the present study to show that a mUED explanation of such a deviation would be immediately available for some value of R^{-1} in the range of $1 - 2$ TeV.

4.4 Summary

To sum up, then, we have studied constraints on the mUED model from the measured Higgs boson signal strengths in the decays $H^0 \to WW^*$, ZZ^*, $\tau\tau$ and $\gamma\gamma$ channels. The mUED calculations have been carried out carefully, taking into account the fact that this model has a very low cutoff due to vacuum stability arguments. Even with the reduced effects due to this low cutoff, however, we find that the present CMS data can push the lower bound on the size parameter R^{-1} of this model as high as 1.3 TeV at 95% C.L. (or 685 GeV at 3σ). ATLAS data are less restrictive, but in any case, do serve to push the value of R^{-1} above about 500 GeV. All this represents an enormous improvement over the 3σ bound of around 260 GeV arising from precision electroweak tests at the LEP collider, as well as a factor close to 2 greater than the 95% dilepton bounds obtained from the early runs of the LHC. We then go on to argue that these signal strengths can be used to probe the mUED model up to $R^{-1} \approx 2$ TeV in the 14 TeV run of the LHC.

CHAPTER 5

CONCLUSIONS

This dissertation has been dedicated to the study of Higgs bosons in various models including several supersymmetric left-right models and a minimal universal extra dimensional model.

In Chapter 2, the Higgs boson spectrum was studied for various iterations of the left-right supersymmetric models differentiated by the symmetry breaking sectors. In some of the models, the lightest neutral Higgs boson tree level mass was significantly higher than in the Standard Model or its minimal supersymmetric extension. For these cases one can easily get the experimentally observed Higgs boson mass of 125 GeV for a relatively small stop squark mass of about 500 GeV and negligible stop squark mixing parameter. A light stop squark can be easily produced at particle accelerators, enhancing the chances of it being seen at the LHC. In some models with right-handed triplet Higgs bosons, the doubly-charged scalar remains massless at the tree level. Radiative corrections to the doubly-charged Higgs boson mass was calculated and it was shown that loop contributions can push the mass to the electroweak symmetry breaking scale.

In Chapter 3, the collider phenomenology of doubly-charged scalars and fermions is studied in the framework of left-right supersymmetric model with automatic R-parity. A new mechanism for production of doubly-charged Higgs boson is presented wherein the pair-production of the right-handed doubly-charged Higgsino and its subsequent decay can produce unique collider signals at the LHC which can easily distinguish itself from other signals, arising especially from the minimal supersymmetric standard

model. The multi-lepton final state of $2l^+2l^- + \not{E}_T$ arises through three distinct sub-processes that contribute to the signal. Applying specific cuts, the background can be suppressed and the signal produced at the colliders can give a strong hint about the presence of doubly-charged particles.

In Chapter 4, the constraints on minimal universal extra dimensional model from the experimentally measured decay strengths of the Higgs boson is studied. The mUED calculations have been carefully done, taking into account that the model has a very low cutoff due to vacuum stability arguments. The Higgs boson cross-section for decays $H^0 \to WW^*, ZZ^*, \tau\tau$ and $\gamma\gamma$ are calculated in the mUED model and compared with the LHC data. The CMS data can push the lower bound on the size parameter R^{-1} of this model as high as 1.3 TeV at 95% C.L.

BIBLIOGRAPHY

[1] S. L. Glashow, Nucl. Phys. **22**, 579 (1961); M. Y. Han and Y. Nambu, Phys. Rev. **139**, B1006 (1965); S. Weinberg, Phys. Rev. Lett. **19**, 1264 (1967).

[2] V. Baluni, Phys. Rev. D **19**, 2227 (1969); R. Crewther, P. di Vecchia, G. Veneziano and E. Witten, Phys. Lett. **88B**, 123 (1979); **91B**, 487 (E) (1980); C. A. Baker, D. D. Doyle, P. Geltenbort, K. Green, M. G. D. van der Grinten, P. G. Harris, P. Iaydjiev and S. N. Ivanov *et al.*, Phys. Rev. Lett. **97**, 131801 (2006) [hep-ex/0602020].

[3] M. A. B. Beg and H. -S. Tsao, Phys. Rev. Lett. **41**, 278 (1978); R. N. Mohapatra and G. Senjanovic, Phys. Lett. B **79**, 283 (1978); K. S. Babu and R. N. Mohapatra, Phys. Rev. D **41**, 1286 (1990); S. M. Barr, D. Chang and G. Senjanovic, Phys. Rev. Lett. **67**, 2765 (1991); R. N. Mohapatra and A. Rasin, Phys. Rev. Lett. **76**, 3490 (1996); R. Kuchimanchi, Phys. Rev. Lett. **76**, 3486 (1996); R. N. Mohapatra, A. Rasin and G. Senjanovic, Phys. Rev. Lett. **79**, 4744 (1997); K. S. Babu, B. Dutta and R. N. Mohapatra, Phys. Rev. D **65**, 016005 (2002).

[4] Y. Fukuda et al. [Super-Kamiokande Collaboration], Phys. Rev. Lett. **81**, 1562 (1998); Y. Fukuda et al. [Super-Kamiokande Collaboration], Phys. Rev. Lett.**82**, 2644 (1999); W. W. M. Allison et al. [Soudan-2 Collaboration], Phys. Lett. B **449**, 137 (1999); S. Fukuda et al. [Super-Kamiokande Collaboration], Phys. Rev. Lett. **85**, 3999 (2000); M. Ambrosio et al. [MACRO Collaboration], Phys. Lett. B **517**, 59 (2001).

[5] B. T. Cleveland et al., Astrophys. J. **496**, 505 (1998); J. N. Abdurashitov et al. [SAGE Collaboration], Phys. Rev. C **60**, 055801 (1999); W. Hampel et al. [GALLEX Collaboration], Phys. Lett. B **447**, 127 (1999); Q. R. Ahmad et al. [SNO Collaboration], Phys. Rev. Lett. **87**, 071301 (2001); Q. R. Ahmad et al. [SNO Collaboration], Phys. Rev. Lett. **89**, 011301 (2002); S. Fukuda et al. [Super-Kamiokande Collaboration], Phys. Lett. B **539**, 179 (2002).

[6] K. Eguchi et al. [KamLAND Collaboration], Phys. Rev. Lett. **90**, 021802 (2003); T. Araki et al. [KamLAND Collaboration], Phys. Rev. Lett. **94**, 081801 (2005).

[7] D. G. Michael et al. [MINOS Collaboration], Phys. Rev. Lett. **97**, 191801 (2006); P. Adamson et al. [MINOS Collaboration], Phys. Rev. Lett. **101**, 131802 (2008).

[8] T. Schwetz, M. Tortola and J. W. F. Valle, New J. Phys. **13**, 063004 (2011).

[9] G. R. Blumenthal, S. M. Faber, J. R. Primack and M. J. Rees, Nature **311** (1984) 517; G. Jungman, M. Kamionkowski and K. Griest, Phys. Rept. **267**, 195 (1996) [hep-ph/9506380]; G. Bertone, D. Hooper and J. Silk, Phys. Rept. **405**, 279 (2005) [hep-ph/0404175]; M. Drees and G. Gerbier, arXiv:1204.2373 [hep-ph].

[10] H. P. Nilles, Phys. Reports **110**, 1 (1984);P. Nath, R. Arnowitt, and A. H. Chamseddine, Applied N = 1 Supergravity (World Scientific, Singapore, 1984);S. Weinberg, The Quantum Theory of Fields, Volume III: Supersymmetry (Cambridge University Press, Cambridge,UK, 2000);S. P. Martin, in Perspectives on Supersymmetry II, edited by G. L. Kane (World Scientific, Singapore, 2010) pp. 1153; see http://zippy.physics.niu.edu/primer.html for the latest version and errata.

[11] L. Girardello and M. Grisaru, Nucl. Phys. B bf 194, 65 (1982);L. J. Hall and L. Randall, Phys. Rev. Lett. **65**, 2939 (1990); I. Jack and D. R. T. Jones, Phys. Lett. B **457**, 101 (1999).

[12] R. N. Mohapatra and A. Rasin, Phys. Rev. Lett. **76**, 3490 (1996); Phys. Rev. D **54**, 5835 (1996); K. S. Babu, B. Dutta and R. N. Mohapatra, Phys. Rev. D **60**, 095004 (1999); Phys. Rev. D **61**, 091701 (2000); Phys. Rev. D **65**, 016005 (2002).

[13] R. N. Mohapatra and J. C. Pati, Phys. Rev. D **11**, 2558 (1975); G. Senjanovic and R. N. Mohapatra, Phys. Rev. D **12**, 1502 (1975); G. Senjanovic, Nucl. Phys. B **153**, 334 (1979).

[14] C. S. Aulakh, A. Melfo, A. Rasin and G. Senjanovic, Phys. Rev. D **58**, 115007 (1998); C. S. Aulakh, A. Melfo and G. Senjanovic, Phys. Rev. D **57**, 4174 (1998); C. S. Aulakh, K. Benakli and G. Senjanovic, Phys. Rev. Lett. **79**, 2188 (1997); Z. Chacko and R. N. Mohapatra, Phys. Rev. D **58**, 015003 (1998);

[15] T. Kaluza, Sitzungsber. Preuss. Akad. Wiss. Berlin (Math. Phys.) **1921**, 966 (1921); O. Klein, Z. Phys. **37**, 895 (1926) [Surveys High Energ. Phys. **5**, 241 (1986)].

[16] N. Arkani-Hamed, S. Dimopoulos and G. R. Dvali, Phys. Lett. B **429**, 263 (1998) [hep-ph/9803315]; I. Antoniadis, N. Arkani-Hamed, S. Dimopoulos and G. R. Dvali, Phys. Lett. B **436**, 257 (1998) [hep-ph/9804398];N. Arkani-Hamed, S. Dimopoulos and G. R. Dvali, Phys. Rev. D **59**,086004(1999).

[17] L. Randall and R. Sundrum, Phys. Rev. Lett. **83**, 4690 (1999) [hep-th/9906064]; L. Randall and R. Sundrum, Phys. Rev. Lett. **83**, 3370 (1999) [hep-ph/9905221].

[18] J. C. Pati and A. Salam, Phys. Rev. D **10**, 275 (1974) [Erratum-ibid. D **11**, 703 (1975)].

[19] K. S. Babu, X. -G. He and E. Ma, Phys. Rev. D **36**, 878 (1987).

[20] E. Ma, Phys. Rev. D **36**, 274 (1987).

[21] R. Kuchimanchi and R. N. Mohapatra, Phys. Rev. D **48**, 4352 (1993); Phys. Rev. Lett. **75**, 3989 (1995).

[22] K. S. Babu and R. N. Mohapatra, Phys. Lett. B **668**, 404 (2008).

[23] Y. Zhang, H. An, X. -d. Ji and R. N. Mohapatra, Phys. Rev. D **78**, 011302 (2008).

[24] K. S. Babu and R. N. Mohapatra, Phys. Rev. Lett. **62**, 1079 (1989); Phys. Rev. D **41**, 1286 (1990).

[25] P. Batra, A. Delgado, D. E. Kaplan and T. M. P. Tait, JHEP **0402**, 043 (2004).

[26] M. Hirsch, M. Malinsky, W. Porod, L. Reichert and F. Staub, JHEP **1202**, 084 (2012).

[27] For a review see: U. Ellwanger, C. Hugonie and A. M. Teixeira, Phys. Rept. **496**, 1 (2010).

[28] R. Kuchimanchi and R. N. Mohapatra, Phys. Rev. D **48**, 4352 (1993).

[29] C. S. Aulakh, A. Melfo and G. Senjanovic, Phys. Rev. D **57**, 4174 (1998); C. S. Aulakh, A. Melfo, A. Rasin and G. Senjanovic, Phys. Rev. D **58**, 115007 (1998).

[30] Z. Chacko and R. N. Mohapatra, Phys. Rev. D **58**, 015003 (1998).

[31] K. S. Babu and R. N. Mohapatra, Phys. Lett. B **668**, 404 (2008).

[32] A. Zee, Nucl. Phys. B **264**, 99 (1986). K. S. Babu, Phys. Lett. B **203**, 132 (1988).

[33] J. Schechter and J. W. F. Valle, Phys. Rev. D **22**, 2227 (1980); G. Lazarides, Q. Shafi and C. Wetterich, Nucl. Phys. B **181**, 287 (1981); R. N. Mohapatra and G. Senjanovic, Phys. Rev. D **23**, 165 (1981).

[34] F. Pisano and V. Pleitez, Phys. Rev. D **46**, 410 (1992); P. H. Frampton, Phys. Rev. Lett. **69**, 2889 (1992).

[35] P. Minkowski, Phys. Lett. **B67**, 421 (1977); T. Yanagida in *Workshop on Unified Theories, KEK Report 79-18*, p. 95 (1979); M. Gell-Mann, P. Ramond and R. Slansky, *Supergravity*, p. 315, North Holland, Amsterdam (1979); S. L. Glashow, *1979 Cargese Summer Institute on Quarks and Leptons*, p. 687, Plenum Press, New York (1980); R. N. Mohapatra and G. Senjanovic, Phys. Rev. Lett. **44**, 912 (1980).

[36] R. N. Mohapatra, Phys. Rev. D **34**, 3457 (1986).

[37] R. N. Mohapatra and A. Rasin, Phys. Rev. Lett. **76**, 3490 (1996); R. N. Mohapatra, A. Rasin and G. Senjanovic, Phys. Rev. Lett. **79**, 4744 (1997); K. S. Babu, B. Dutta and R. N. Mohapatra, Phys. Rev. D **61**, 091701 (2000); K. S. Babu, B. Dutta and R. N. Mohapatra, Phys. Rev. D **65**, 016005 (2002).

[38] S. Chatrchyan *et al.* [CMS Collaboration], Eur. Phys. J. C **72**, 2189 (2012).

[39] G. Aad *et al.* [ATLAS Collaboration], Eur. Phys. J. C **72**, 2244 (2012).

[40] P. Fileviez Perez and S. Spinner, Phys. Lett. B **673**, 251 (2009); S. Patra, A. Sarkar, U. Sarkar and U. Yajnik, Phys. Lett. B **679**, 386 (2009).

[41] R. M. Francis, M. Frank and C. S. Kalman, Phys. Rev. D **43**, 2369 (1991).

[42] K. Huitu and J. Maalampi, Phys. Lett. B **344**, 217 (1995); B. Dutta and R. N. Mohapatra, Phys. Rev. D **59**, 015018 (1999); M. Frank and B. Korutlu, Phys. Rev. D **83**, 073007 (2011).

[43] H. Georgi and M. Machacek, Nucl. Phys. B **262**, 463 (1985); K. Huitu, P. N. Pandita and K. Puolamaki, arXiv:hep-ph/9904388;

[44] P. Fileviez Perez, T. Han, G. -y. Huang, T. Li and K. Wang, Phys. Rev. D **78**, 015018 (2008).

[45] A. Melfo, M. Nemevsek, F. Nesti, G. Senjanovic and Y. Zhang, Phys. Rev. D **85**, 055018 (2012).

[46] D. A. Demir, M. Frank, K. Huitu, S. K. Rai and I. Turan, Phys. Rev. D **78**, 035013 (2008); D. A. Demir, M. Frank, D. K. Ghosh, K. Huitu, S. K. Rai and I. Turan, Phys. Rev. D **79**, 095006 (2009).

[47] S. Chatrchyan *et al.* [CMS Collaboration], Phys. Rev. Lett. **109**, 261802 (2012).

[48] A. Pukhov, arXiv:hep-ph/0412191.

[49] T. Sjostrand, S. Mrenna and P. Skands, JHEP **0605**, 026 (2006).

[50] J. Pumplin, D. R. Stump, J. Huston, H. L. Lai, P. Nadolsky and W. K. Tung, JHEP **0207**, 012 (2002); D. Stump, J. Huston, J. Pumplin, W. K. Tung, H. L. Lai, S. Kuhlmann and J. F. Owens, JHEP **0310**, 046 (2003); T. Sjostrand, S. Mrenna and P. Skands, JHEP **0605**, 026 (2006).

[51] J. Abdallah *et al.* [DELPHI Collaboration], Phys. Lett. B **552**, 127 (2003); G. Abbiendi *et al.* [OPAL Collaboration], Phys. Lett. B **577**, 93 (2003); P. Achard *et al.* [L3 Collaboration], Phys. Lett. B **576**, 18 (2003); D. E. Acosta *et al.* [CDF Collaboration], Phys. Rev. Lett. **93**, 221802 (2004); D. E. Acosta *et al.* [CDF Collaboration], Phys. Rev. Lett. **95**, 071801 (2005); T. Aaltonen [CDF Collaboration], FERMILAB-PUB-07-709-E; S. Chatrchyan *et al.* [CMS Collaboration], Eur. Phys. J. C **72**, 2189 (2012); G. Aad *et al.* [ATLAS Collaboration], Eur. Phys. J. C **72**, 2244 (2012).

[52] B. Meirose, A. A. Nepomuceno and , Phys. Rev. D **84**, 055002 (2011). E. Ramirez Barreto, Y. A. Coutinho, J. Sa Borges and , Nucl. Phys. B **810**, 210 (2009). E. Ramirez Barreto, Y. A. Coutinho, J. Sa Borges, Phys. Rev. D **83**, 075001 (2011).

[53] R. Barbier, C. Berat, M. Besancon, M. Chemtob, A. Deandrea, E. Dudas, P. Fayet and S. Lavignac *et al.*, Phys. Rept. **420**, 1 (2005).

[54] G. Aad *et al.* [ATLAS Collaboration], Phys. Lett. B **716**, 1 (2012) [arXiv:1207.7214 [hep-ex]]; S. Chatrchyan *et al.* [CMS Collaboration], Phys. Lett. B **716**, 30 (2012) [arXiv:1207.7235 [hep-ex]]; TEVNPH Working Group (for the CDF, D0 Collaborations), Fermilab preprint FERMILAB-CONF-12-318-E, arXiv:1207.0449 [hep-ex] (2012).

[55] S. Dimopoulos and L. Susskind, Nucl. Phys. B **155**, 237 (1979); E. Eichten and K. D. Lane, Phys. Lett. B **90**, 125 (1980); C. Csaki, C. Grojean, H. Murayama, L. Pilo and J. Terning, Phys. Rev. D **69**, 055006 (2004) [hep-ph/0305237].

[56] B. W. Lee, C. Quigg and H. B. Thacker, Phys. Rev. D **16**, 1519 (1977).

[57] W. J. Marciano, G. Valencia and S. Willenbrock, Phys. Rev. D **40** (1989) 1725; C. F. Kolda and H. Murayama, JHEP **0007** (2000) 035 [hep-ph/0003170].

[58] See M. Sher, Phys. Rept. **179**, 273 (1989), and references therein, for early work on the subject; for more recent work, see J. Ellis, J. R. Espinosa, G. F. Giudice, A. Hoecker and A. Riotto, Phys. Lett. B **679**, 369 (2009) [arXiv:0906.0954 [hep-ph]]; J. Elias-Miro, J. R. Espinosa, G. F. Giudice, G. Isidori, A. Riotto and A. Strumia, Phys. Lett. B **709**, 222 (2012) [arXiv:1112.3022 [hep-ph]]; G. Degrassi, S. Di Vita, J. Elias-Miro, J. R. Espinosa, G. F. Giudice, G. Isidori and A. Strumia, JHEP **1208**, 098 (2012) [arXiv:1205.6497 [hep-ph]]; F. Bezrukov, M.Y. Kalmykov, B.A. Kniehl and M. Shaposhnikov, JHEP **1210**, 140 (2012); M. Holthausen, K.S. Lim and M. Lindner, JHEP **1202**, 037 (2012).

[59] S. Alekhin, A. Djouadi and S. Moch, Phys. Lett. B **716** (2012) 214 [arXiv:1207.0980 [hep-ph]].

[60] For a comprehensive discussion, see G. Bertone, J. Silk, B. Moore, J. Diemand, J. Bullock, M. Kaplinghat, L. Strigari and Y. Mellier *et al.*, *Particle Dark Matter: Observations, Models and Searches*, (Cambridge University Press, 2010).

[61] P. J. E. Peebles and B. Ratra, Rev. Mod. Phys. **75**, 559 (2003) [astro-ph/0207347].

[62] A. Riotto and M. Trodden, Ann. Rev. Nucl. Part. Sci. **49**, 35 (1999) [hep-ph/9901362].

[63] See, for example, S. P. Martin, *A Supersymmetry Primer*, (in Kane, G.L. (ed.): "Perspectives on supersymmetry II", p.1), [hep-ph/9709356]; M. Drees, R. Godbole and P. Roy, *Theory and phenomenology of sparticles* (Hackensack, USA: World Scientific, 2004); H. Baer and X. Tata, *Weak scale supersymmetry*, (CUP ,2006).

[64] T. Appelquist, H.C. Cheng, B.A. Dobrescu, Phys. Rev. **D64**, 035002 (2001).

[65] D. Hooper and S. Profumo, Phys. Rept. **453**, 29 (2007) [hep-ph/0701197].

[66] H.-C. Cheng, K.T. Matchev, M. Schmaltz, Phys. Rev. **D66**, 036005 (2002); A.K. Datta, K.C. Kong, K.T. Matchev, New J. Phys. **12**, 075017 (2010); B. Bhattacherjee *et al*, Phys. Rev. **D81**, 035021 (2010);

[67] A.K. Datta, K.C. Kong, K.T. Matchev, Phys. Rev. **D72**, 096006 (2005); Erratum-ibid. **D72**, 119901 (2005); B. Bhattacherjee *et al*, Phys. Rev. **D82**, 055006 (2010).

[68] K.R. Dienes, E. Dudas, T. Gherghetta, Phys. Lett. **B436**, 55 (1998) and Nucl. Phys. **B537**, 47 (1999).

[69] G. Bhattacharyya *et al*, Nucl.Phys. **B760**, 117 (2007).

[70] M. Blennow *et al*, Phys. Lett. **B712**, 419 (2012).

[71] [ATLAS Collaboration], ATLAS-CONF-2013-102 (2013).

[72] [ATLAS Collaboration], CERN preprint CERN-PH-EP-2013-103 (2013).

[73] [CMS Collaboration], CMS-PAS-HIG-13-005 (2013).

[74] G. Belanger, A. Belyaev, M. Brown, M. Kakizaki and A. Pukhov, Phys. Rev. D **87**, 016008 (2013) [arXiv:1207.0798 [hep-ph]]; U. K. Dey and T. S. Ray, Phys. Rev. D **88**, 056016 (2013) [arXiv:1305.1016 [hep-ph]].

[75] A. Datta and S. Raychaudhuri, Phys. Rev. D **87**, 035018 (2013) [arXiv:1207.0476 [hep-ph]].

[76] L. Edelhauser, T. Fläcke and M. Kramer, JHEP **1308**, 091 (2013) [arXiv:1302.6076 [hep-ph]].

[77] CMS Collaboration], CMS-PAS-EXO-12-061 (2012).

[78] T. Kakuda, K. Nishiwaki, K. -y. Oda and R. Watanabe, Phys. Rev. D **88**, 035007 (2013) [arXiv:1305.1686 [hep-ph]].

[79] [ATLAS Collaboration], ATLAS-CONF-2013-034 (2013).

[80] V. Barger and R.J.N. Phillips, *Collider Physics*, (Addison-Wesley, 2nd ed., 1997).

[81] M. Schreck and M. Steinhauser, Phys. Lett. B **655**, 148 (2007) [arXiv:0708.0916 [hep-ph]].

[82] J. Beringer et al. (Particle Data Group), Phys. Rev. D86, 010001 (2012).

[83] W. -Y. Keung and W. J. Marciano, Phys. Rev. D **30**, 248 (1984).

[84] F. J. Petriello, JHEP **0205**, 003 (2002) [hep-ph/0204067].

[85] W. Beenakker, R. Hopker and M. Spira, hep-ph/9611232.

[86] See, for example, P. Giacomelli, *LHC: future measurements and reach*, Solvay Workshop on "Facing the Scalar Sector", Brussels (May 2013).

APPENDIX A

MINIMIZATION CONDITIONS AND SCALALR HIGGS MASS-SQUARED MATRIX

Inverse seesaw model

The minimization conditions for the potential are given as:

$$\begin{aligned}
4m_3^2(-v_L^2+v_R^2) &= (g_V^2v_L^4+g_L^2v_L^2(-v_1^2+v_2^2+v_L^2)+g_R^2v_1^2v_R^2-g_R^2v_2^2v_R^2-g_R^2v_R^4-g_V^2v_R^4 \\
&+ 4v_1^2v_L^2\lambda^2-4v_1^2v_R^2\lambda^2), \\
-4B\mu(v_1^2-v_2^2) &= -v_2v_1\left[g_L^2(-v_1^2+v_2^2+v_L^2)+g_R^2(-v_1^2+v_2^2+v_R^2)-2(v_L^2+v_R^2)\lambda^2)\right] \\
&- 2\lambda A_\lambda v_Lv_Rv_2+4v_1v_Lv_R\lambda\mu, \\
4m_1^2(v_2^2-v_1^2) &= [g_R^2v_1^4-g_R^2v_2^4+g_L^2(v_1^2+v_2^2)(v_1^2-v_2^2-v_L^2)-g_R^2v_1^2v_R^2-g_R^2v_2^2v_R^2 \\
&+ 4\lambda^2v_1^2v_L^2+4\lambda^2v_1^2v_R^2-4A_\lambda\lambda v_1v_Lv_R-8\lambda\mu v_2v_Lv_R+16\mu^2v_1^2-16\mu^2v_2^2], \\
8\mu v_2(\frac{v_L\lambda}{v_R}-\frac{v_R\lambda}{v_L}) &= \frac{4\lambda A_\lambda v_1v_L}{v_R}-\frac{4\lambda A_\lambda v_1v_R}{v_L}+(g_R^2-g_L^2)(v_1^2-v_1^2)+g_L^2v_L^2-g_R^2v_R^2 \\
&+ 2g_V^2(v_L^2-v_R^2)+4\lambda^2(v_R^2-v_L^2). \qquad \text{(A.1)}
\end{aligned}$$

The mass-squared matrix elements $M_{ij}(=M_{ji})$ in this case can be given by:

$$\begin{aligned}
M_{11} &= \frac{g_R^2(v_1^2-v_2^2)^2+g_V^2v_L^2+g_L^2(v_1^2-v_2^2-v_L^2)^2+8\lambda^2v_1^2v_L^2}{2(v_1^2+v_2^2+v_L^2)}, \\
M_{12} &= \frac{g_R^2v_R(v_2^2-v_1^2)-g_V^2v_rv_l^2+4\lambda(-A_\lambda v_1v_L+\lambda v_R(v_1^2+v_L^2)+2\mu v_2v_L}{2\sqrt{(v_1^2+v_2^2+v_L^2)}}, \\
M_{13} &= \frac{v_1v_L\left[g_R^2(v_2^2-v_1^2)+g_V^2v_L^2+2g_L^2(v_2^2-v_1^2+v_L^2)+4\lambda^2(v_1^2-v_L^2)\right]}{2\sqrt{(v_1^2+v_2^2+v_L^2)(v_1^2+v_L^2)}}, \\
M_{14} &= \frac{v_2\left[g_V^2v_L^4+2g_L^2v_1^2(v_1^2-v_2^2-v_L^2)+g_R^2(v_1^2-v_2^2)(2v_1^2+v_L^2)+8\lambda^2v_1^2v_L^2\right]}{2(v_1^2+v_2^2+v_L^2)\sqrt{(v_1^2+v_L^2)}}, \\
M_{22} &= \frac{g_R^2v_R^3+g_V^2v_R^3+2\lambda A_\lambda v_1v_L-4\lambda\mu v_2v_L}{2v_R},
\end{aligned}$$

$$
\begin{aligned}
M_{23} &= \frac{(g_R^2-g_V^2)v_1v_Lv_R+2\lambda\left[A_\lambda(v_L^2-v_1^2)+2\mu v_1v_2\right]}{2\sqrt{v_1^2+v_L^2}},\\
M_{24} &= \frac{v_2v_R\left[-2g_R^2v_1^2-(g_R^2+g_V^2)v_L^2+4\lambda^2(v_1^2+v_L^2)\right]-4\lambda v_L\left[A_\lambda v_1v_2+\mu(v_1^2-v_2^2+v_L^2)\right]}{2\sqrt{(v_1^2+v_2^2+v_L^2)(v_1^2+v_L^2)}},\\
M_{33} &= \frac{(4g_L^2+g_R^2+g_V^2)v_1^3v_L^3+4m_2^2v_2v_L^2+2\lambda A_\lambda v_R(v_1^2+v_L^2)^2-8\lambda^2v_1^3v_L^3-4\lambda\mu v_1^3v_2v_R}{2v_1v_L(v_1^2+v_L^2)},\\
M_{34} &= [-4m_2^2v_L(v_1^2+v_2^2+v_L^2)+v_1v_2v_L(4g_L^2v_1^2-g_V^2v_l^2+g_R^2(2v_1^2+v_L^2))+4\lambda^2v_2v_L(v_L^2-v_1^2),\\
&+ 4\lambda\mu v_R(v_1^2+v_2^2+v_L^2)]/\left[2(v_1^2+v_L^2)\sqrt{v_1^2+v_2^2+v_L^2)}\right]\\
M_{44} &= [g_L^2(-2v_1^6+20v_1^4v_2^2-2v_1^2v_2^4-3v_1^4v_L^2+10v_1^2v_2^2v_L^2+v_2^4v_L^2+5v_2^2v_L^4+v_L^6)\\
&+ g_L^2v_R^2(v_1^2-v_1v_2+v_L^2)(v_1(v_1+v_2)+v_L^2))+4m_1^2(v_1^4+v_L^4+v_1^2(v_2^2+2v_L^2))\\
&+ v_2(16m_2^2v_1(v_1^2+v_L^2)+v_2(v_L^2(4m_3^2+g_V^2(3v_L^2-v_R^2))-8\lambda A_\lambda v_1v_Lv_R\\
&+ 4(6v_1^2v_L^2+(v_1^2+v_L^2)v_R^2)\lambda^2))-16\lambda\mu v_2v_L(v_1^2+v_L^2)v_R\\
&+ 16\mu^2(v_1^4+v_L^4+v_1^2(v_2^2+2v_L^2))]/\left[8(v_1^2+v_L^2)(v_1^2+v_2^2+v_L^2)\right].
\end{aligned}
\tag{A.2}
$$

Case with two pair of triplets and two bidoublets

The minimization conditions for this case are given as:

$$
\begin{aligned}
&4m_{12}^2v_{d_1}+4B_{12}\mu_{12}v_{d_2}+4m_{11}^2v_{u_1}+8B_{11}\mu_{11}v_{u_2}+g_L^2v_{u_1}(v_{d_1}^2-v_{d_2}^2+v_{u_1}^2-v_{u_2}^2)\\
&+g_R^2v_{u_1}(v_{d_1}^2-v_{d_2}^2+2{v_R}^2-2\overline{v}_R^2+v_{u_1}^2-v_{u_2}^2)+4\left[v_{u_1}(\mu_{11}^2+\mu_{12}^2)+v_{d_1}\mu_{12}(\mu_{11}+\mu_{22})\right]=0,\\
&4B_{12}\mu_{12}v_{d_1}+4m_{12}^2v_{d_2}+8B_{11}\mu_{11}v_{u_1}+4m_{11}^2v_{u_2}+g_L^2v_{u_2}(-v_{d_1}^2+v_{d_2}^2-v_{u_1}^2+v_{u_2}^2)\\
&+g_R^2v_{u_2}(-v_{d_1}^2+v_{d_2}^2-2{v_R}^2+2\overline{v}_R^2-v_{u_1}^2+v_{u_2}^2)+4\left[v_{u_2}(\mu_{11}^2+\mu_{12}^2)+v_{d_2}\mu_{12}(\mu_{11}+\mu_{22})\right]=0,\\
&4m_{22}^2v_{d_1}+8B_{22}\mu_{22}v_{d_2}+4m_{12}^2v_{u_1}+4B_{12}\mu_{12}v_{u_2}+g_L^2v_{d_1}(v_{d_1}^2-v_{d_2}^2+v_{u_1}^2-v_{u_2}^2)\\
&+g_R^2v_{d_1}(v_{d_1}^2-v_{d_2}^2+2{v_R}^2-2\overline{v}_R^2+v_{u_1}^2-v_{u_2}^2+4\left[v_{u_1}\mu_{12}(\mu_{11}+\mu_{22})+v_{d_1}(\mu_{12}^2+\mu_{22}^2)\right]=0,\\
&8B_{22}\mu_{22}v_{d_1}+4m_{22}^2v_{d_2}+4B_{12}\mu_{12}v_{u_1}+4m_{12}^2v_{u_2}+g_L^2v_{d_2}(-v_{d_1}^2+v_{d_2}^2-v_{u_1}^2+v_{u_2}^2)\\
&+g_R^2v_{d_2}(-v_{d_1}^2+v_{d_2}^2-2{v_R}^2+2\overline{v}_R^2-v_{u_1}^2+v_{u_2}^2)+4\left[v_{u_2}\mu_{12}(\mu_{11}+\mu_{22})+v_{d_2}(\mu_{12}^2+\mu_{22}^2))\right]=0,\\
&2B_2\mu_2\overline{v}_R+v_R(2m_5^2+2\mu_2^2+2g_V^2({v_R}^2-{\overline{v}_R}^2)+g_R^2(v_{d_1}^2-v_{d_2}^2+2{v_R}^2-2\overline{v}_R^2+v_{u_1}^2-v_{u_2}^2)=0,\\
&2B_2\mu_2v_R+\overline{v}_R(2m_6^2+2\mu_2^2+2g_V^2(\overline{v}_R^2-{v_R}^2)+g_R^2(v_{d_2}^2-v_{d_1}^2-2{v_R}^2+2\overline{v}_R^2-v_{u_1}^2+v_{u_2}^2)=0.
\end{aligned}
\tag{A.3}
$$

Universal seesaw model with a singlet

The mass-squared matrix elements are given by:

$$
\begin{aligned}
M_{11} &= \frac{g_L^2\left({v_L}^2-{\overline{v}_L}^2\right)^2+{g_V}^2\left({v_L}^2-{\overline{v}_L}^2\right)^2+8{v_L}^2{\overline{v}_L}^2\lambda^2}{2\left({v_L}^2+{\overline{v}_L}^2\right)},\\
M_{12} &= \frac{v_L\overline{v}_L\left({v_L}^2-{\overline{v}_L}^2\right)\left({g_L}^2+{g_V}^2-2\lambda^2\right)}{{v_L}^2+{\overline{v}_L}^2},\\
M_{13} &= \frac{-{g_V}^2\left({v_L}^2-{\overline{v}_L}^2\right)\left({v_R}^2-{\overline{v}_R}^2\right)-8v_L\overline{v}_Lv_R\overline{v}_R\lambda^2}{2\sqrt{{v_L}^2+{\overline{v}_L}^2}\sqrt{{v_R}^2+{\overline{v}_R}^2}},\\
M_{14} &= \frac{{g_V}^2\left(-{v_L}^2+{\overline{v}_L}^2\right)v_R\overline{v}_R+2v_L\overline{v}_L\left({v_R}^2-{\overline{v}_R}^2\right)\lambda^2}{\sqrt{{v_L}^2+{\overline{v}_L}^2}\sqrt{{v_R}^2+{\overline{v}_R}^2}},\\
M_{15} &= \frac{2\lambda\left(A_\lambda v_L\overline{v}_L+\left({v_L}^2+{\overline{v}_L}^2\right)v_S\lambda\right)}{\sqrt{{v_L}^2+{\overline{v}_L}^2}},\\
M_{22} &= 2[{g_L}^2{v_L}^2{\overline{v}_L}^2+2{g_V}^2{v_L}^2{\overline{v}_L}^2+{m_3}^2\left({v_L}^2+{\overline{v}_L}^2\right)+{m_5}^2\left({v_L}^2+{\overline{v}_L}^2\right)\\
&+ {v_L}^4\lambda^2-2{v_L}^2{\overline{v}_L}^2\lambda^2+{\overline{v}_L}^4\lambda^2+2{v_L}^2{v_S}^2\lambda^2+2{\overline{v}_L}^2{v_S}^2\lambda^2]/\left({v_L}^2+{\overline{v}_L}^2\right),\\
M_{23} &= \frac{{g_V}^2v_L\overline{v}_L\left(-{v_R}^2+{\overline{v}_R}^2\right)+2\left({v_L}^2-{\overline{v}_L}^2\right)v_R\overline{v}_R\lambda^2}{\sqrt{{v_L}^2+{\overline{v}_L}^2}\sqrt{{v_R}^2+{\overline{v}_R}^2}},\\
M_{24} &= \frac{-2{g_V}^2v_L\overline{v}_Lv_R\overline{v}_R-\left({v_L}^2-{\overline{v}_L}^2\right)\left({v_R}^2-{\overline{v}_R}^2\right)\lambda^2}{\sqrt{{v_L}^2+{\overline{v}_L}^2}\sqrt{{v_R}^2+{\overline{v}_R}^2}},\\
M_{25} &= -\frac{A_\lambda\left({v_L}^2-{\overline{v}_L}^2\right)\lambda}{\sqrt{{v_L}^2+{\overline{v}_L}^2}},\\
M_{33} &= \frac{{g_R}^2\left({v_R}^2-{\overline{v}_R}^2\right)^2+{g_V}^2\left({v_R}^2-{\overline{v}_R}^2\right)^2+8{v_R}^2{\overline{v}_R}^2\lambda^2}{2\left({v_R}^2+{\overline{v}_R}^2\right)},\\
M_{34} &= \frac{v_R\overline{v}_R\left({v_R}^2-{\overline{v}_R}^2\right)\left({g_R}^2+{g_V}^2-2\lambda^2\right)}{{v_R}^2+{\overline{v}_R}^2},\\
M_{35} &= \frac{\lambda\left(-2A_\lambda v_R\overline{v}_R+2\left({v_R}^2+{\overline{v}_R}^2\right)v_S\lambda\right)}{\sqrt{{v_R}^2+{\overline{v}_R}^2}},\\
M_{44} &= [2{g_R}^2{v_R}^2{\overline{v}_R}^2+2{g_V}^2{v_R}^2{\overline{v}_R}^2+{m_4}^2\left({v_R}^2+{\overline{v}_R}^2\right)+{m_6}^2\left({v_R}^2+{\overline{v}_R}^2\right)\\
&+ {v_R}^4\lambda^2-2{v_R}^2{\overline{v}_R}^2\lambda^2+{\overline{v}_R}^4\lambda^2+2{v_R}^2{v_S}^2\lambda^2+2{\overline{v}_R}^2{v_S}^2\lambda^2]/\left({v_R}^2+{\overline{v}_R}^2\right),\\
M_{45} &= \frac{A_\lambda\left({v_R}^2-{\overline{v}_R}^2\right)\lambda}{\sqrt{{v_R}^2+{\overline{v}_R}^2}},\\
M_{55} &= m_S^2+(v_L^2+\overline{v}_L^2+v_R^2+\overline{v}_R^2). \qquad \text{(A.4)}
\end{aligned}
$$

APPENDIX B

FEYNMAN RULES

Here we list down all the Feynman rules necessary for analyzing productions and decays of doubly-charged Higgsinos in the LRSUSY model.

Fermion-Fermion-Z Boson, γ:

- $\bullet\gamma^\mu\tilde{\delta}^{--}_{L,R}\bar{\tilde{\delta}}^{--}_{L,R}:\ 2ie\gamma^\mu$
- $\bullet Z^\mu_L\tilde{\delta}^{--}_{L}\bar{\tilde{\delta}}^{--}_{L}:\ i\dfrac{g_L\cos 2\theta_W}{\cos\theta_W}\gamma^\mu$
- $\bullet Z^\mu_L\tilde{\delta}^{--}_{R}\bar{\tilde{\delta}}^{--}_{R}:\ -i\dfrac{2g_L\sin^2\theta_W}{\cos\theta_W}\gamma^\mu$
- $\bullet Z^\mu_R\tilde{\delta}^{--}_{L}\bar{\tilde{\delta}}^{--}_{L}:\ -i\dfrac{g_L\sin^2\theta_W}{\sqrt{\cos 2\theta_W}\cos\theta_W}\gamma^\mu$
- $\bullet Z^\mu_R\tilde{\delta}^{--}_{R}\bar{\tilde{\delta}}^{--}_{R}:\ i\dfrac{g_L(1-3\sin^2\theta_W)}{\cos\theta_W\sqrt{\cos 2\theta_W}}\gamma^\mu$
- $\bullet Z^\mu_R u\bar{u}:\ i\dfrac{g_L(3-8\sin^2\theta_W+3\gamma_5\cos 2\theta_W)}{12\cos\theta_W\sqrt{\cos 2\theta_W}}\gamma^\mu$
- $\bullet Z^\mu_R d\bar{d}:\ -i\dfrac{g_L(3-4\sin^2\theta_W+3\gamma_5\cos 2\theta_W)}{12\cos\theta_W\sqrt{\cos 2\theta_W}}\gamma^\mu$ Appendix **??** data goes here

VITA

Ayon Patra

Candidate for the Degree of

Doctor of Philosophy

Dissertation: THEORY AND PHENOMENOLOGY OF HIGGS BOSONS IN LEFT-RIGHT SUPERSYMMETRIC MODELS

Major Field: Physics

Biographical:

Personal Data: Born in West Bengal, India on March 22, 1984.

Education:

Received B. Sc. degree from Calcutta University, Kolkata, West Bengal, India, 2005, in Physics.
Received M. Sc. degree from Indian Institute of Technology, Kanpur, Uttar Pradesh, India, 2007, in Physics.
Completed the requirements for the degree of Doctor of Philosophy with a major in Physics at Oklahoma State University in May, 2014.

Publications:

K. S. Babu, A. Patra and S. K. Rai, Phys. Rev. D **88**, 055006 (2013).
A. Datta, A. Patra and S. Raychaudhuri, arXiv:1311.0926 [hep-ph].

Recognition:

National Merit Scholarship, Government of India, India, 2005.
Academic Excellence Award, Department of Physics, Indian Institute of Technology, Kanpur, 2006.

Name: Ayon Patra Date of Degree: May, 2014

Institution: Oklahoma State University Location: Stillwater, Oklahoma

Title of Study: THEORY AND PHENOMENOLOGY OF HIGGS BOSONS IN LEFT-RIGHT SUPERSYMMETRIC MODELS

Pages in Study: 126 Candidate for the Degree of Doctor of Philosophy

Major Field: Physics

Scope and methods. In this dissertation, I study the theory and phenomenology of Higgs bosons in the framework of various models with supersymmetry, left-right symmetry and universal extra dimensions. In Chapter 1, I summarize the various models studied and motivation for each. Chapter 2 is devoted to the study of Higgs boson mass spectrum in various left-right supersymmetric models with different symmetry breaking sectors. Chapter 3 involves the collider phenomenology of relatively light doubly-charged Higgs bosons and Higgsinos which arise naturally in supersymmetric left-right models. In Chapter 4, I look at the constraints on a minimal universal extra dimensional model from the measured signal strength for Higgs boson decay at the large hadron collider.

Findings and conclusions. In Chapter 2, I study Higgs boson mass spectrum in supersymmetric left-right models based on the gauge group $SU(3)_c \times SU(2)_L \times SU(2)_R \times U(1)_{B-L}$. The constraints on the lightest neutral Higgs boson mass m_h is studied in detail. A variety of symmetry breaking scenarios is considered. Several of these models with Higgs triplets and Higgs doublets for $SU(2)_R$ symmetry breaking are studied, with additional bidoublets and possibly a gauge singlet. Many of these cases lead to a much higher tree-level neutral Higgs boson mass compared to MSSM. With this enhanced Higgs boson mass, it is possible to accommodate the experimentally observed mass of 126 GeV with a relatively light stops that mix negligibly. In Chapter 3, I look at the collider phenomenology of the doubly-charged Higgs bosons and Higgsinos in the framework of left-right supersymmetric model with automatic R-parity conservation. I analyze a new collider signal resulting from the pair production and decay of a light doubly-charged Higgsino into an even lighter doubly-charged Higgs boson. I investigate the collider signature of these particles with four leptons and missing transverse energy final state at the Large Hadron Collider and show that the discovery reach for both particles can be increased in this channel. In Chapter 4, I investigate the impact of the latest data on Higgs boson branching ratios on the minimal extra dimensional model. The experimental data along with the constraints from the vacuum stability requirements allow for a realistic prediction for the signal strengths in this model. Comparing the calculated results with the observed data, the size parameter R^{-1} of the model can be shown to have a lower bound of 1.3 TeV at 95% confidence level.